METALLIC FIBRE REINFORCEMENT OF PLASTICS AND THE EFFECT OF COLD WORKING

By

Ekrem Pakdemirli, B.S., M.S. in Mech.Eng.

Thesis presented for the degree of Doctor of Philosophy in the University of London

May 1967

ABSTRACT

In Part I.a general survey of the theories for the evaluation of the physical constants of composites is given. A theory to predict the moduli of metal fibre/plastic systems is developed for an arbitrary distribution of fibres, which takes into account the micro and macro strain differences of two media.

Unidirectional and cross reinforcement as well as randomly distributed types of reinforcement are considered. The theory is also applied to helically wound thin-walled cylinders to optimise the orientation of the fibres.

In Part II.a the effect of cold working on the mechanical properties of plastics and composites is described. Detailed experimental techniques employed during this investigation are given.

In Part II.b the experimental results obtained from tensile tests, plane strain compression tests, impact and creep tests for various combinations of polythene, propathene, aluminium, copper, bronze and steel systems are presented.

Acknowledgement

The author wishes to thank Professor Hugh Ford, F.R.S. and Dr. J.G. Williams for their supervision during the course of study. He would also like to thank Professor Emeritus W.G. Bickley for his helpful discussions on the mathematical side of this work. Last but not least he thanks his wife whose patience and understanding have done so much in helping him to complete this work.

CONTENTS

	page
General introduction	6
PART I. Reinforcement of plastics	8
1.0 General	9
2.0 Theoretical predictions for the physical constants of metallic fibre reinforced plastics	11
2.1 Uni-directional reinforcing	23
2.2 Cross reinforcing	29
2.3 Randomly distributed fibres reinforcement	33
2.4 Application of the theory to helically wound metal fibre reinforced thin walled cylinders	34
2.5 Ultimate strength of a composite	39
3.0 Deformation mechanism	40
PART II. a. Experimental methods, cold rolling of plastics and composites	47
1.0 Manufacturing process of reinforced plastics	48
2.0 Mechanical testing of plastics	54
2.1 Simple tensile tests	56
2.2 Plane strain compression tests	58
2.3 Impact tests	60
2.4 Creep tests	61
3.0 The effect of cold working on mechanical peoperties of plastics	63
3.1 Cold rolling	65

4.0 Cold rolling of composites 69

PART II. b. The results 72

1.0 The results 73

2.0 Reinforced plastics 73

3.0 Cold rolling of plastics 77

4.0 Cold rolling of composites 78

5.0 Discussion of the results 79

6.0 Conclusions 89

REFERENCES 93

GRAPHS AND FIGURES 100

GENERAL INTRODUCTION

Recently there has been great interest in multiphase materials, especially in the applications where high strengths per unit weight are necessary. Glass/thermosetting and metal/metal systems are produced in considerable quantities (the annual consumption of glass fibre reinforced plastics is over 50,000 tons). Usually the embedded fibres (or whiskers) have very high ultimate strength and are brittle. The cost of production of such fibres (except glass fibres) is high and limits the application.

There is a trend towards using thermoplastics with glass fibres. This allows generally any production process for the manufacturing of composites. This investigation is confined to metal/thermoplastics systems. Such composites conduct electricity and heat, they have higher yield and rupture strains. Therefore it is believed that they will be used where these properties are dominant factors in the design criteria.

It is known that there are generally two ways to improve mechanical properties of a material. One of the methods is to embed high strength fibres into a matrix where the load is transferred by means of shear tractions at the fibre-matrix interphase. The second method is to introduce high dislocation density by cold working (usually by drawing or rolling). In this investigation both methods

have been tried, and also an attempt has been made to find out what happens if a composite is subjected to a cold working. There is evidence that for small reductions in thickness (less than 8 percent) an improvement in the yield strength of the composite is obtained.

The results are presented in two parts. The first part deals with the theoretical aspects of reinforcement and cold rolling of materials. Some details have been omitted in order to consider a wider range of problems. Part II deals mainly with the experimental approach and comparison of the results with the theories given in Part I.

PART I

REINFORCEMENT OF PLASTICS

1.O GENERAL

In the last few years, relatively inexpensive materials of high strength have been obtained with different reinforcing processes. Metallic and non-metallic fibres of high tensile strength have been embedded in metal or non-metal matrices for obtaining new materials with improved mechanical and physical properties. Copper and aluminium base tungsten and molybdenum fibre reinforced composites are being used in limited quantities for high stress applications. Glass-fibre reinforced thermo-setting plastics have found many applications in the aircraft and car industries. It is reported that up to 190,000 lbf/in^2 ultimate strength has been obtained from glass-fibre reinforced epoxy resins. This strength, of course, can be achieved only in the direction of fibre alignment. Because glass is very brittle these composites have very low rupture strains and transverse ultimate strengths. Metal fibres embedded in plastics in particular orientation remove the forementioned shortcomings. However, DELMONTE (1)* reports that the gain in the tensile strength in metal-fibre reinforced plastics is not always impressive. This is largely due to imperfect adhesion of the two media which have very high ratios of elastic moduli. The

---

*Numbers in the brackets show the references listed at the end.

smaller the value of this ratio the better is the cohesion of the contacting surfaces. Generally the results obtained so far are encouraging and the future of composite materials is bright.

WILLIAMS (2) produced aluminium steel composite (E_f/E_m = 3) in which the experimental breaking stress value for 6 percent reinforcement was 45 percent of that expected from the theory (Eqn. 2). This percentage deteriorated as the percentage of reinforcement increased. TEWU (3) produced metal/metal sintered composites (E_f/E_m = 10) and found that the Young's modulus of them is doubled with respect to the Young's modulus of the matrix, when the volumetric reinforcement ratio was around 0.2. General surveys on experimental achievement of composite materials are found in many papers (4-10). There is a considerable volume of experimental data on glass fibre reinforced thermo-setting plastics and on aluminium-base composites in these papers.

Although metal-fibre reinforced thermoplastics have the potential of becoming structural materials, very little work has been done in this field. The use of thermoplastics as the matrix and the incorporation of metal fibres as the reinforcing elements will give two advantages, namely: (a) most normal fabricating processes can be used; (b) the composite can be re-used. A composite of this nature is more ductile than the glass-

fibre reinforced plastics which in some cases may be desirable. There is therefore a need for more theoretical and experimental work directed towards determining the characteristics of such composites. This work intends to provide some information on both experimental and theoretical aspects of the problem.

2.0 THEORETICAL PREDICTIONS FOR THE PHYSICAL CONSTANTS OF METALLIC FIBRE-REINFORCED PLASTICS

The theoretical work done to determine the physical constants of the composites can be generally classified into three groups as follows:

1) A stress distribution under given tractions with suitable boundary conditions is found and appropriate body averages taken throughout the volume. Hence the elastic constants of inhomogeneous medium are determined. This approach to the problem is called 'the direct method'. However, phase geometry complicates the boundary conditions and in some cases makes it impossible to calculate the exact values. This approach has been used by some authors (11, 12) for hexagonal arrays of round fibres.

2) By using known and regular phase geometries and gross approximations to the nature of the stress and strain field, composites are modelled and represented by various combinations of series and parallel connected

constituent elements. Thus, it becomes possible to find the physical constants of the composites. This approach has been widely used in the field of composites (13-21).

3) By using variational methods of elasticity the moduli of the composites are bounded. The effective elastic moduli are expressed in terms of strain energy for any particular stress/strain field. Hence the upper and lower bounds are determined (references (17-26)).

As is clear from the definitions, one cannot draw sharp lines between these three approaches. The method which the author uses can be assumed to be a mixture of the first and second. This has more engineering appeal than that of the variational-methods approach, which involves highly sophisticated mathematical procedures.

WHITNEY (12) obtained an expression for the Young's modulus of composite along the fibre alignment in terms of physical constants of the constituents . This is

$$E_c = E_m + c(E_f - E_m) + 2(\nu_f - \nu_m)^2 c(1-c)E_m E_f / \{E_m(1-c)L_f + [cL_m + (1+\nu_m)E_f]\} \qquad 1.$$

together with

$$L = 1 - \nu - 2\nu^2 \qquad 1.a$$

where E, ν, c are Young's modulus, Poisson's ratio and

---

* The subscripts c, m, f stand for composite, matrix and fibre respectively.

the volumetric concentration of the fibres respectively. In the case of equal Poisson's ratio equation 1 reduces to

$$E_c = E_m(1-c) + E_f c \qquad 2.$$

which in engineering is called the law of mixtures. This expression was obtained by PAUL (17) as the theoretical upper bound for composites of arbitrary phase geometry. In fact equation 2 was suggested by McDANELS (13) earlier for the ultimate strength of the composite in the form of

$$\sigma_c = \sigma_m(1-c) + \sigma_f c \qquad 3.$$

where σ_m is the stress within the matrix when the brittle (fibre) phase attains its ultimate stress.

TEWU (3) derived formulae for the bulk and shear moduli of composites which involve complicated expressions due to phase geometry. The expressions are

$$K_c = K_m/[1+cP(\frac{K_m-K_1}{K_c})]$$
$$G_c = G_m/[1+cQ(\frac{G_m-G_f}{G_c})] \qquad 4.$$

where K and G are bulk and shear moduli, and P, Q are functions of phase geometry and the physical constants of the constituent materials.

HASHIN (18, 19, 27) gives the bounds on shear and bulk moduli using variational principles of elasticity. The predicted lower bounds are;

$$K_c^* = K_f + \frac{(K_m - K_f)C_m}{1 + \frac{3(K_m - K_f)}{3K_f + 4G_f}} \qquad 5.a$$

$$G_c^* = G_f + \frac{(G_m - G_f)C_m}{1 + \frac{6(G_m - G_f)(K_f + 2G_f)}{5(3K_f + 4G_f)G_f} C_f} \qquad 5.b$$

where upper bounds are obtained by interchanging of subscripts (m, f) in equations 5. The method employed by Hashin et al. involved Fourier transform operation whose mathematical rigour is not established. "It is however believed that the results are exact in the sense of statistics."

HILL (22) gave expressions for bulk and shear moduli of a two-phase composite with ellipsoidal inclusions. The method that he used takes account of the inhomogeneity of the stress and strain field, in a similar way to Hershey-Kröner theory of crystalline aggregates. The equations, with the notation adopted here are;

$$\frac{1}{K_c + \frac{4}{3}G_c} = \frac{c}{K_f + \frac{4}{3}G_c} + \frac{1-c}{K_m + \frac{4}{3}G_c}$$

$$\left[\frac{cK_f}{K_f + \frac{4}{3}G_c} + \frac{(1-c)K_m}{K_m + \frac{4}{3}G_c}\right] + 5\left[\frac{cG_m}{G_c - G_m} + \frac{(1-c)}{G_c - G_f}\right] + 2 = 0 \qquad 6.a$$

where the symbols have previous definitions.

HILL (26) derived inequalities between various moduli of composites with arbitrary phase geometries. Additionally exact solutions for the moduli are given when the phases have equal rigidities. The exact solutions are

$$E_c = \frac{cE_f + (1-c)E_m - E_fE_m/4G_m}{1-(cE_m+(1-c)E_f)/4G_m}$$

$$K_c = K_m + \frac{c(K_f - K_m)}{1+(K_f-K_m)(1-c)/(K_m+\frac{4}{3}G_m)} \qquad 6.b$$

$$\nu_c = \frac{c\nu_f + (1-c)\nu_m - \nu_m\nu_f}{1-c\nu_m - (1-c)\nu_f}$$

of course with $G_m = G_f = G_c$.

HILL (23) also found an exact solution for a composite reinforced with a cylindrical element, when the phases have equal transverse rigidities. The expression is

$$E_c = cE_f + (1-c)E_m + \frac{4c(1-c)(\nu_f - \nu_m)^2}{\frac{c}{K_m} + \frac{1-c}{K_f} + \frac{1}{G_m}} \qquad 6.c$$

Again equation 6c reduces to the law of mixtures when the Poisson's ratios of the phases are the same.

We shall begin to derive a new theory for fibre reinforced composites for arbitrary concentrations. Throughout the derivations it will be assumed that: a) Every fibre lies in a plane and all the planes are parallel to each other. b) Each phase alone is isotropic while the composite itself is anisotropic. c) The strain

field is neither homogeneous nor continuous (see the Deformation mechanism for the justification). d) The fibres have large aspect ratios so that they can sustain only axial loads. e) The matrix has a load-carrying capacity. The basic assumptions made by authors who used the three approaches described in section I.2 are: a) The material has transverse isotropy (12, 17, 20-23). b) The strain field is continuous (11-26). c) The boundary conditions are adjustable to express gross phase geometry (17-26). d) The matrix has load-carrying capacity (11-26). e) The fibres can sustain only axial loads (31, 34).

Furthermore a representative volume element (R.V.E) of the composite is defined with the following properties. It is a unit volume element of the composite such that it has the same properties as the composite and the directional physical constants are the same as the directional constants of the composite. Now a distribution function for fibres $\varphi(\theta)$ and its complementary function $\varphi^*(\theta)$ (which is the distribution function of the matrix) are introduced with the following property:

$$\int_0^{\pi} \varphi(\theta)d\theta + \int_0^{\pi} \varphi^*(\theta)d\theta = 1 \qquad 7.$$

This distribution function is representing the distribution of the volume of bundles of fibres (and is also propor-

tional to the number of the fibres which are perpendicular to their alignment) per unit thickness.

In most applications the thickness of the composite will be small compared to the other dimensions of it; thus it will not be unrealistic if one assumes that the system will be under plane stress state. This assumption makes the calculations easier, and reduces the number of independent variables of anisotropic media to five. Fig. 1.1 shows a fibre oriented at an angle of θ^{o} to the 1st axis within the R.V.E. To begin with, let σ_{ij} and ε_{ij} be the known stress and strain tensor fields in a deformed elastic body of volume unity and surface of S.

The axial strain of any fibre which is inclined θ^{o} to the 1st axis (which is also the strain of the composite and matrix) will be

$$\varepsilon_{rs} = a_{ir}a_{js}\varepsilon_{ij} \qquad 8$$

Now constant α^{*} is introduced to account for the adhesion efficiency between the two media. This constant is purely empirical and rising from the experimental evidence that the bond between metal and the plastics (polyethylene, propathene) breaks before any constituent element fails (ruptures). If there is a

perfect adhesion at the interface (in that case the plastic phase may rupture before the bond is broken) then the value of α is 1.0 and similarly no adhesion case is represented by $\alpha = 0.0$ (Thus the adhesion efficiency is the fractional value of the constant α).

Another variable β^* must be introduced to account for the inhomogeneity of the strain field, even though perfect adhesion does exist. An exaggerated picture is given in Fig.17 where strain inhomogeneity (strain concentration) is shown. For simplicity we let $\psi = \alpha\beta$. Of course in most general case ψ is a tensor quantity of second rank. But it gives great simplicity to the mathematical procedures if it is considered to be a constant.

Some authors (8,30,31) have introduced similar constants to modify the law of mixtures** (as in the case $E_y = (1-c)E_m + \psi c E_f$ second of eqn. 26). Therefore in the light of the forementioned arguments the introduction of ψ is justifiable both from technological and theoretical points of view. Thus the average strain sustained by the matrix is greater than the average strain within the metal phase. Therefore the effective strain within the fibre will be

---

* In general α, β are tensor quantitis but for simplicity they had been regarded as scalar.

** For more discussion see page 42.

$$\varepsilon'_{rs} = \psi\varepsilon_{rs} \qquad 9.$$

Consequently the stress within the fibre and the matrix will be

$$E_f\varepsilon'_{rs} = E_f\psi\varepsilon_{rs}, \qquad E_m\varepsilon_{rs} \qquad 10.$$

respectively.

To find the resultant stresses in the directions of 1, 2 (i.e. x, y) one has to find the distribution of the fibres which are along the respective axis. The resolution of the resultant forces along the axis must generate the stress field.* In mathematical terms the foregoing argument is

$$\sigma'_{kn} = \int_0^{\pi} (\psi E_f \varepsilon_{rs} \varphi(\theta)) a_{1k} a_{1n} d\theta \qquad k,n = 1,2 \qquad 11.$$

where (') stands for fibre. At this point using generalised Hooke's law with the LOVE's (28) notation** the stresses are related to the strains with the following coupling matrices

$$X_a = C_{ab} e_b \,, \quad e_a = S_{ab} X_b \qquad a,b = 1, 6 \qquad 12.$$

---

* The stress field which is found within the metal phase

** $X_1 = \sigma_{11}$, $X_2 = \sigma_{22}$, $X_3 = \sigma_{33}$, $X_4 = \sigma_{13}$, $X_5 = \sigma_{23}$, $X_6 = \sigma_{12}$

$e_1 = \varepsilon_{11}$, $e_2 = \varepsilon_{22}$, $e_3 = \varepsilon_{33}$, $e_4 = 2\varepsilon_{13}$, $e_5 = 2\varepsilon_{23}$, $e_6 = 2\varepsilon_{12}$.

where C_{ab} and S_{ab} are called stiffness and compliance matrices, and it must be recalled that both are symmetric. The plastic itself is assumed to be homogeneous and isotropic (within the composite). Hence under plane stress state the coefficient of the stiffness matrix for the resin itself can be obtained by transforming the well-known equations 13 in the matrix form.

$$\sigma_1 = \frac{E}{1-\nu^2}(e_1+\nu e_2)$$

$$\sigma_2 = \frac{E}{1-\nu^2}(e_2+\nu e_1) \qquad 13$$

$$\sigma_6 = \frac{E}{2(1+\nu)} e_6$$

Then one gets,

$$C^*_{ab} = \begin{vmatrix} \frac{E}{1-\nu^2} & \frac{\nu E}{1-\nu^2} & \cdot & \cdot & \cdot & \cdot \\ \frac{\nu E}{1-\nu^2} & \frac{E}{1-\nu^2} & \cdot & \cdot & \cdot & \cdot \\ \cdot & \cdot & \cdot & \cdot & \cdot & \cdot \\ \cdot & \cdot & \cdot & \cdot & \cdot & \cdot \\ \cdot & \cdot & \cdot & \cdot & \cdot & \cdot \\ \cdot & \cdot & \cdot & \cdot & \cdot & \frac{E}{2(1+\nu)} \end{vmatrix} \qquad 14.$$

where the dots stand for either insignificant or null terms, and (*) for the matrix.

The part of the stress field sustained by the matrix itself will be

$$\begin{vmatrix} X_1 \\ X_2 \\ X_6 \end{vmatrix} = \begin{vmatrix} \frac{1}{1-\nu^2} & \frac{\nu}{1-\nu^2} & \cdot \\ \frac{\nu}{1-\nu^2} & \frac{1}{1-\nu^2} & \cdot \\ \cdot & \cdot & \frac{1}{2(1+\nu)} \end{vmatrix} \times \begin{vmatrix} \int_o^\pi e_1 E_m \varphi^*(\theta) d\theta \\ \int_o^\pi e_2 E_m \varphi^*(\theta) d\theta \\ \int_o^\pi e_6 E_m \varphi^*(\theta) d\theta \end{vmatrix} \qquad 15.$$

Of course due to isotropy, equation 15 is invariant under any rotation or translation of the axes. For the fibres, however, the stiffness matrix coefficients must be calculated from the combination of equations 8, 11 and 12. Combining equations 8 and 11, one obtains

$$X'_{kn} = \int_o^\pi \psi E_f \varphi(\theta) a_{i1} a_{j1} e_{1j} a_{1k} a_{1n} d\theta \qquad k,n=1,2, \qquad 16.$$

With the notation adapted and making use of equation 12. the terms of the stiffness matrix are found as follows

$$C'_{11} = E_f \int_o^\pi \psi\varphi(\theta) a_{11}^4 d\theta$$

$$C'_{12} = E_f \int_o^\pi \psi\varphi(\theta) a_{11}^2 a_{21}^2 d\theta$$

$$C'_{16} = E_f \int_o^\pi \psi\varphi(\theta) a_{11}^3 a_{21} d\theta$$

$$C'_{21} = E_f \int_o^\pi \psi\varphi(\theta) a_{11}^2 a_{12}^2 d\theta$$

$$C'_{22} = E_f \int_o^\pi \psi\varphi(\theta) a_{21}^2 a_{12}^2 d\theta \qquad 17.$$

$$C'_{26} = E_f \int_o^{\pi} \psi\varphi(\theta) a_{12}^2 a_{11} a_{21} d\theta$$

$$C'_{66} = E_f \int_o^{\pi} \psi\varphi(\theta) a_{12}^2 a_{11}^2 d\theta$$

where (') stands for the metal phase, and with the usual understanding of $-a_{12}=a_{21} = \sin\theta$, $a_{22}=a_{11}=\cos\theta$ for the planar cartesian coordinates.

For the composite itself the equation 12 holds, and its stiffness matrix can be written as the sum of two matrices.

$$X_t = C_{tr} e_r = (C'_{tr} + C^*_{tr}) e_r \qquad 18.$$

Combining equations 15, 17, 18 one gets the coefficient of the stiffness matrix for the composite. They are

$$C_{11} = \frac{1}{1-\nu^2} E_m \int_o^{\pi} \varphi^*(\theta) d\theta + E_f \int_o^{\pi} \psi\varphi(\theta) a_{11}^4 \, d\theta$$

$$C_{12} = \frac{\nu}{1-\nu^2} E_m \int_o^{\pi} \varphi^*(\theta) d\theta + E_f \int_o^{\pi} \psi\varphi(\theta) a_{11}^2 a_{21}^2 d\theta$$

$$C_{16} = E_f \int_o^{\pi} \psi\varphi(\theta) a_{11}^3 a_{21} d\theta$$

$$C_{21} = \frac{\nu}{1-\nu^2} E_m \int_o^{\pi} \varphi^*(\theta) d\theta + E_f \int_o^{\pi} \psi\varphi(\theta) a_{11}^2 a_{12}^2 d\theta \qquad 19.$$

$$C_{22} = \frac{1}{1-\nu^2} E_m \int_o^{\pi} \varphi^*(\theta) d\theta + E_f \int_o^{\pi} \psi\varphi(\theta) a_{12}^2 a_{21}^2 d\theta$$

$$C_{26} = E_f \int_o^{\pi} \psi\varphi(\theta) a_{12}^2 a_{11} a_{21} d\theta$$

$$C_{66} = \frac{1}{2(1+\nu)} E_m \int_o^{\pi} \varphi^*(\theta)d\theta + E_f \int_o^{\pi} \psi\varphi(\theta)a_{12}^2 a_{11}^2 d\theta$$

or, in engineering terms, the Young's and shear moduli of the composite in terms of these coefficients are given by

$$E_x = C_{11}\lambda, \quad E_y = C_{22}\lambda, \quad G_{12} = C_{66} \qquad 20.$$

$$\nu_{12} = C_{12}/C_{11} \quad \nu_{21} = C_{12}/C_{22} \quad \lambda = 1-\nu_{12}\nu_{21}$$

The coefficients from equation 19 can be evaluated of course only if ψ and $\varphi(\theta)$ are given; in other terms, if the distribution function of the fibres and the bondage efficiency are known throughout the composite, the directional physical constants can be obtained from equation 20.

The moduli of various types of reinforced composites will be evaluated and compared with the existing theories. Particular reference will be made to unidirectional, cross-reinforced and random types of composite materials. Furthermore, physical constants will be obtained for helically wound pipes and hoses.

2.1 UNIDIRECTIONAL REINFORCING

In this particular type of reinforcement all the fibres are parallel and supposed that they are not touching each other. Assuming the cross-sections are circular and

have equal diameters the maximum volumetric concentration can be worked out for any type of fibre orientation. Fig. 1.2 shows a cross-section of unidirectionallly reinforced composite. The element KLMN is a repeating one and it can be assumed to be the Representative Volume Element (the unit thickness is not shown in the figure). The volumetric concentration of fibres is obtained by dividing the total area occupied by the fibres by the cross-sectional area of R.V.E. It is

$$c = \frac{\pi D^2}{4S^2} \qquad 21.$$

where D and S are diameter and interspacing distance between the fibres respectively. Note that as $S \to D$ the maximum volumetric concentration obtained as 78.4 percent. This type of packing the fibres is called 'loose pack'. Another type of packing is called 'close pack' or 'hexagonal array' which is shown in Fig. 1.3. Here the R.V.E. is ABC. The concentration ratio is obtained as

$$c = \frac{\pi D^2}{2\sqrt{3}S^2} \qquad 22.$$

Maximum volumetric concentration of fibres is achieved by setting S=D; and it is 90.8 percent. Of course in theory if the diameter of the fibres is not equal, these maximum concentration ratios can be increased. In practice, beyond 60 percent reinforcing the properties

of the composite deteriorates.

For any kind of orientation the material is orthotropic (symmetrical with respect to xy, xz, yz, planes). Unfortunately there is no real function to be used as the distribution function of the fibres. However a function of $\varphi(\theta)$ can be defined analogous to DIRAC-delta function as follows:

$$\varphi(\theta) \begin{cases} = 0 & 0 < \theta < \frac{\pi-\varepsilon}{2} \\ = \frac{c}{\varepsilon} & \frac{\pi-\varepsilon}{2} \leq \theta \leq \frac{\pi+\varepsilon}{2} \\ = 0 & \frac{\pi+\varepsilon}{2} < \theta < \pi \end{cases} \qquad 23.$$

with the following properties

$$\int_0^\pi \varphi(\theta)d\theta = c$$

$$\int_0^\pi \varphi(\theta)G(\theta)d\theta = cG(\pi/2) \qquad 24.$$

$$\int_0^\pi \varphi(\theta-a)G(\theta)d\theta = cG(\frac{\pi}{2} - a)$$

for any continuous function of $G(\theta)$. Now assuming that ψ is independent of θ and using the definition of $\varphi^*(\theta)$ from equation 7, together with equation 24, after integration of equations 19, the coefficients of stiffness matrix are obtained as follows

$$C_{11} = \frac{1-c}{1-\nu^a} E_m$$

$$C_{12} = C_{21} = \frac{(1-c)\nu}{1-\nu^2} E_m$$

$$C_{22} = \frac{1-c}{1-\nu^2} E_m + \psi c E_f \qquad 25.$$

$$C_{66} = \frac{1-c}{2(1-\nu)} E_m$$

$$C_{16} = C_{26} = 0$$

The directional physical constants are obtained from the solution of equations 25 and 20, as

$$E_x = \frac{1-c}{1-\nu^2} E_m \left[1 - \frac{(1-c)\nu^2 E_m}{(1-c)E_m + (1-\nu^2)c\psi E_f}\right]$$

$$E_y = (1-c)E_m + \psi c E_f \qquad 26.$$

$$G_{xy} = \frac{(1-c)}{2(1+\nu)} E_m$$

In the case of $\psi = 1.0$ (which its max. value is 1) the second of equation 26 reduces to the equation $E_y = (1-c)E_m + cE_f$ which is found in the literature (2, 6, 8, 10-18, 23, 30). Dividing both sides by E_m of equations 26, we have (in the direction of reinforcement)

$$\frac{E_y}{E_m} = (1-c) + \psi c \frac{E_f}{E_m} \qquad 27.$$

which is perhaps a single equation to describe the Young's modulus of the composite for different states of constituent elements (such as elastic fibre, elastic resin,

elastic fibres, plastic resin, plastic fibre, plastic resin). The gradient of the straight line depends on the strain transfer coefficient (ψ) as well as on the volumetric concentration of the fibres. Thus the corners in the stress/strain curve of a reinforced plastics can be explained in the best way by the different values that ψ assumes (see the deformation mechanism).

The transverse and shear moduli E_x, G_{xy}, are affected slightly due to the presence of the fibres. Furthermore if $E_f = E_m$, then the composite has constants of $E_x = E_y = E_m = E_f$. Shaffer (15) derived an expression for transverse Young's modulus in his "strength of materials type of approach" which is differing from the first of equations 26 by a factor of slightly more than two. However, there is no experimental evidence given to support his theory, and in fact if there is for glass-fibre reinforced plastics, it is very doubtful that it can be generalised to metallic fibre composites, where the fibres have high E_f / E_m ratios compared to glass fibres. Baer (29) quotes that "A fibre provides reinforcement primarily in a direction parallel to the fibre. In direction perpendicular to the fibre, either its effect is negligible or it may be detrimental to the ultimate strength and fracture strain of the composite". Hence E_x and G_{xy} expressions obtained above

are in agreement with the above statement.

The moduli at an arbitrary direction, say at a direction which makes an angle of $(\frac{\pi}{2}-\lambda)$to the fibres, can be found by using the property of the defined impulse function (third of equations 24). The constants of the stiffness matrix are evaluated through the equations 7, 19 and 24. The results are;

$$C_{11} = \frac{1-c}{1-\nu^2} E_m + \psi c E_f \cos^4\lambda$$

$$C_{12} = C_{21} = \frac{(1-c)\nu E_m}{1-\nu^2} + \psi c E_f \sin^2\lambda \cos^2\lambda$$

$$C_{16} = \psi c E_f \cos^3\lambda \sin\lambda$$

$$C_{22} = \frac{1-c}{1-\nu^2} E_m + \psi c E_f \sin^4\lambda \qquad 27$$

$$C_{26} = \psi c E_f \sin^3\lambda \cos\lambda$$

$$C_{66} = \frac{1-c}{2(1+\nu)} E_m + \psi c E_f \sin^2\lambda \cos^2\lambda$$

and the Young's modulus along this direction is

$$E_\lambda = C_{11} + \frac{C_{12}(C_{16}C_{26}-C_{12}C_{66})+C_{16}(C_{12}C_{26}-C_{16}C_{22})}{C_{22}C_{66}-C_{26}^2}$$

28

Note that equation 28 yields the first of the two equations 26 when λ has the values of 0 and $\frac{\pi}{2}$ respectively.

The maximum value of E_λ occurs at $\lambda = \frac{\pi}{2}$ which is logical. The variation of E_λ versus fibre orientation angle 'λ' is shown in G.1.1.

Comparison of the theories found in the literature and the one derived here for the unidirectional reinforced composites is given in G.1.2 and Table 1.1.

2.2 CROSS REINFORCEMENT

Fig. I.4 shows a model of wire mesh reinforcing. If P is the distance between two wire meshes then the volumetric concentration ratio is found as described in section 2.1. This is

$$c = \frac{\pi D^2}{2SP}$$

c has its largest value when $P \rightarrow 2D$ and for the case where $\frac{D}{S} = \frac{1}{3}$; the maximum value of c obtained to be 26.2 percent. With this type of reinforcing, one implicitly assumes that equal amount of fibres are found in x, y directions. With the help of this information, the distribution function $\varphi(\theta)$ can be assumed to be composed of two pulse functions, with the following properties,

$$\varphi(\theta) = \varphi^1(\theta) + \varphi^2(\theta) \qquad 30\text{-a}$$

where

$$\varphi^1(\theta) = 0 \quad \varepsilon < \theta < \pi/2$$
$$= \frac{c}{2\varepsilon} \quad 0 \leq \theta \leq \varepsilon$$

Specifications for the Matrix and Fibre.

Theory	Composite	E_f/E_m	ν_m	ν_f	c	E_c/E_m	Remarks
HILL Ref.(23)	Polythene/ Steel	1000	.5	.333	.5	500.509	In the direction of reinforcement
WHITNEY Ref. (12)	"	"	"	"	"	500.509	"
McDANELS Ref. (13)	"	"	"	"	"	500.500	"
THE PRESENT for ψ=1.0	"	"	"	"	"	500.500	"
THE PRESENT for ψ = .8	"	"	"	"	"	400.500	"
THE PRESENT for ψ = .7	"	"	"	"	"	350.500	"

TABLE 1.1. Comparison of the theories for 50% unidirectional reinforcement.

$$\varphi^2(\theta) = \frac{c}{2\varepsilon} \qquad \frac{\pi}{2} \leq \theta \leq \frac{\pi}{2} - \varepsilon$$
$$= 0 \qquad 0 < \theta < \frac{\pi}{2} - \varepsilon \qquad \text{30-b}$$

$$\int_0^{\pi} \varphi^1(\theta)d\theta = \frac{c}{2}$$

$$\int_0^{\pi} \varphi^2(\theta)d\theta = \frac{c}{2}$$

$$\int_0^{\pi} \varphi^1(\theta)G(\theta) = G(0) \cdot \frac{c}{2}$$

$$\int_0^{\pi} \varphi^2(\theta)G(\theta) = G(\tfrac{\pi}{2}) \cdot \frac{c}{2} \qquad 31$$

$$\int \varphi^1(\theta)G(\theta-\lambda) = \frac{c}{2}G(-\lambda)$$

$$\int \varphi^2(\theta)G(\theta-\lambda) = \frac{c}{2}G(\tfrac{\pi}{2} - \lambda)$$

Introducing the equations 30-31 into equations 19, the constants are obtained as follows,

$$C_{11} = C_{22} = \frac{1-c}{1-\nu^2} E_m + .5\psi c E_f$$

$$C_{12} = C_{21} = \frac{1-c}{1-\nu^2} E_m$$

$$C_{66} = \frac{1-c}{2(1+\nu)} E_m \qquad 32$$

$$C_{16} = C_{26} = 0$$

where the Young's and rigidity moduli are obtained readily and they are,

$$E_x = E_y = \frac{1-c}{1-\nu^2} E_m + .5c\psi E_f - \frac{(1-c)^2\nu^2 E_m^2}{(1-\nu^2)(1-c)E_m + .5(1-\nu^2)\psi c E_f}$$

$$G_{xy} = \frac{(1-c)E_m}{2(1+\nu)} \qquad 33.$$

Note that as $c \to 0$ the equations 24, 28 give the physical constants of the resin. To the best knowledge of the author there is no theoretical work published on this type of reinforcement. However, it seems to be a logical outcome to think that first of equations 33 will be roughly half of the value of that second of equations 26, due to equal share of fibres in two orthogonal directions. The variation of the Young's modulus with respect to volumetric concentration is given in G.1.3.

The Young's modulus at any direction can be obtained by carrying out similar calculations as in the case of unidirectional reinforced composite; the coefficients of the stiffness matrix are found to be

$$C_{11} = C_{22} = \frac{1-c}{1-\nu^2} E_m + .5\psi c E_f [\cos^4\lambda + \sin^4\lambda]$$

$$C_{12} = C_{21} = \frac{\nu(1-c)}{1-\nu^2} E_m + \psi c E_f [\sin^2\lambda \cos^2\lambda]$$

$$C_{16} = C_{26} = .5c\psi E_f [\cos^3\lambda \sin\lambda + \sin^3\lambda \cos\lambda]$$

$$C_{66} = \frac{(1-c)E_m}{2(1+\nu)} + \psi c E \sin^2\lambda \cos^2\lambda \qquad 34$$

and the directional Young's modulus will be

$$E_\lambda = C_{11} + \frac{C_{12}(C_{16}C_{26}-C_{12}C_{66})+C_{16}(C_{12}C_{26}-C_{16}C_{22})}{(C_{22}C_{66}-C_{26}^2)}$$

Again, the last of equations 34 yields the first of equations 33 for the values of 0, or $\frac{\pi}{2}$ of λ. Of course this is due to the fact that the composite has three axes of symmetry, namely at 0, $\frac{\pi}{4}$ and $\frac{\pi}{2}$. The variation of E_λ versus the orientation angle λ is shown in G.1.4.

2.3 'RANDOMLY DISTRIBUTED FIBRES' REINFORCEMENT

The fibres are assumed to be found in the same amount in any direction; thus the distribution functions are continuous functions of concentration ratio of c, and are independent of (θ). They are

$$\varphi(\theta) = \frac{c}{\pi}, \qquad \varphi^*(\theta) = \frac{1-c}{\pi} \qquad 35$$

Substituting Eqns. 35 into Eqns. 19 one gets

$$C_{11} = C_{22} = \frac{1-c}{1-\nu^2} E_m + \frac{3c}{8} \Psi E_f$$

$$C_{21} = C_{12} = \frac{(1-c)\nu E_m}{1-\nu^2} + \frac{c}{8} \Psi E_f$$

$$C_{16} = C_{26} = 0 \qquad 36$$

$$C_{66} = \frac{E_m}{2(1+\nu)} (1-c) + \frac{c}{8} \Psi E_f$$

The moduli are

$$E_x = E_y = \frac{1-c}{1-\nu^2} E_m + \frac{3c}{8} \psi E_f - \frac{(\frac{1-c}{1-\nu^2} \nu E_m + \frac{c}{8} \psi E_f)^2}{(\frac{1-c}{1-\nu^2} E_m + \frac{3c}{8} \psi E_f)}$$

$$G_{xy} = \frac{(1-c)E_m}{2(1+\nu)} + \frac{c}{8} \psi E_f \qquad 37$$

Since the distribution function is independent of orientation angle θ, the Young's and shear moduli are constant throughout the plane x,y.

Note that as $c \rightarrow 0$ the equations 37 reduce to $E_x = E_y = E_m$ and $G_{xy} = G_m$.

Comparison of the theories found in the literature and the one derived here for the randomly distributed fibres reinforcement is given in G.1.5. Note also that when there is a planar mat of fibres (no resin case, which is impossible for plastic/fibre systems) and ψ=1.0 equation 37 yields the expressions given by COX (31). They are

$$E_x = E_y = \frac{E_f}{3} \; ; \qquad G_{xy} = \frac{1}{8} E_f .$$

2.4 APPLICATION OF THE THEORY TO 'HELICALLY WOUND, METAL-FIBRE REINFORCED THIN-WALLED CYLINDERS'.

Fig. 1.5 shows a cylinder under internal pressure P, For simplicity, a single fibre with a helix angle λ is shown on it. The axial and circumferential stresses are given by well-known equilibrium conditions. For

plane stress state the stresses are,

$$\sigma_x = \frac{PR}{2t} \quad , \quad \sigma_\theta = \frac{PR}{t} \quad , \quad \sigma_t = 0 \qquad 38$$

where R and t are radius and thickness of the cylinder respectively.

It is clear from equation 38 that if the failure of cylinder occurs in tension; it will be due to σ_θ approaching the yield stress of the composite. Assuming that composite fails at certain value of strain in any direction, one has

$$\sigma_x = \frac{PR}{2t} = E_x \varepsilon^y \quad , \quad \sigma_\theta = \frac{PR}{t} = E_y \varepsilon^y \qquad 39$$

where ε^y is the yield strain of the composite. Eliminating ε^y from the equations 38 one gets

$$E_y = 2E_x \qquad 40$$

Thus if the equation 40 is satisfied, failure of the cylinder may occur at any principal direction.

The equations of fibres in parametric form in three dimensions are

$$\begin{aligned} x &= R \cos \theta \\ y &= R \sin \theta \\ z &= R\theta \tan \lambda \end{aligned} \qquad 41$$

where λ is called the helix angle.

The length of a line segment such as AB (in Fig.I.5) is given by

$$AB = \int_{\theta_1}^{\theta_2} ds = \int_{\theta_1}^{\theta_2} (dx^2+dy^2+dz^2)^{\frac{1}{2}} d\theta = \int_{\theta_1}^{\theta_2} R\sec\lambda\, d\theta \qquad 42$$

As the geometry of the reinforcement is uniform, it is enough to consider a unit height of the cylinder. Let the average diameter of the fibres be 2r, then the volume occupied by the continuous (n) fibres will be

$$n\pi r^2 L \qquad 43$$

where L is the length of the fibre. Thus the volumetric concentration is given by

$$c = \frac{n\pi r^2 \int_0^{2\pi} R\sec\lambda\, d\theta}{2\pi Rt} = \frac{\pi r^2 \operatorname{cosec}\lambda}{2Rt} \qquad 44\text{-a}$$

or

$$c = a \operatorname{cosec}\lambda \qquad a = \frac{nr^2}{2Rt} \qquad 44\text{-b}$$

where R, t are the mean radius and the thickness of the thin-walled cylinder respectively. And 'a' is constant for any particular reinforcement. For close and loose packing* the maximum volumetric concentrations are 90.5 and 78.7 percent respectively.

To use the composite in the most efficient way the equation 40 must be satisfied. For this, a general rela-

---

* The number of fibres is a function of λ which is $\pi D/K\sin\lambda$ where K is the distance between the axis of two fibres. For maximum cases K=t = 2r.

tionship between fibre orientation, fibre concentration, and the physical constants of the constituent elements will be derived. If the fibres are parallel to each other and have a particular orientation, the distribution function is again a pulse function with the following properties

$$\varphi(\theta) = 0 \quad \lambda + \frac{\varepsilon}{2} < \theta < \frac{\pi}{2}$$

$$= \frac{c}{\varepsilon} \quad \lambda - \frac{\varepsilon}{2} \leq \theta \leq \lambda + \frac{\varepsilon}{2}$$

$$= 0 \quad 0 < \theta < \lambda - \frac{\varepsilon}{2}$$

$$\int_0^{\pi} \varphi(\theta)d\theta = c \qquad 45$$

$$\int_0^{\pi} \varphi(\theta)G(\theta)d\theta = cG(\lambda)$$

$$\int_0^{\pi} \varphi(\theta-a)G(\theta)d\theta = cG(\lambda-a)$$

Using the equations 19 and 45 and carrying out the necessary operations, one gets equations 27. Recalling equations 20 the followings are written immediately:

$$C_{11} = 2C_{22}$$

$$T^4 + 2T^2 + PT - (aP+1) = 0 \qquad 46\text{-a}$$

where

$$T = \sin\lambda, \quad P = \frac{E_m}{aE_f(1-\nu^2)\psi}, \quad a = \frac{nr^2}{2Rt} \qquad 46\text{-b}$$

Of course equation 46-a including the volumetric concentration of the fibres has the following form:

$$(T^2+1)^2 - 2 + \frac{1-c}{c\psi(1-\nu^2)} \frac{E_m}{E_f} = 0 \qquad 47$$

As it is clear from the equation 47, below certain values of 'c' there is no solution to the problem; hence it is necessary to find bounds for the concentration. They can be found by simply satisfying the inequality of

$0 \leq T^2 \leq 1$. For real material these are found to be

$$1 \geq c \geq \frac{1}{1+\psi(1-\nu^2)\frac{E_f}{E_m}} \qquad 48$$

The variation of λ versus the concentration ratio is shown in G.1.6. Maximum orientation angle of the fibres obtained when $\frac{E_m}{E_f}$ approaches zero. In this case the value of helix angle is 40 degrees.

In some literature (33) it has been suggested that the reinforcing cords are inextensible and carry all the load (matrix has no load carrying capacity). Thus the helix angle (for the most efficient use of fibres) can be calculated from the equilibrium conditions. The equilibrium condition provides

$$\cos\lambda - 2\sin\lambda = 0 \qquad 49$$

which gives $\lambda = 26^{o}36'$.

For this case, the volumetric concentration is calculated from the maximum allowable stress. And the helix angle is independent of the concentration ratio of the fibres.

The variation of hoop and axial stiffnesses versus orientation angle λ are given in G.1.7. A substantial agreement of this theory with the experimental results given by TSAI (32) is obtained. For 40 percent reinforced, helically wound glass-epoxy composite ($\frac{E_f}{E_m} = 10$) the helix angle is obtained to be 35^{o} from both experiment (32) and the above theory, if the ratio of the hoop to the axial stiffness is 2.0.

2.5 ULTIMATE STRENGTH OF A COMPOSITE

In most cases the designer is interested in the ultimate strength of a material as well as in its physical constants. For multiphase materials there is as yet no convention for the definition of ultimate strength. Therefore, here, it is defined as follows - 'The ultimate strength of a composite is the strength attained when one of the phases reaches its ultimate yield strain' - Under crude assumption* numerical values for the ultimate strength of different types of reinforcement can be obtained from the corresponding formulae given for the

---

* One of the Young's modulus is replaced by the ratio of ultimate strength to the ultimate strain.

Young's modulus of the composite. As an example consider unidirectional reinforcement; from equation 26 we have

$$E_c = (1-c)\, E_m + \psi c E_f$$

dividing both sides by $e_m = e_c = \frac{e_f}{\psi}$, one has

$$\sigma_c = (1-c)\sigma_m + \psi^2 c \sigma_f$$

(for $\psi = 1$.) This expression is given by many authors (1, 2,6,7,8,14,16,29,30,51,53). In the same way similar expressions can be obtained for other types of reinforcement.

3.0 DEFORMATION MECHANISM

In a typical stress strain curve of fibre-strengthened composite, generally there are three regions in which the constituent elements behave differently. In the first region, both the plastic and the metal phases are in the elastic state. The stresses within the composite can be evaluated by simply replacing E_m and E_f with $\sigma_m, \psi\sigma_f$. This region extends to the point where one of the phases reaches the plastic state. In the second region the reinforcing phase is still in the elastic state. To evaluate the constants of the composite, one has to substitute the gradient of the stress/strain curve as the current Young's modulus of the ductile phase (matrix) to the above formulae. The average stress within the composite is evaluated by replacing the moduli with the stresses of the corresponding phases for the same strain. By further application of load, the fibre phase also reaches to plastic state. The composite fails when the

fibres break. The ultimate breaking stress is evaluated from the derived formulae by substituting the ultimate stress of the fibres and the corresponding stress within the matrix itself, i.e. the ultimate strength of an uniformly distributed fibre reinforced composite, is

$$\sigma_c = \frac{\left(\frac{1-c}{1+\nu}\sigma_m + \frac{c}{2}\psi^2\sigma_f\right)\left(\frac{1-c}{1-\nu}\sigma_m + \frac{c}{4}\psi^2\sigma_f\right)}{\left(\frac{1-c}{1-\nu^2}\sigma_m + \frac{3c}{8}\psi^2\sigma_f\right)} \qquad 63$$

The composite ruptures if the work hardening of the matrix is not sufficient to resist the applied load, when the brittle phase breaks. This implicity defines a critical volumetric concentration for the reinforcement, which can be formulated as,

$$\sigma_c > \sigma_u^m (1-c)$$

or $$c > 1 - \frac{\sigma_c}{\sigma_u^m} \qquad 64$$

where σ_u^m is the ultimate strength of the matrix.

The overall strain transfer efficiency coefficient ψ has different values in the above three zones of deformation. An explanation is given below.

I. Elastic matrix,elastic fibre. Fig. I.6 shows a fibre embedded in the matrix. The shear stress evaluated at the interface $r=r_o$ is maximum at the end of the fibre ($z=0$) and it decreases as z increases. Since the shear stress is not constant, the axial stress within

the fibre builds up gradually (30). Different envelopes for the stress build up were considered (30-31) for the evaluation of average load carried by a fibre. The result obtained by COX (31) is

$$P = E_f A e \left[1 - \frac{\tanh(\zeta \ell/2)}{\zeta \ell/2}\right] \qquad 65$$

$$\zeta = \left[2G_m/E_f r_o^2 \log_e \left(\frac{r_1}{r_o}\right)\right]^{\frac{1}{2}}$$

where r_1, r_o are the radii of the matrix and fibre respectively and G_m is the shear modulus of the matrix, and A, e are cross-sectional area of the fibre and the applied strain respectively.

Recasting the equation 65 one has

$$\frac{P}{AE_f} = e\left[1 - \frac{\tanh(\zeta \ell/2)}{(\frac{\zeta \ell}{2})}\right] \qquad 66$$

which the left-hand side is the actual average strain within the fibre. This justifies the introduction of β as a coefficient to account for the microscopic strain differences between the matrix and the fibre. See Fig. 1.7. Furthermore, since the adhesion between two media is not perfect, the coefficient α had been introduced to account for this. Equation 65 is not applicable when the matrix is in plastic state, because when the shear stress at the interface reaches the magnitude of the yield stress in shear, of the matrix, the axial

stress function becomes monotonic, hence the build up ceases. The maximum value that ψ can have is given by the expression in brackets in the equation 66.

The variation of ψ (for the case $\alpha = 1$) for different types of composites is shown in Table 1.2.

Composite	E_f/G_m	ψ(max)	Aspect ratio (a)	E_f/G_m	ψ(max)	Composite
Tungsten/ copper	10	.8138	10	750	.1111	Alum/L.D.P.
		.9069	20		.3183	
		.9535	40		.6025	
		.9767	80		.7985	
		.9884	160		.8992	
		.9934	280		.9424	
		.9942	320		.9496	
		.9959	450		.9642	
		.9971	640		.9748	
Iron/ propathene	240	.2710	10	1200	.0731	Bronze/M.D. Polyethylene
		.5551	20		.2318	
		.7720	40		.5099	
		.8860	80		.7452	
		.9430	160		.8725	
		.9674	280		.9272	
		.9715	320		.9363	
		.9797	450		.9547	
		.9857	640		.9681	

Table 1.2.

(The values are given for 25 percent fibre concentration and $\frac{r_o}{r_1} = \sqrt{c} = .5$).

II. Plastic media. Elastic fibre. Further application of load causes the matrix to deform plastically; the load transfer between two media is done by the shear stresses along the interface, thus the load build up gradient is more or less constant and it is,

$$\frac{de}{dz} = 2\pi r_o \tau_{rz} \qquad 67$$

where τ_{rz} is the yield stress in shear of the matrix. If the work hardening effects are small so that τ_{rz} is constant, the integration of equation 67 gives the load that can be transferred to the fibres. This is

$$P = 2\pi r_o z \tau_{rz}$$

or

$$\sigma_{zz} = \frac{2\tau_z}{r_o} \qquad 68$$

The fibre also reaches the plastic state as σ_{zz} approaches the yield strength value. The value of 'z' is called the critical length [in some works (4,16,30), $\frac{z}{2r_o}$ is named as critical aspect ratio].

The average stress within the fibre is calculated from the equation 69

$$\frac{1}{\ell} \int_o^p \sigma_{zz}\, dz \qquad 69$$

Combining equations 68 and 69, one obtains an effective stress within the fibre as;

$$\bar{\sigma}_f = \frac{\sigma_f}{\ell}(\ell-\ell_c) + \frac{\sigma_f \ell_c}{2\ell} = \sigma_f\left(1-\frac{\ell_c}{2\ell}\right) \qquad 70$$

Of course, this is true when one assumes linear stress build up. As it is clear from equation 70, in the case of perfect adhesion ψ^2 has the value in brackets in equation 70.

As a conclusive statement to the nature of the strain transfer efficiency coefficient one may write in general

$$\psi = f(E_f, E_m, \ell, d, c, \alpha) \qquad 71$$

where the symbols have the previous definitions. Of course α depends entirely on the molecular distance and surface conditions as well as impurities at the interface of the two media. It can be determined purely by experiments or from the fact that when β and ψ are known the value of α is the ratio of ψ/β.

III. Plastic matrix, plastic fibre. When the composite reaches complete plastic state, the interreaction of fibres becomes appreciable, due to large deformations; thus the coefficient β decreases in magnitude. This sharp decrease in β creates a corner in the stress/strain curve for high volumetric concentrations. Although in some cases it is possible to determine the value of ψ, it is easier and more reliable, if it is found from small number of experiments.

The type of experiments that can be made for this assessment are found in the work by KELLY, A, TYSON,W.R. (16).

PART II.a

EXPERIMENTAL METHODS, COLD ROLLING OF PLASTICS AND COMPOSITES

1.0 MANUFACTURING PROCESS OF REINFORCED PLASTICS

Generally there are four methods of fabricating two phase materials: a) liquid infiltration of the matrix; b) injection; c) powder metallurgy processes; d) physico - chemical process. The first method has found widest application within glass-fibre reinforced plastics manufacturing. Copper/tungsten (16), plastics/sapphire (50) systems were also produced with the same technique for experimental purposes. Injection moulding is used where good surface finish and homogeneity are required. However, this process limits the maximum length and the concentration of glass fibres used, and thus limits the maximum strength obtainable. Powder metallurgy processes have been used to fabricate aluminium/steel (51) and plastics/metal [the author] composites. With this method, the fibres are placed in a mould with the matrix in powder, flake or granular form, and then the mixture is hot pressed. With the last method the fibres are formed directly within the matrix with sophisticated physical and chemical processes. Most of the plastics/metal systems produced within the course of this research were by compression moulding, which is economical for small quantity production.

The magnitude of pressure used for fabrication changes considerably from process to process, the range that is used now is between 0 - 12,000 psi. The higher the pressure the more costly is the tooling and running cost of the set up, but the better surface finish and homogeneity of the composite. The temperature range is between 0-210°C. For thermo-setting plastics, generally the application of heat cuts the necessary curing time of the resin, and the variation in temperature during the process - provided it is below a certain limit - do not become a problem. However, for thermoplastics the right processing temperature is necessary because the viscosity and interadhesion of the resin itself are functions of it.

Overheating of the resin causes the plastic to degrade which subsequently produces a higher density of gas bubbles trapped near the fibres. This is detrimental to the properties of the material, and must be eliminated, or at least minimized, if the composite is to be used to its fullest extent.

An extensive account of information about the manufacturing process of glass fibre reinforced plastics are found in the literature, (29, 52, 53, 54), where metal fibre reinforced plastics are either unknown or they are in the research and development stages.

One of the aims of this work was to combine the most commonly known and cheap plastics with the cheapest fibres found on the market, to produce composite at costs where many industrial applications can be afforded. To this aim polythene (low, medium, high density), propathene (polypropylene) which were supplied by I.C.I. were combined with aluminium bronze and steel fibres (supplied by Brillo). The cross-sections of the fibres were not necessarily uniform and circular.

Table 2.1 shows the information about the dimensions of the fibres supplied by the manufacturers. Fig. 2.4, 2.12, 2.13, show the cross-section of randomly distributed fibres type of composites. It is clear from the photographs (taken under microscope) and from the Table 2.1 that the fibres can be assumed to be circular in cross-section. Some irregularities in the cross-section contributes towards better mechanical gripping of the two media but also disturbs the strain field. However it is believed that inhomogeneity of the strain field contributed by these irregularities in the cross-section does not play a great role in determining the strain transfer efficiency coefficient.

Material	ℓ/d	Min-Max width x 10^{-3} in.	Min-Max thickness x 10^{-3} in.
BRONZE	∞	2. - 2.3	2. - 2.4
STEEL	∞	2. - 2.3	2. - 2.4
ALUMINIUM	∞	8. - 9.0	8. - 9.0

Table 2.1. Fibre dimensions and specifications supplied by Brillo. Monu. Comp.

The information about the physical properties of the forementioned plastics supplied by I.C.I. is tabulated in Table 2.2. Copper and iron wire meshes were also incorporated with propathene. Angular testing of the meshes are given in G2.1, G2.2 [Angle measured from one of fibre directions].

A general idea can be obtained from Fig. 2.1 about the type of compression moulding which was used for the production of the specimens. A plastics layer was put into the female die, either in granular or sheet form; a planar mat, prepared from the fibres was pressed against preheated plastics of the right quantity. Then the mould was heated to the right temperature. After a certain period of time the system was cooled under slight pressure to ensure warping and bending did not occur. A method of layering the constituents was also used with high density polythene (G 2). Programmes of moulding processes were

found experimentally for the elimination of air traps and for good distribution of fibres. Approximate figures for applied pressure preheating, moulding temperature, and the duration of pressure are given in Table 2.3.

Material	Density gr/cm^3	U.Strength psi	Young's Modulus† psi	Elongation at break %
L.D. Polythene	.915	1820	4.0×10^4	550-600
M.D. Polythene	.922	2050	4.5×10^4	500-560
H.D. Polythene**	.934	2100	11.0×10^4	450-500
Propathene	.905	5000	31.0×10^4	210-240
Alum. Wool*	2.70	31000	10.3×10^6	-
Bronze Wool*	8.83	89300	18.6×10^6	-
S.Steel Wool*	7.72	130000	30.5×10^6	-
Copper Mesh	10.40	40250	15.6×10^6	26
Iron Mesh	7.95	56700	26.6×10^6	15
Copper Wire	10.40	36300	15.6×10^6	25

Table 2.2

It was found that for polythene the heat had to be applied from the bottom plate to avoid air trapping within

---

* The properties of the material from which the fibres are produced.

† For plastics it is .10 percent secant modulus, under .2 in/min testing speed.

** Measured quantities for the moulded plastics as supplied by I.C.I. (code , G.2)

the composite, while for polypropylene two faces of the die had to have nearly the same temperatures. The pressure was applied by a 100-ton capacity Denison testing machine. The temperature was controlled by a servotronik temperature indicator/controller. After maintaining the pressure and heat to the prescribed time the mould was left to cool under a pressure of 200 psi. Fig. 2.2 shows the actual set-up for moulding reinforced plastics. Fig. 2.3 shows composites removed from the mould.

MATERIAL	PRE-HEATING TEMP. ^{o}C	MOULDING TEMP. ^{o}C	PRESSURE APPLIED psi	DURATION OF PRESSURE (min)
Polythene/metal	75	112	1000	20
Propathene/metal	140	175	3200	10

Table 2.3

Different surface treatment of fibres such as washing in carbon tetrachloride, or heating the fibres or applying both had been tried. The best results from the adhesion point of view was obtained when the fibres were dipped into carbon tetrachloride and then heated to 200^{o}C in the closed die. Fig. 2.4 shows a cross section of aluminium and bronze wool* (randomly distributed) reinforced propathene.

*Not in the sense of ordinary wool the fibres are fairly straight but the manufacturing company names them as metal wool.

2.0 MECHANICAL TESTING OF PLASTICS AND COMPOSITES

The mechanical properties of composites and plastics are of great interest in any application where they are used as structural materials. The use of such materials is determined primarily by their mechanical properties rather than by their chemical behaviour. The question is always will the material be strong enough to serve its purpose and will it be tough enough to withstand being subjected to dynamic loading. These are very important questions to the design engineer.

If the comparison of physical data obtained from two or more sources is to have any meaning, the testing methods have to be standardised. The results of physical tests carried out on a material often depend on the environmental conditions (humidity, temperature, etc.) the size, shape and method of preparation of the test pieces, and the techniques of measurement employed.

Many of the standard tests applied to the plastics and to the composites have been derived from A.S.T.M. methods, where they were originally introduced for metals. Plastics and composites, due to their molecular structure and orientation, are much more anisotropic than metals. Therefore the crystallinity, flow and freeze patterns of

the material can affect the properties to a great extent. Testing the composites by these standard tests may lead sometimes to wrong data interpretations. This is mostly due to anisotropy of the composite. It must be borne in mind that a structure, rather than a material, is under test. Misalignment of the composite with the testing direction, inappropriate machining, and different geometry of the specimens lead one to wrong conclusions. Great care must be taken to avoid these pitfalls.

It is wrong for example to conclude that the behaviour of a composite under simple tension is the same as the behaviour of the composite under a complex loading system. To avoid these shortcomings of standard tests many non-standard tests have been developed for special purposes. Many non-standard tests for flats, rings, ring segments and cylinders have been published (56). Perhaps the best method is to test the component itself under the loading system that it will have in future, but it must be realized that the more reliable the data required, the more money must be devoted to testing procedures. To what extent this can be realized is the problem of the engineer in charge.

In this work few different types of tests (but with a large quantity of specimens) have been carried out. These tests are 1) Simple tensile tests, 2) Plane

strain compression tests, 3) Impact tests, 4) Creep tests. The particulars about these tests are outlined in the following pages.

2.1 SIMPLE TENSILE TESTS

This test is the most common used in the testing of materials and applied to the plastics without any modification. This is the simplest test which gives load/extension relationship over the testing range. For plastics, it can be used satisfactorily to find out a true stress/strain relationship up to the point where severe necking takes place. Beyond this point it becomes useless unless a very elaborate set-up is used to detect the cross section of the neck. Great care must be paid to the right alignment of the test specimen when the directional properties of a material are to be obtained.

The tensile tests were made with an Instron testing machine. For tests with standard dumbell shape specimens an electro-mechanical type of extensometer (manufactured in Imperial College) was used with a X-Y plotter to record the load and extension. Fig. 2.7 shows the actual set-up used to perform such tests. Test specimens of strip shape were milled to .375x4.50 in. and were left for a day to relax prior to testing. True stress/strain curves were obtained from the load/extension diagrams using a digital computer.

Here it will not be proper if few words are not said about the principals of the electro-mechanical type of extensometer and its accuracy. This extensometer was designed by the author specially to measure the true strain in plastics. The extensometer was built from aluminium for light weight. It is attached to plastic specimen on four knife edges. The gauge length is adjustable in the range of .5 - 4.0 in. The movement within the gauge length is stepped down by a gear mechanism in the ratio of 1 : 40 and then fed into a high frequency transducer. The output of transducer is amplified and fed to an X-Y plotter. The amplification can be adjusted from 1 to 10.000. Thus with the arrangement shown in Fig.2.7 1 percent strain (.5 m gauge length) corresponds to 1.25 inch chart displacement.

For small strains (below 1%) a strain gauge extensometer built by INSTRON was used. The gauge length is constant and it is .5 in. With the amplifier 1 percent strain causes 10 in. of chart displacement. Thus, better accuracy is obtained.

Errors that might have been introduced to the results due to measurings are maximum of 4 percent in the electro-mechanical and .5 percent in the Instron extensometers respectively.

2.2 PLANE STRAIN COMPRESSION TESTS

WATTS and FORD (57) studied experimentally, a plane strain compression of strips and slabs between two smooth and parallel dies. Although this was devised for metals, it can be applied to plastics. Fig.2.8b shows the plane strain compression test diagrammatically. The actual set-up and subpress instrumentation is shown in Fig.2.8a To ensure a plane strain state during compression the width to thickness ratio of the strips was kept greater than 8. The friction between the die and the specimen (plastics or plastics/metal composite) was minimised by applying Molyslip (molybednum disulphide grease) to the contacting surfaces of the subpress and the material being tested. The effect of friction and die specimen geometries on the stress/strain relationship of the plastics had been studied by WILLIAMS (58, 59). The basic principle of this test is that a strip of material to be tested is pressed between two highly polished parallel dies at a constant rate. The deflection of the material and the load applied are recorded automatically. The main advantages over simple tensile test is that, the area under the die remains practically constant, thus ensuring the stability in the load-deflection diagram. A typical stress/strain diagram for polyvinylchloride obtained from such test is

shown in G.2.3. A correction has to be made in each case for the true origin of the curve. The origin shift is mainly due to that molyslip is squeezed out at the beginning of the experiment as the load is applied. This error is sometimes as high as 1% of strain which, in some cases, may be great limitation to its application.

It is found that the stress - in plane strain compression test - varies with the die width, because of external elastic forces(40,53) To overcome this shortcoming, a minimum of four experiments with different die breadths were carried out for each case. Stresses for constant strains were picked off from such curves, and stress versus the reciprocal of die width graphs were produced. By extra polation* the stress corresponding to an infinite die breadth was obtained as the intercept of the fitted line with the stress axis. The values of stress obtained in this way are free of elastic forces error.

The test specimens were carefully milled to 2.0x4.0 in. size and left overnight for relaxation. Between two successive testings at least 0.5 in. was left.

---

* The calculations were done by an IBM 7090 digital computer.

2.3 IMPACT TESTS

Toughness is important in structural design. But the term itself has not been clearly defined; however it is related to impact strength which is only a guide to it. Impact strength is more important than the tensile strength data to a designer, if the component to be designed will be subjected to shocks and dynamic loadings in the future. The impact strength of a material is a function of strength, elasticity and internal damping of itself. The work done in breaking a test piece is taken to be a measure of this strength. An approximate assessment of this, is the area under the stress/strain curve. For perfectly elastic materials, it is given by

$$\frac{\sigma^2}{2E}$$

where E, σ are the Young's modulus and the yield strength of the material respectively.

For impact strength evaluation notched or plain bars are used. Factors influencing the impact strength measured from such tests are

1) The dimensions of the test piece.
2) The notch (its shape and sharpness).
3) The rate of loading.
4) The ambient temperature.
5) The anisotropy of the test piece.

Two types of tests, namely simple beam (Charpy) and cantilever beam (Izod) had been standardised. The tests that were carried out during the course of this work were of Charpy type. For this Zwick and K.G. impact machine was used, with a pendulum rating of 150 kg.cm. The specimens were milled to 10. x 55. mm and notched with a 55^{o} milling cutter to a depth of 2.0 mm. The span between the supports was 40 mm.

2.4 CREEP TESTS

The dimensional stability of materials during their usage is important in most of the applications. When a load is applied to a material an instantaneous strain takes place which is followed by gradually increasing deformation. This is called creep. Some portion of this deformation is recoverable upon the removal of the applied load. For the plastics, the recoverable part of the creep is greater than the metals. For the designer, the creep behaviour of a material is important if the component to be designed will be subjected to continuous loadings in future. The useful life of the component is determined from the applied stress level and the maximum allowable creep. To obtain data of such long term behaviour of materials many different types of tests have come into use. Some of the important types of tests are, long-time creep

test under constant tensile load, stress-rupture, stress-relaxation, and constant-strain rate tests. The long-time creep test is conducted by applying a dead weight to one end of a lever while the specimen is attached to the other end of it.

The deformation may be determined by periodically measuring the distance between two fiducial marks on the specimen with a cathetometer or in special cases by a travelling microscope. With rigid materials strain gauges can be used to measure small deformations accurately. If there is no slippage in the grips holding the specimen the device for measuring elongation may be attached to the specimen grips, and the change in length may be measured from the separation of the grips. Dial-gauges and transducers can be used for this purpose which provide very good accuracy.

During the course of this work creep tests were done by applying a dead weight to one end of the material. The gauge length of the specimen was 2.00 in. and the deformation was measured by a 'Betty' dial gauge*(with a scale of 1/10.000 in.) at certain intervals. Only four experiments with reinforced plastics were done. Fig.2.9 is a diagrammatical representation of the creep tests performed.

---

*excluding the end effects an accuracy of .05%.

3.0 THE EFFECT OF COLD WORKING ON MECHANICAL PROPERTIES OF PLASTICS

There has been very little recent work on the cold rolling* of plastics. ELEY (36) calculated the roll pressure and heat dissipation for imaginary polymeric substances when they are subjected to cold rolling. MAXWELL and ROTSCHILD (37) and CARMICHAEL (38) examined the behaviour of unidirectional rolled polyethylene and found that the ductility (which is about 500-600 percent for unrolled material) reduces to a negligible amount while the proportional limit is increased by a factor of 20, (for 80 percent unidirectional rolling). Furthermore, it had been pointed out that the density of the plastic changes by less than 1 percent for 80 percent reduction in thickness. It has been observed (38, 39, 40) that the primary yield point of the rolled plastics varies with the degree of cold rolling but the change in Young's modulus is not substantial. The relationships which relate the Young's modulus to the amount of cold working have not been given.

To the best knowledge of the author HSIAO (41) was the first author to relate the increase in primary yield point to the degree of molecular orientation caused by cold drawing. The general mathematical approach in the forementioned work can be outlined as follows. A statistical

* Rolling below the crystallite melting temperature and above glass transition temperature.

mean fracture strength in the vicinity of a point in a system of randomly oriented ideal linear elements was obtained. After making some simplifications for the integrands and using statistics, he found that for a complete unidirectional orientation, the mean fracture strength was about three times that of the oriented one. However by taking the change of volume and the modifications of the molecular kinetic process into account, the strength of a perfectly unidirectional oriented system was obtained as six times the unoriented strength. WILCHINSKY (42) studied the orientation in cold rolled polypropylene by X-ray diffraction methods and explained indirectly the phenomenon of preferred orientation of the crystallites after subjected to cold rolling. A theoretical explanation of this has not been given yet.

TAKASHI and others (43) studied the deformation mechanism for polyethylene spherulites and gave a mechanical model which takes into account the crystal transformation from the folded chain type to the fringed-micellar* type within the crystal lamella.

Although we are still very far from a complete molecular interpretation of polymer behaviour, many features can be explained qualitatively by consideration of spatial relations between the crystallites, and how these vary with time. The author intends to publish a theoretical argument on this line

---

* The individual molecules are assumed to be able to pass from one crystalline region to another through the amorphous region and thus hold the polymer together

3.1. COLD ROLLING

For the cold working operation, two types of rolling were investigated; a) unidirectional, b) cross rolling. For this purpose a laboratory type of rolling mill was employed which was described adequately elsewhere (60). The rollers were of 4 in diameter and had a surface roughness of 7 C.L.A.(Fig.2.5).

In order to have plane strain condition in unidirectional rolling the dimensions of the specimens were chosen to satisfy $\frac{h_i}{w} < .125$ (OROWAN and PASCOE (49)) where h_i is the initial thickness and w is the width of the specimen. Furthermore the reduction in each pass never exceeded 4% at the extreme case for keeping $(\frac{2\Delta h}{D})^{\frac{1}{2}} << \eta$ where Δh is the reduction in thickness per pass and D is the roll diameter, η is the coefficient of friction.

Cast alkathene, p.v.c. and acetal copolymer specimens with the dimensions of $2\frac{1}{2}$ x 4" were rolled to various degrees. The specimens were chosen to keep the thickness variation before rolling to under 2%. A term which is used frequently in engineering and also used here is "percentage reduction" which is defined as change in thickness divided by the original thickness.

The density of the unrolled and rolled plastics were measured by a density column (Fig.2.6) which is fully explained in ref. (61). It is found from the measure-

ments that the density increase for 80% rolled polythene is around .3 percent.

Table 3.4 shows the initial and final dimensions of the rolled materials which were used to prepare tensile and plane strain compression test specimens.

Material	h_i (in.)	$L_i x w_i$ (in.)	h_f (in.)	L_f x w_f (in.)	$\Delta w/w$ (%)	r (%)
ALKATHENE	.249	4.00x4.00	.229	4.31x4.02	.5	8.0
	.245	4.00x4.00	.196	4.95x4.03	.7	20.0
	.246	3.00x4.00	.171	4.24x4.05	1.2	30.5
	.246	3.00x4.00	.122	5.90x4.10	2.5	50.4
	.246	2.00x4.00	.073	6.40x4.16	4.0	70.3
P.V.C.	.251	4.00x4.00	.220	4.51x4.03	.7	12.3
	.248	4.00x4.00	.180	5.37x4.05	1.2	27.4
	.251	4.00x4.00	.163	5.89x4.06	1.5	35.0
	.248	3.00x4.00	.141	5.15x4.08	2.0	43.0
ACETAL COPOLYMER	.133	4.00x2.50	.104	5.06x2.51	.4	21.7
	.133	3.00x2.50	.066	5.94.2.54	1.6	50.4
	.133	3.00x2.50	.048	8.11x7.55	2.0	64.0
	.133	2.00x2.50	.039	6.64x2.56	2.4	70.7

Table 3.4

For cross rolling, square shape materials were cut with the initial dimensions such that after the required degree of rolling the final dimensions would be in the

ominal range of 4.5x4.5 in. The initial dimensions can e obtained from the following expression (it is derived rom the assumption that the volume remains constant)

$$L_f = L_i(1-r)^{\frac{1}{2}}$$

where L_f, L_i and r are final and initial dimensions of the material and the percentage reduction in thickness respectively.

Cold working operation usually imparts large strain to the material. The stress/strain relationship depends on how this large strain is imposed on the body. Let this large strain be defined as the resultant of the principal strain components (55). In tensor form this is

$$\bar{\sigma} = \lambda[\delta_{ij}e'_{ij}e'_{ij}]^{\frac{1}{2}} \qquad 1$$

where λ is an adjustable constant, δ_{ij} is the Kronecker delta (unit matrix) and e' is the natural (logarithmic) strain. The repeated suffix means summation throughout the index range (1,2,3). Constant volume may be expressed in tensor form as

$$\delta_{ij}e_{ij} = 0 \qquad 2$$

Combining equations 1, 2 and simplifying we have,

$$\bar{e} = \lambda'[(e_{11}-e_{22})^2 + (e_{11}-e_{33})^2+(e_{22}-e_{33})^2]^{\frac{1}{2}} \qquad 3$$

where λ' is another constant. As an example, a plastic

which was cross-rolled and then subjected to plane strain compression tests will be examined.

During cross rolling, the reduction per pass is considerably smaller than the total reduction, and the reductions are cyclic. The total strain induced in two directions at the end of rolling can be considered to be equal to a close approximation, or in other terms, $e_{11} = e_{22}$. Then the equation 2 gives

$$e_{33} = -2e_{11} = -2e_{22}$$

substituting this in equation 3 yields

$$\bar{e}_{cr} = \frac{3}{\sqrt{2}} \lambda' e_{33}^{cr}$$

where $\bar{e}_{cr}$ is the average large strain in cross-rolling. e_{33}^{cr} is the natural strain across the thickness of the material ($\text{Log}_e \frac{h}{h_o}$). Setting $\lambda' = \frac{\sqrt{2}}{3}$ one equates these two strains. Thus all the other strains must be expressed in terms of $\bar{e}_{cr}$. Now suppose that the same material is subjected to plane strain compression test, the total large strain can be calculated from the equation 3 by setting $e_{22} = 0$ and $e_{11} = -e_{33}$ and it is

$$\bar{e}_{ps} = \sqrt{6}\, \lambda' e_{33}^{p.s}$$

using the adjusted value of λ' we have

$$\bar{e}_{ps} = \frac{2}{\sqrt{3}} e_{33}^{p.s}$$

Now for the same amount of large strain (for the cases

of cross-rolling and plane strain compression test) one has

$$e_{33}^{p.s.} = \frac{\sqrt{3}}{2} e_{33}^{c.r.}$$

A 50 percent strain due to cross rolling will be equivalent to 45.2% strain due to plane strain compression.

It is clear that, the simple tensile test is analogous to cross rolling and if a tensile test result is to be compared with the result of the plane strain compression test, then the natural strain axis of the tensile test must be contracted by a factor of $\frac{\sqrt{3}}{2}$.

To find the total reduction resulting from two operations (say by cold rolling and then plane straining) the following expression must be used, (it is derived from equation 2)

$$r_t = r_c + r_r - r_c r_r$$

where r_r, r_c and r_t are reductions due to rolling and compressing and the total reduction respectively.

4.0 COLD ROLLING OF COMPOSITES

In theory cold working improves the yield strength and the Young's modulus (in the direction of cold working) of single phase materials. This may also be true for alloys and composites. In this investigation, randomly distributed bronze/polethene composites were subjected to cold rolling in order to assess the changes in the

mechanical properties of such two phase materials. It has been found experimentally that up to 7-8 percent of rolling the ultimate strength increases; it then starts to decrease. At around 30 percent rolling the ultimate strength has a smaller value than it had before the rolling. This may be due to the following reasons namely, a) the value of strain transfer efficiency coefficient 'ψ' decreases, due to broken bonds, b) mechanical breakdown of the fibre shortens the length which reduces the value of ψ further. The reasoning is indirect and is as follows: the fibres within the composite are long, and as cold rolling is applied one of the fibre ends rotates in the plane of rolling. This causes the bond between matrix and the fibre to fail (an exaggerated geometrical construction of what happens to a single fibre when it is subjected to rolling is shown in Fig. 2.14). Although small reductions per pass minimize the rotation which reduces the number of broken bonds, the cumulative rotation causes the interaction of the fibres (however the decrease in mechanical properties of the composite due to this fibre interaction is not known). Secondly if mechanical breakdown occurs during cold working, the value of ψ is reduced further. This reduction can be seen from the Table 1.2. (The values are given for 25 percent fibre concentration and

$\frac{r_o}{r_1} = \sqrt{c} = .5.)$

Thus if a conclusion is to be drawn from a limited number of experiments and the forementioned reasonings one can say that there is an optimum point for the degree of rolling which can be applied to composites. Rolling beyond this point causes deterioration in the ultimate strength and yield point of the composites.

PART II.b

THE RESULTS

1.0 THE RESULTS

Generally in this work, four different types of tests have been carried out to assess the mechanical properties of the plastics and composites. These were simple tensile tests, plane strain compression tests, impact and creep tests. The experimental procedure for such tests have been described in previous sections. Fig. 2.2, 2.5, 2.6, 2.7, 2.8 show the actual set-up for the mechanical testing of plastics and composites. For cold rolled composites only plane strain compression tests have been performed. This was merely due to the rough surface acquired by the composite after rolling (it is nearly impossible to get a true picture about the mechanical properties of a material which has cracks on the surface, by testing it in simple tension). The experimental results will be given in the following three subsections, namely reinforced plastics, cold rolling of plastics and cold rolling of composites.

2.0 REINFORCED PLASTICS

One of the aims of the present investigation was to assess the effect of fibre distribution within the composites. For this, three types of fibre distribution were considered, namely, uni-directional, cross and randomly distributed type. The tensile stress/strain relationships for the metal fibres (obtained

from the bulk material) that have been used to reinforce polypropylene, polyethylene (three grades) are given in G.2.4.

For unidirectional reinforcement, copper wires were embedded in polypropylene (the cross-section of such a composite is given in Fig.2.10). The resulting composite was subjected to simple tensile tests. The stress strain relationships for different volumetric fibre concentrations are given in G.2.5 for quick comparison; the stress/strain curve for the unreinforced matrix is also given in each case. The experimental results are compared with the maximum predicted theoretical values (for $\psi = 1.0$ where uniform strain field and perfect adhesion is assumed) in G.2.6. Also in each case the corresponding average ψ value is given for the experimental points. (This value for ψ is obtained from the best fitting theoretical curve as they have been given in Part I.)

For cross-reinforced composites copper and iron gauze were embedded in polypropylene and tested in simple tension. The stress/strain relationships and the gain in the Young's modulus are given in G.2.7 - G.2.10. Cross-sections of iron propathene is seen in Fig. 2.11. (The dark lines are due to grinding of the cross-section prior to microscopic investigation.)

As it is seen in the photograph the probability of having mechanical interaction between fibres is less. This fact reflected in ψ (due to better wetting of the fibres by the matrix, higher experimental values were obtained for the strain transfer efficiency coefficient).

Propathene and polyethylene (three grades) were reinforced with chopped aluminium, bronze and steel fibres (the aspect ratio of the fibres were in the range of 160-280). Then specimens were tested to verify the theory for the randomly distributed type of reinforcement. The stress/strain relationships obtained from tensile tests are given in G.2.11 - G.2.24. Theoretical maximum values (ψ = 1.0) are compared. G.2.25 gives stress/strain curves for randomly distributed bronze reinforced medium density polyethylene, obtained from plane strain compression tests, as explained on page 59.

The variations of computed α and experimental values of ψ with respect to E_f/E_m are presented in G.2.42 and G.2.43 respectively.

G.2.26 - G.2.29 show the results obtained from Charpy tests. These tests were carried out only with randomly distributed type of various composites. For each case a curve is fitted to indicate the trend

of the behaviour of the composites. Table 2.5 shows the variation of the impact strength for various composites (with 150 kg cm pendulum).

Impact strength (kg cm)

Materials	Polymer	Composite	% Reinforcement
Polyethylene (g=.915)	90	55	5
Randomly distributed		35	10
Steel fibres.		40	15
		48	20
Polyethylene (g=.922)	78	45	5
Randomly distributed		32	10
steel fibres.			
Polyethylene (g=.910)	100	60	10
Randomly distributed		40	15
Aluminium fibres		50	20
Polyethylene G.2 (g=.934)	14	30	20
Randomly distributed		33	25
Aluminium fibres.		38	30

Table 2.5. Variation of the impact strength for various composites (some of the strength figures are interpolated values).

Long term creep tests have been performed for randomly distributed types of composites and the results are presented in G.2.30 - G.2.32. These tests have been performed as shown in diagrammatical figure Fig. 2.9.

3.0 COLD ROLLING OF PLASTICS

Polyethylene, P.V.C. and acetal copolymer were rolled, then tested in tension and plane strain compression to assess the effect of cold rolling. G.2.33 shows the stress/strain relationships for 71% unidirectionally rolled polyethylene tested at 0^{o}, 45^{o}, 90^{o} to the rolling direction. It has been found experimentally (G.2.34) that on the basis of large strain definition (page 68) the results obtained from tensile tests and plane strain compression tests are the same. Therefore, tensile tests results will not be reproduced.

G.2.35 - G.2.41 show plane strain compression tests results for the unidirectional and cross-rolled polymers. Again large strain concepts have been used to show that the effect of cross-rolling on the stress/strain relationships is the same as the effect of uni-directional rolling. Thd dotted line curves were obtained from transposing the stress/strain values according to the large strain theory. As is clear

from the graphs that good agreement is obtained up to 50 percent rolling. The deviation might be due to structural changes caused by uncontrollable heat dissipation and temperature rise during rolling.

4.0 COLD ROLLING OF COMPOSITES

Randomly distributed bronze fibre reinforced low density polyethylene composites were uni-directionally and cross-rolled. Then they were tested in plane strain compression (due to rolling, surface conditions deteriorate and cracks are formed. This is detrimental to the tensile stress/strain properties, therefore only plane strain compression tests were carried out.) G. 2.46, G.2.47 show the variation of stresses for constant strains with respect to degree of rolling. From the experiments it seems that the stress increments at constant strains are proportional to the applied reduction in thickness (up to 10 percent rolling) during compression. Then a peak value is reached, at around 12 percent uni-directional rolling. This is followed by fairly linear decrease in the stress values. Roughly the same trend was observed with cross-rolled randomly distributed bronze reinforced low density polyethylene.

5.0 DISCUSSION OF THE RESULTS

The theory developed in Part I for predicting the Young's and shear modulus of a fibre reinforced composite material is a general one in the sense that it takes into account the orientation of the fibres, the adhesion efficiency of the two media, as well as the effect of the non-homogeneous strain field. The distribution function reflects the effect of a fibre orientation in the coefficients of stiffness (or compliance) matrix. COX (31), GORDON (34) used the idea of 'distribution function' but neither of them could obtain results for uni-directional and cross-reinforced composites.

The constants α, β introduced on page 17 account for the adhesion efficiency and non-homogeneous character of the strain field respectively. For simplicity the product of these two constants was replaced by new constant ψ. Although some authors (8, 26, 31, 35) had used the idea of introducing a constant to modify the law of mixtures (eq. 2 on page 13) the basic concept was the effective Young's modulus of the fibres (or reinforcing phase) is different from that of the one before reinforcing. NIELSEN (35) used the idea of 'stress concentration' and introduced a constant to modify the modulus of the filled polymers.

As it has been pointed out earlier, when α is less than unity and thus determined purely by experimental methods, the whole approach becomes empirical (62). The range of α is between 0 and 1, where $\alpha = 0$. corresponds to no adhesion between the two media. In this case, the only contribution to the strength of the composite comes from the continuous phase which is the matrix. This contribution is slightly less than that predicted by the theoretical lower bound (17)*.

The inhomogeneous character of the strain field is governed by β. Theoretically it can be calculated for small strains. Calculated variation [for the case of elastic matrix and fibre (solid lines) and elastic fibre, plastic matrix (dotted lines)] is shown in G.1.8. A comparison of maximum theoretical ψ value (where $\psi = \beta$) (elastic fibre, elastic matrix) and actual values is given in G.2.45.

The application of the derived reinforcement theory to helically wound thin walled cylinders is successful. Because any degree of anisotropy in a given direction can be obtained by varying the concentration, E_f/E_m

---

*This bound corresponds to Reuss model (uniform stress field throughout the constituent media) and is $\frac{E_m E_f}{cE_m + (1-c)E_f}$

ratio and the helix angle. Good agreement is obtained with the experimental results (32) when the hoop stiffness is twice the axial stiffness.

Tests with unidirectional copper fibre reinforced polypropylene show that the results are roughly 15 percent below the law of mixtures (or maximum E_c values* corresponding to $\psi = 1$ case). For the copper fibres β is found from the calculations to be .975 (aspect ratio of 280 and 6% volumetric concentration) which in turn suggests that there is a lack of perfect adhesion between the two constituents of the composite. However by leeting $\psi = .85$ the experimental and theoretical results coincide. Here the adhesion coefficient α is found to be .873, but some contribution might have come from the fact that the fibres were slightly kinked and not perfectly parallel to each other.

Tests with copper and iron gauze reinforced polypropylene gave good agreement with the theoretical predictions. It was observed that up to moderate fibre concentrations perfect adhesion was achieved ($\alpha = 1$, $\beta = \psi = .95$). This is thought to be due to two reasons, a) as the fibres are not quite straight better mechanical gripping takes place and thus an

---

*This corresponds to Voigt model (uniform strain field) and it is $E_c = (1-c)E_m + cE_f$.

improved value of α is obtained. b) Mechanical interaction of the fibres is avoided since parallel fibres do not touch each other.

It was also observed that higher ψ value was obtained for copper/propathene composite than that of iron/propathene which again is in accord with the theoretical expectations. The results presented in graph form are quite accurate since strain gauge type of extensometer was employed (maximum of .5 percent error due to reading or measuring). For randomly distributed fibre reinforced composites (various combinations of steel, bronze, aluminium, propathene and three grades of polyethylene gave results in reasonable agreement with the theoretical predictions found on page 34. From the experiments Table 2.6 is constructed to show the variation of the strain transfer efficiency coefficient.

Composite	E_f/E_m	ψ	Remarks
Al/P.Propylene	33.2	.87	Randomly reinforced.
Copper/P.Propylene	50.4	.85	Uni-directionally reinforced.
Copper/P.Propylene	50.4	.95	Cross-reinforced (gauze wire)
Bronze/P.Propylene	60.0	.79	Randomly reinforced.
Iron/P.Propylene	85.7	.88	Cross-reinforced (gauze wire).
Al/H.D.Polyethylene (G.2)	93.6	.78	Randomly distributed.
Steel/P.Propylene	98.3	.77	"
Al/L.D.Polyethylene	257	.75	"
Bronze/M.D. Polyethylene	414	.72	"
Steel/L.D. Polyethylene	762	.71	"

Table 2.6 The variation of strain transfer efficiency coefficient with respect to E_f/E_m ratio.

From the inspection of Table 2.6 it is clear that the adhesion of the fibres and the plastics deteriorates as the ratio of E_f/E_m increases (the variation of aspect ratio does not affect significantly the β value in the elastic range of the constituents). The range of the strain transfer efficiency coefficient is between .71 - .95 for the whole range of composites.

Plane strain compression tests with randomly distributed bronze fibre reinforced medium density polypropylene gave $\psi = .41$ compared with the $\psi = .72$ in tension. Of course owing to the fact that metal/plastics composites are heterogeneous materials the Bauschinger effect is appreciable. Thus the properties in compression and flexure are more complex and hence it is not easy to analyse them mathematically. However the behaviour of such composites under compressive stresses is beyond the scope of the present work. Thus the discussion on the results of P.S.C. tests will not be taken further.

From Charpy tests it is observed that by metal fibre reinforcement the ductile material (such as L.D. polyethylene) becomes brittle up to certain fibre concentration and then its ductility improves slightly. Since the fibres are randomly distributed, for high fibre concentrations, mechanical interaction takes place. This might be the cause for the apparent improvement in the impact strength. Brittle material (such as polyethylene G.2) reinforced with aluminium fibres exhibits a reverse trend. This is again thought to be due to mechanical interaction of the fibres (at high concentrations). For small fibre concentrations, fibres contribute to the strength of

the composite, but as the reinforcement ratio increases complete wetting of the fibres cannot be reached (the effective cross-sectional area becomes smaller) and interaction of the fibres reduces the impact strength of the material.

The creep tests results reveal that the amount of creep reduces considerably for even small amounts of metallic fibre reinforcement and reaches almost steady state long before the unreinforced one (see G.30). At low fibre concentrations the response of the composite to small change of stress levels is high; this can be observed from G.2.32.* But at moderate fibre concentration the change in the creep rate is very small compared with the previous one. The creep for 10.1 percent randomly distributed steel fibre reinforced M.D. Polyethylene tends to become steady within a short time (one minute or so) after the load is applied.

The stress/strain curves for two types of rolled (uni-directional and cross-rolled) plastics agree on the basis of large strain definition up to roughly 50 percent thickness reduction. For the heavier reductions the deviation is caused by the uncontrollable

---

* The first readings for the deformations were taken 5 seconds after loading, and the creep was assumed to be linear within the 0 and 5 seconds interval.

temperature rise during rolling (as is well known, plastics are sensitive to ambient temperature), which affects greatly the mechanical properties of the plastics. From the tensile tests, it was observed that the Young's modulus of the cold rolled L.D. polyethylene decreased up to 30 percent thickness reduction and then started to improve again, G.2.44. At around 50 percent thickness reduction the modulus reached its original value. Beyond 55 percent thickness reduction the rate of increase in the Young's modulus increased, and at around 80 percent rolling the modulus was nearly twice the value than what it was before.

The plane strain compression tests carried out for cold rolled plastics showed that P.V.C. becomes anisotropic in the direction of rolling. Nearly 50 percent increase in the stress value (for 32% strain) in the direction of rolling was obtained for moderate thickness reduction (38.6%).

It is clear that all the stress/strain curves for the cold rolled plastics tend to be asymptotic to the unrolled stress/strain curve. If the case is so, theoretically it is possible to find a parametric differential equation for the family of the curves (44) which will take the rolling effect into account.*

---

*This is an example of Liapunov's stability at large theorem.

But practically this will be immensely difficult problem, because, the plastics suffer structural changes to an unpredictable degree (since local temperature rises during rolling cannot be controlled). The numbers of the parameters that must be involved in the differential equation will be high, which in turn will complicate mathematical procedures.

Generally the plane strain compression test bears much more inaccuracy at the small strains region compared to simple tensile tests. (This is due to the shift of origin when the lubricative grease is squeezed out, see G.2.3.) But it has the advantage that the test is stable, even though high strains are involved.

The plane strain compression tests that were carried out for the cold rolled composites reveal very little. This is partly because the behaviour of the metallic fibre reinforced plastics towards the compressive stresses was beyond the scope of this work (tensile tests could not have been carried out due to surface conditions after the rolling). However, the test results show that there is a gain in the stressvalues (at constant strains). This gain exists up to 12 percent uni-directional rolling and beyond this point the stress values decrease. Around 30 percent

rolling (at 3.5% strain) the stress becomes smaller than the value before rolling.

6.0 CONCLUSIONS

For fibre reinforced composites, the stiffness and the strength generally increase with the percent of reinforcement though the fibre alignment is equally important. In addition, the ratio of the moduli of the reinforcing fibre to the resin is the prime factor in determining the stiffness, strength and strain transfer efficiency coefficient ψ. According to the developed theory there is no reinforcement effect of the fibres in the transverse direction to their axis. This view is supported by the experimental results given in the references(29, 63, 64). Although the developed theory predicts the rigidity modulus and the Poisson's ratio, the validity of the derived equations with various composites must be checked. It is possible that the predicted values are considerably departed from the actual measurements. Since composites are heterogeneous materials the Bauschinger effect is much higher, and hence the theory developed in part I is not expected to hold in compression.

The introduction of ψ is justified substantially by the experiments carried out. Although strictly speaking its nature is a tensor quantity, mathematical complications force one to treat it as a scalar in the domain of 0 - 1. One of the components of ψ, α,

expresses the adhesion efficiency, mechanical interaction of the fibres and the irregularities in the fibre geometry. This gives flexibility to the derived theory. The coefficient β also plays an important role when E_f/E_m is high (non-homogeneity of the strain field is increased with higher E_f/E_m ratios). Generally speaking this theory implies a mechanical model which is between Reuss and Voigt models th ough it gives closer results to the Voigt estimates. Finally, the theory is not expected to hold for stresses approaching failure.

It has been noticed that for low concentrations perfect adhesion is achieved for nearly all types of reinforcement with the exception of randomly distributed steel fibre reinforced L.D. polyethylene. Furthermore, it is clear from the experiments that the lower the value of E_f/E_m the higher is the value of strain stransfer efficiency coefficient. The ductility of the brittle matrix is improved while the reverse holds for ductile matrix. As the reinforcement ratio increases the effect of mechanical interaction of the fibres becomes appreciable.

By metallic fibre reinforcement the creep properties of the plastics are greatly improved. And it was observed that most of the creep is recovered upon the removal of the load. However, with the results

obtained in the course of this investigation it is not possible to state general rules to the creep behaviour of the metal fibre reinforced composites. Therefore extensive research is necessary on the creep behaviour of such materials.

It must be pointed out that this work is far from giving a complete picture of the behaviour of the metal/plastics composites. And it is believed that detailed investigations of failure mechanism, fibre interactions and the variation of ψ must be carried out. Research into the behaviour of such composites under compressive stresses is also worthwhile.

On the basis of large strain definition (p. 68) it has been found that for the plastics a) the stress/strain curves obtained from tensile tests and plane strain compression tests are the same; b) cross-rolling and uni-directional rolling have the same effect on the stress/strain relationship in the principal rolling direction, and c) an envelope exists for the stress/strain curves of cold rolled polyethylene, P.V.C., and acetal copolymer, as is in the case of metals (65), though the scatter around the envelope is greater than metals.

By uni-directional rolling, the plastics become non-isotropic and the more reduction applied to it the more non-isotropism is introduced to the material.

However by cross-rolling the degree of non-isotropism is reduced, and it appears that this is proportional to the applied thickness reduction. There is evidence that the Young's modulus of polyethylene is a function of the degree of rolling. Thus more experimental and theoretical analyses on the behaviour of the Young's modulus must be carried out.

When a randomly distributed metal fibre/plastic composite is cold rolled, it is found that there is a moderate improvement in the Young's modulus and the yield strength of the composite up to certain thickness reduction. However surface conditions deteriorate and a number of crack initiations are created. If the surface conditions can be improved after rolling it is possible that higher improvements in the yield strength will be obtained. The general impression obtained from rolling of such composites is that there is no technological advantages (at least for the time being) that can be obtained from cold working of composites with high E_f/E_m ratios.

REFERENCES

1. DELMONTE, J. Metal filled plastics. Plastics Application Series, Chapman and Hall Ltd., London 1961.
2. WILLIAMS, R.U. and O'BRIEN D.J. The reinforcement of metals with metal fibres. App. Mat. Research July 1964.
3. TAI TEWU. Effects of Powder particle shape on elastic properties of sintered alloys. Int. J. of Powder Met. V.1 N3, 1965.
4. Fiber Composite Materials. Am. Soc. for Metals, Chapman and Hall Ltd. London, 1965.
5. HAWARD, R.N., MANN, J. Reinforced Thermo plastics. Rubber Chemistry and Technology, Rubber reviews for 1965.
6. HIBBARD, W. Composite materials for the future. Chem. Eng. 1963.
7. HOLLIDAY, L., MANN, J. The structure and properties of complex and heterophase materials. R.CPL75, Shell C.C.
8. KELLY, A., DAVIES, G.J. Properties of reinforced materials. Metallurgical Review 10, 1965.
9. OGORKIEWICZ, R.M. Glass fibre plastics. The Chartered Mech. Eng. Apr. 1964.
10. TURNER, S. A study of plastic composites., App. Mat. Research V.4, N.1, 1965.

11. PICKETT, G. Analytical procedures for predicting the mechanical properties of fibre reinforced composites. AFML-TR-65-220, June 1965.

12. WHITNEY, J.M., RILEY, M.B. Elastic properties of fibre reinforced composite materials, AIAA, V.4, N.9.

13. McDANELS, D.L., JEH, R.W., and WEETON, J.W. Metal Progress, 1960 78(6), 118.

14. McDONALD, N.F., RANSLEY, C.E. Preparation of high modulus alloys. Powder Metallurgy, Rep. No.58,1954.

15. SHAFFER, B.W. Stress/strain relations of reinforced plastics parallel and normal to their internal filaments. AIAA Journal, V.2, N.2, pp. 348-352.

16. COOPER, A.G., Orientation effects in fibre reinforced metals. J. Mech. Physics of Solids Vol:14, pp 103-111, 1966.

17. PAUL, B. Prediction of elastic constants of multi-phase materials. Trans. AIME 218, p.36, 1960.

18. HASHIN, Z., SHTRIKMANS, S. A variational approach to the theory of the elastic behaviour of multiphase materials. J. Mech. Phys. Solids, V.11 pp.127-140, 1963.

19. HASHIN, Z., SHTRIKMAN, S. A variational approach to the theory of the elastic behaviour of polycrystals, J. Mech. Phys. Solids, V.10, pp343-352, 1962.

20. HASHIN, Z. On elastic behaviour of fibre reinforced materials of arbitrary transverse phase geometry,

J. Mech. Phys. Solids, V.13, pp.119-134, 1965.

21. HASHIN, Z., SHTRIKMAN, S. On some variational principles in anisotropic and non-homogeneous elasticity, J. Mech. Phys. Solids, V.10, 335-342, 1962.

22. HILL, R. Self consistent mechanisms of composite materials, J. Mech. Phys. Solids, V.13, pp213-222, 1965.

23. HILL, R. Theory of mechanical properties of fibre-strengthened materials, I. Elastic Behaviour, J. Mech. Phys. Solids, V.12, pp.199-212, 1964.

24. HILL, R. Theory of mechanical properties of fibre-strengthened materials, II. Inelastic Behaviour, J. Mech. Phys. Solids, V.12, pp.213-218, 1964.

25. HILL, R. Theory of mechanical properties of fibre-strengthened materials,III, Self consistent model, J. Mech. Phys. Solids, V.13, pp.189-198, 1965.

26. HILL R. Elastic properties of reinforced solids. Some theoretical principles, J. Mech. Phys. Solids, V.11, N.4, pp.305-326, 1963.

27. HASHIN, Z. Theory of mechanical behaviour of heterogeneous media. Appl. Mech. Rev. V.17, No.1, 1964.

28. LOVE, A.E.H. A treatise on the mathematical theory of elasticity, N.Y. Dover publications 1944, Chap.III, p.99.

29. BAER, E. Engineering design for plastics. Society of Plastics Engineering, Reinhold Publications.

30. KELLY, A., TOYSON, W.R. Tensile properties of fibre reinforced metals, copper/tungsten and copper molybdenum. J.Mech. Phys.Solids. V.13, 1965.

31. COX, H.L. The elasticity and strength of paper and other fibreous materials. British Journal of Applied Physics, 1952, N.3, p.72.

32. TSAI, S.W., ADAMS, D.F., DONER, D.R. Analysis of composite structures. NASA :CR-620.

33. GREEN, A.E., ADKINS, J.E. Large elastic deformations and non-linear continum mechanics. Oxford Press, 1960, Chapter 7.

34. GORDON, J.E. J. Roy. Aeron. Soc. 56 (1952) 710.

35. NIELSEN, E.L. Simple theory of stress-strain properties of filled polymers. J. Applied Polymer Sci. V.10, pp.97-103 (1966).

36. ELEY, D.D., Theory of rolling plastics, I, II. J. of Polymer Science, 1946, pp.529.

37. MAXWELL, B., ROTHSCHILD, P.H. Cold working of polyethylene, J. App. Polymer Science, V.5, p.5.11 1961.

38. CARMICHAEL, A.J. The effect of deformation on the volume and mechanical properties of polythene, 1962. (Report presented to Mech. Eng. Clayton Committee.)

39. FORD, H. Engineering properties of plastics. Symposium on Plastics, The Inst. of Mech. Eng. 7-8 October 1964.

40. PAKDEMIRLI, E., WILLIAMS, J.G. Cold working of plastics (to be published).

41. HSIAO, C.C. Theory of mechanical breakdown and molecular orientation of a model linear high polymer solid. J. of App. Phys. 1959.

42. WILCHINSKY, W.Z. Orientation in cold rolled polypropylene. J. App. Polymer Science, pp.923, V.7, No.3, 1964.

43. TAKASHI, O., SHUNJI, N., KAWAI, H. Deformation mechanism of polyethylene spherulite. J. of Polymer Science, Part A, V.3, pp.1943, 1965.

44. LASALLE, J., LEFSETSZ, S. Stability by Liapunov's direct method. Academy Press, pp52-55, 1961

45. MARIN, J. Theories of strength for combined stresses and nonisotropic materials. J.Aero. Sci. V.24, n.4, 1957

46. WINDING, C.C., HIATT, G.D. Polymeric materials. McGraw-Hill, 1961, Ch.1.

47. FREER, D.W. An investigation of the effect of cold rolling on the mechanical and structural properties of linear polyethylene. M.Sc. Thesis, Imperial College, 1966.

48. KELLY. Proc. Roy. Soc. (London) 282A, (1964) 63.

49. OROWAN, P.W., PASCOE, K.J. First report of the rolling mill research sub-committee. The Iron and Steel Inst. Spec. Report No.34, 1946.

50. SCHUSTER, D.M., SCALA, E. Trans. Met. Soc. A.J.M.E. 230, 1491, 1965.

51. CRATCHLEY, D. Experimental aspects of fibre reinforced metals. Met. Reviews, V.10, No.97, 1965.

52. DE DANI, A. Glass fibre reinforced plastics. George Newnes Ltd. 1960.

53. SONNEBORN, R.S. Fibreglass reinforced plastics, 1954, Reinhold, New York.

54. PICKTHALL, D. Glass reinforced plastics. Engineering Materials and Design, June, 1963.

55. FORD, H. Advanced Mechanics of Materials, Longmans 1963.

56. FRIED, N. Survey of methods of tests for parallel filament wound plastics, ASTM, STP.327, 1963, pp13-39.

57. WATTS, A.B., FORD,H. An experimental investigation of the yielding of strip between smooth dies. Proc. Inst. Mech. Eng., V.1B, No.10, 1952-53.

58. WILLIAMS, J.G. Stress/strain relationships for plastics. Ph.D. Thesis, London University, 1963.

59. WILLIAMS, J.G. Shoulder and friction effects in the compression testing of plastics. Imperial College Int. Report September 1965.

60. WHITTON, P.W., FORD, H. Surface friction and lubrication in cold strip rolling. Proc. Inst. Mech. Eng. pp.123-135, 1955.

61. PAYN, S. Materials and Standards, Vol.4, No.2, 1964.

62. HILL, R. Private communication. 1967.

63. LOEWENSTEIN, K.L. Composite materials. Elsevier, Amsterdam, 1966. (Ed. by L.Holliday)

64. DONALDSON, A.L. SP1/12 R.P. Conf. 1957, 9-D.

65. FORD, H. Researches into the deformation of metals by cold rolling. Proc. Instn. Mech. Engrs. 1948.

GRAPHS AND FIGURES

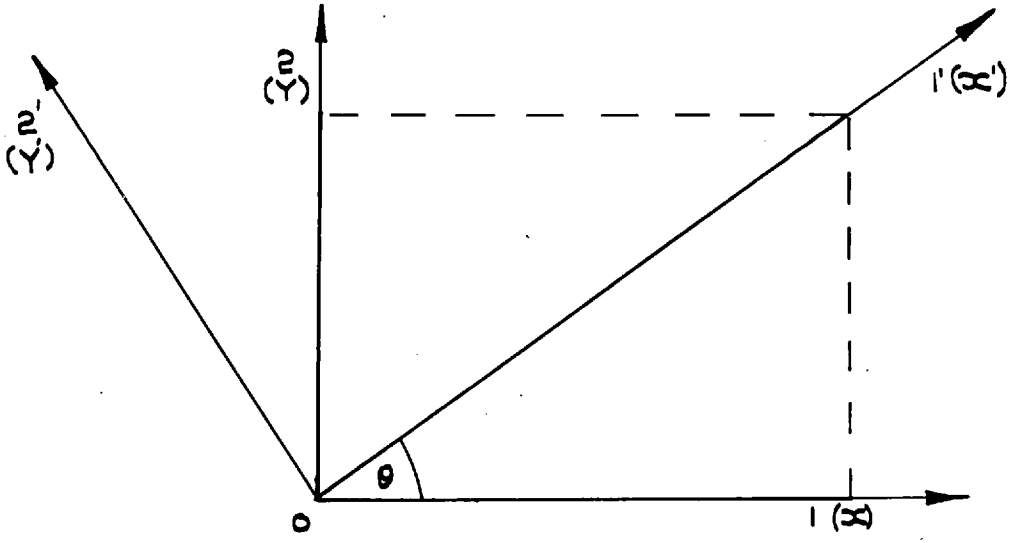

FIG. 1·1 Reference Axes

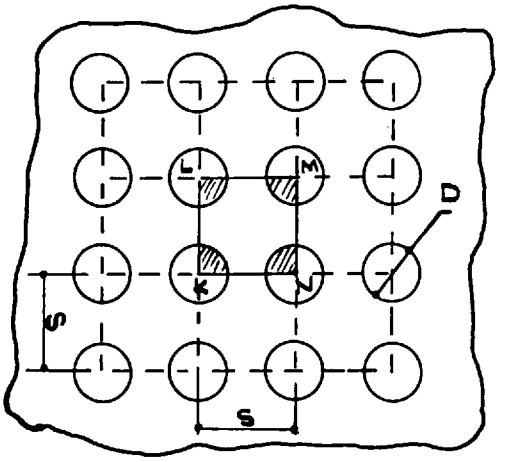

FIG 1.2

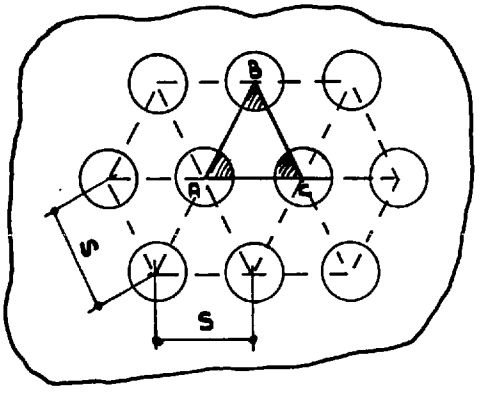

FIG 1.3

Two Types of Fibre Arrangement

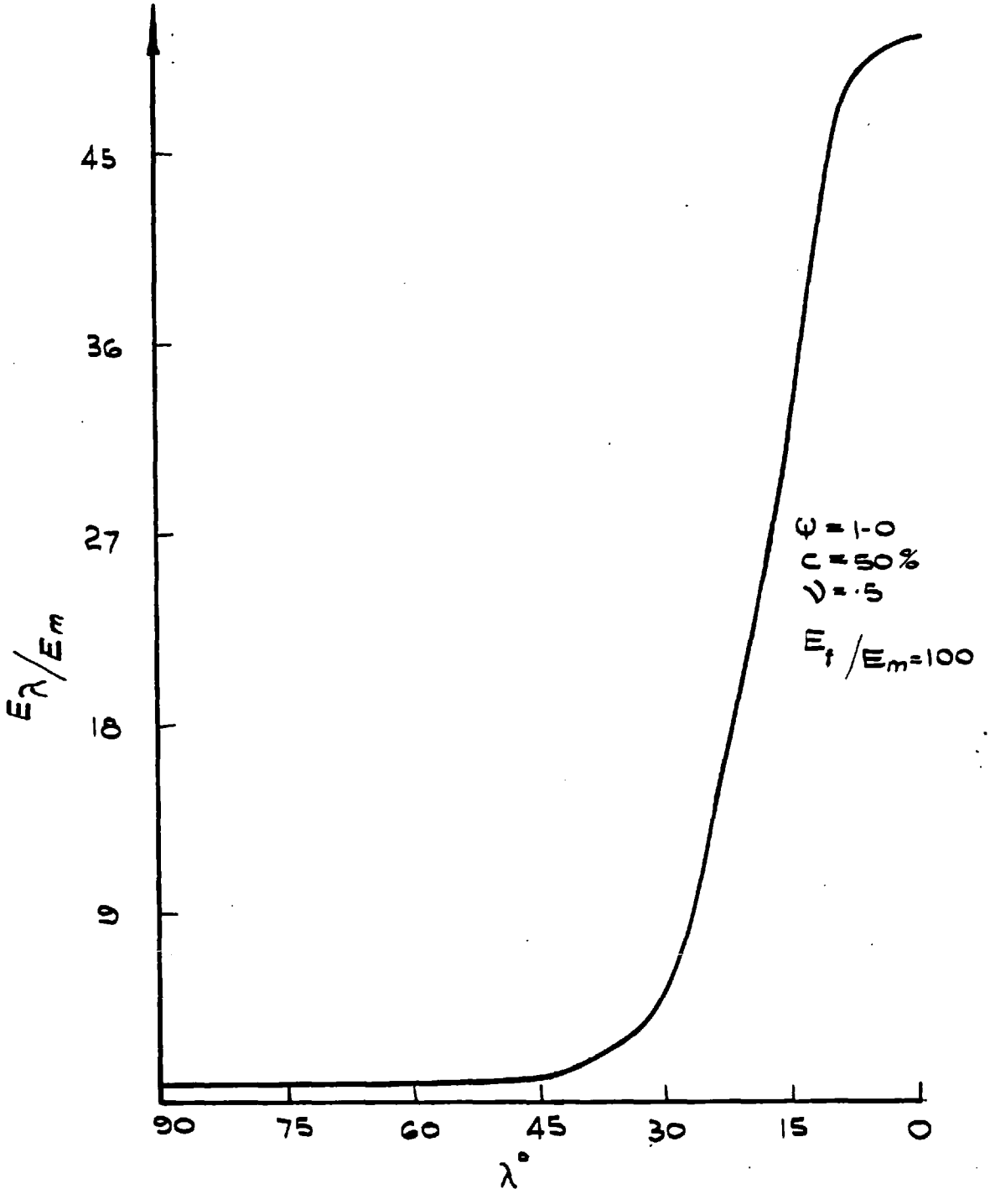

G.1.1 The variation of the directional Young's modulus for a unidirectional reinforced composite.

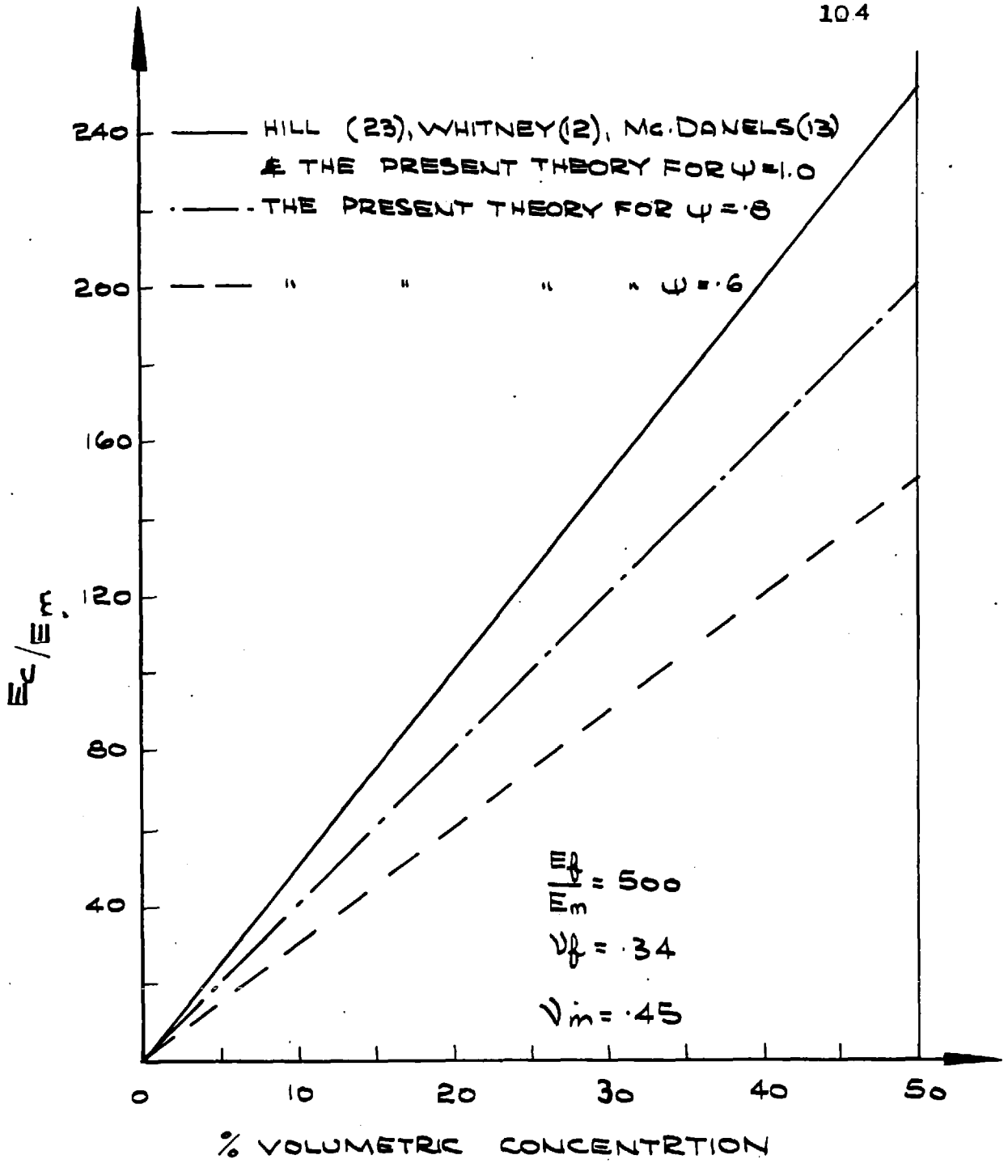

G.1.2 **The variation of the Young's modulus of a unidirectional reinforced composite.**

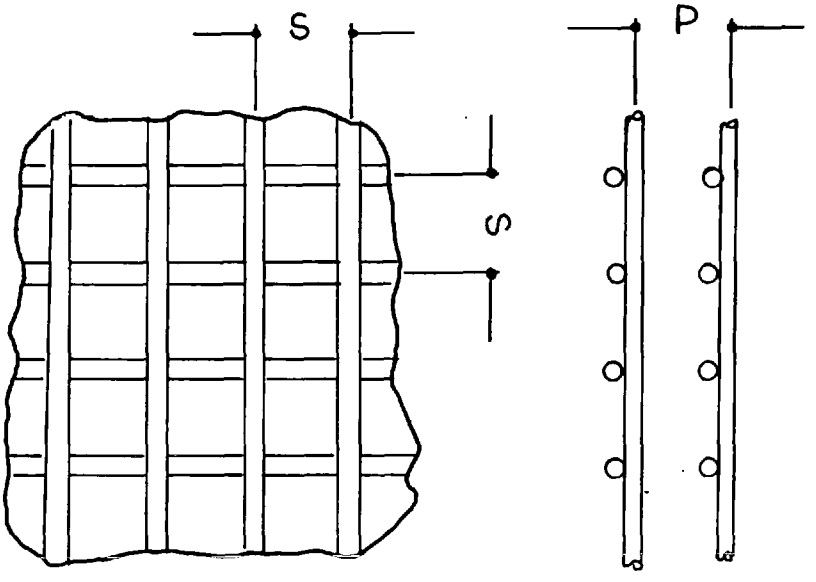

FIG.1.4 **Fibre array for cross-reinforcement**

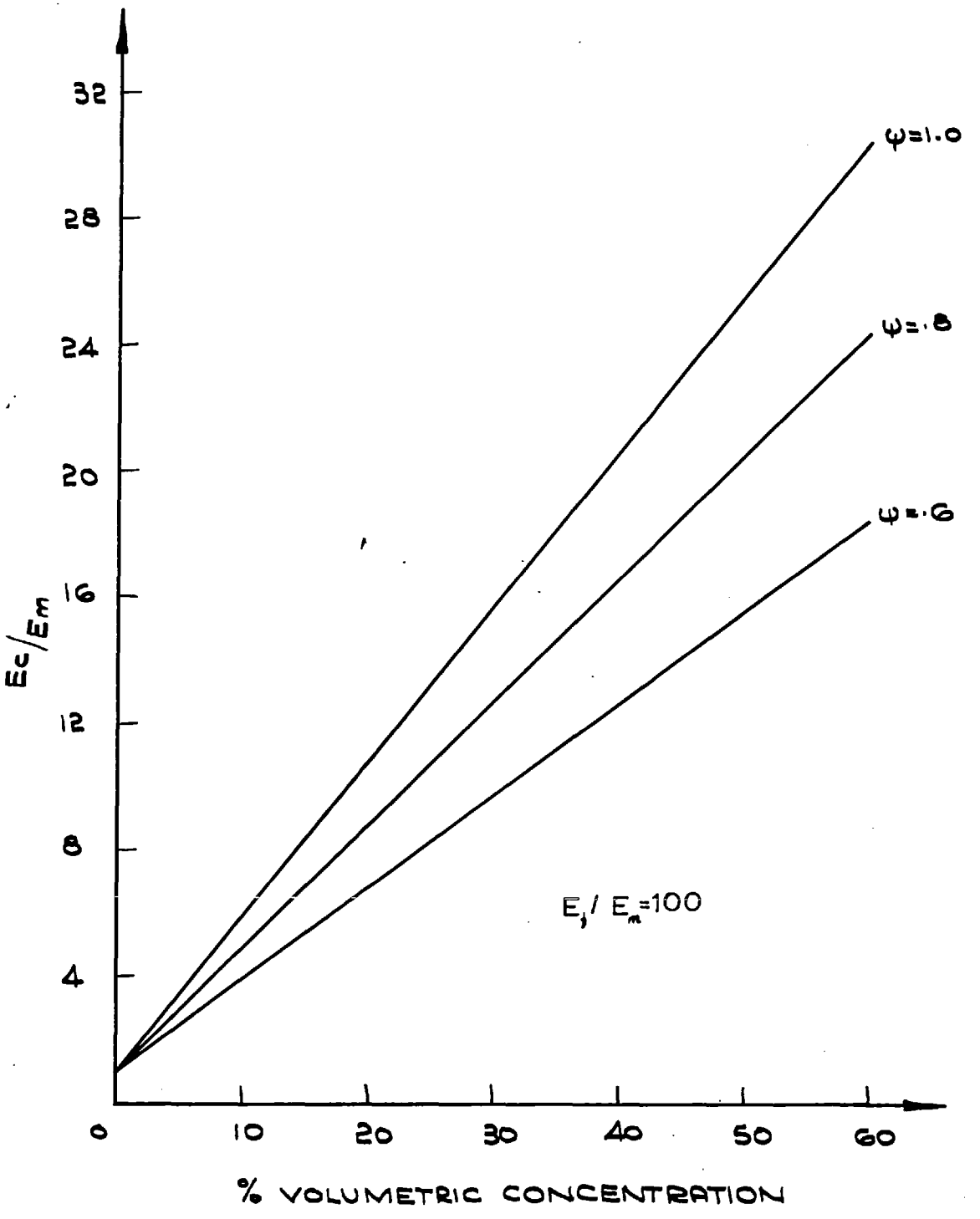

G.1.3 **Variation of the Young's modulus for a cross-reinforced composite.**

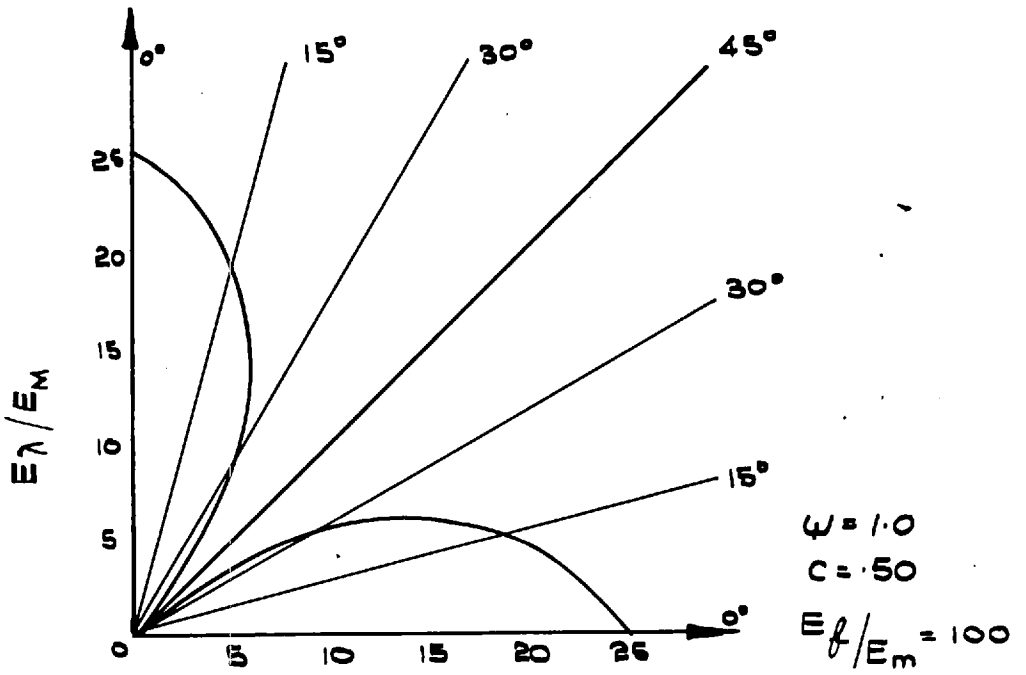

G.I.4 Variation of the directional Young's modulus for a cross-reinforced composite.

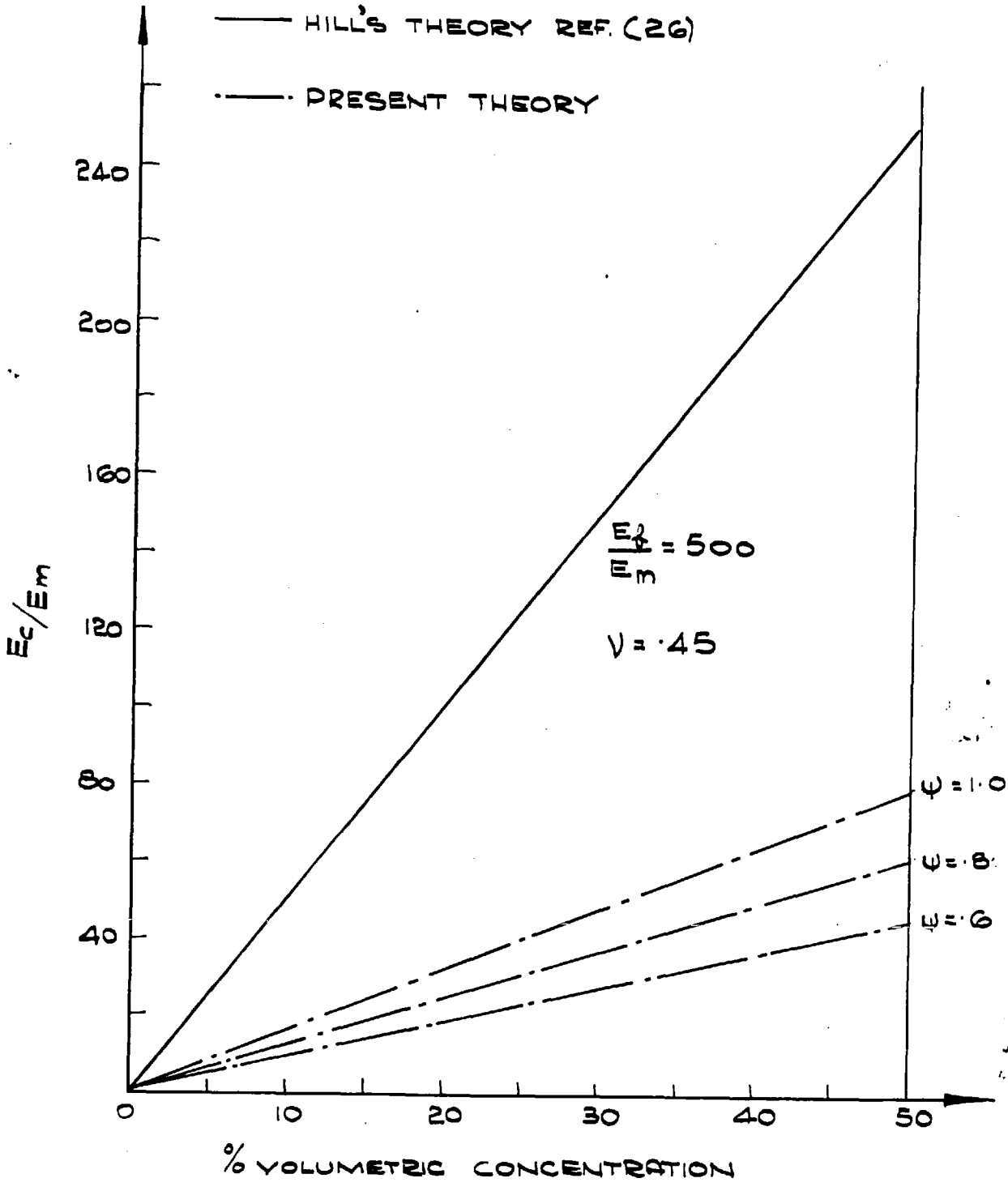

G.1.5 Comparison of the theories for 'randomly distributed' fibres reinforcement.

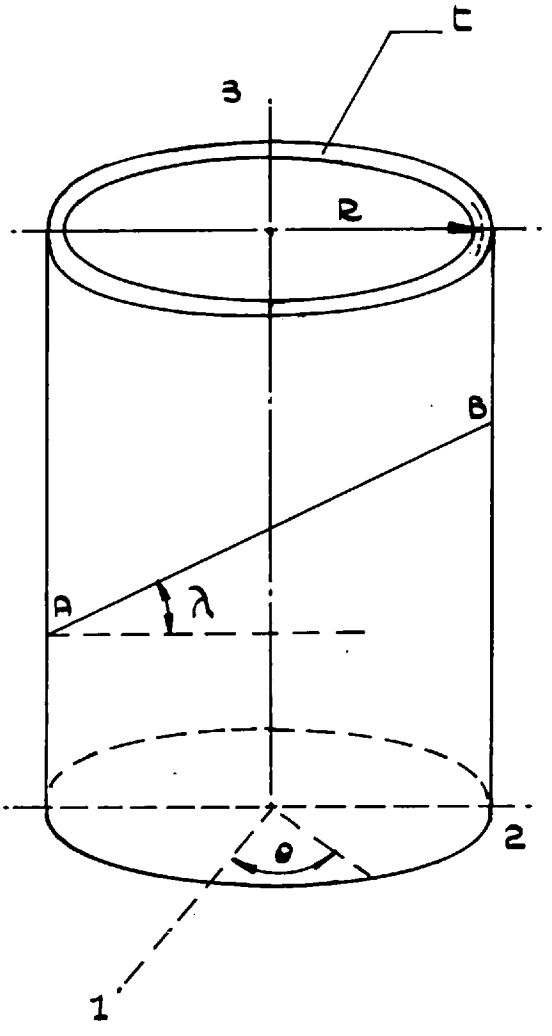

FIG. I.5. Fibre reinforced cylinder

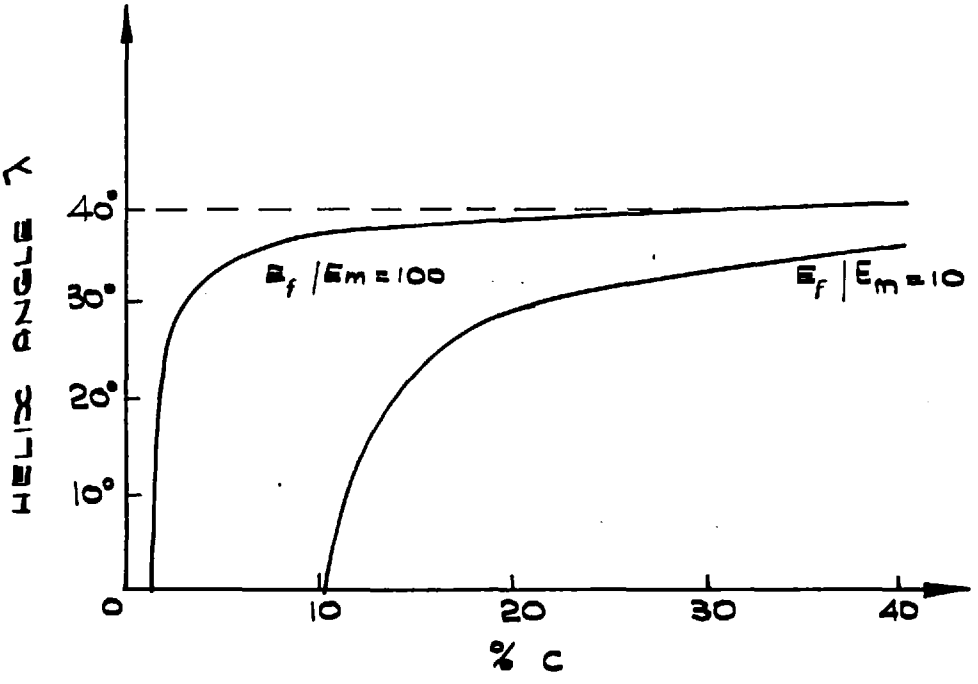

G.1.6 The variation of helix angle with respect to fibre concentration (for axial stiffness/ hoop stiffness = .5)

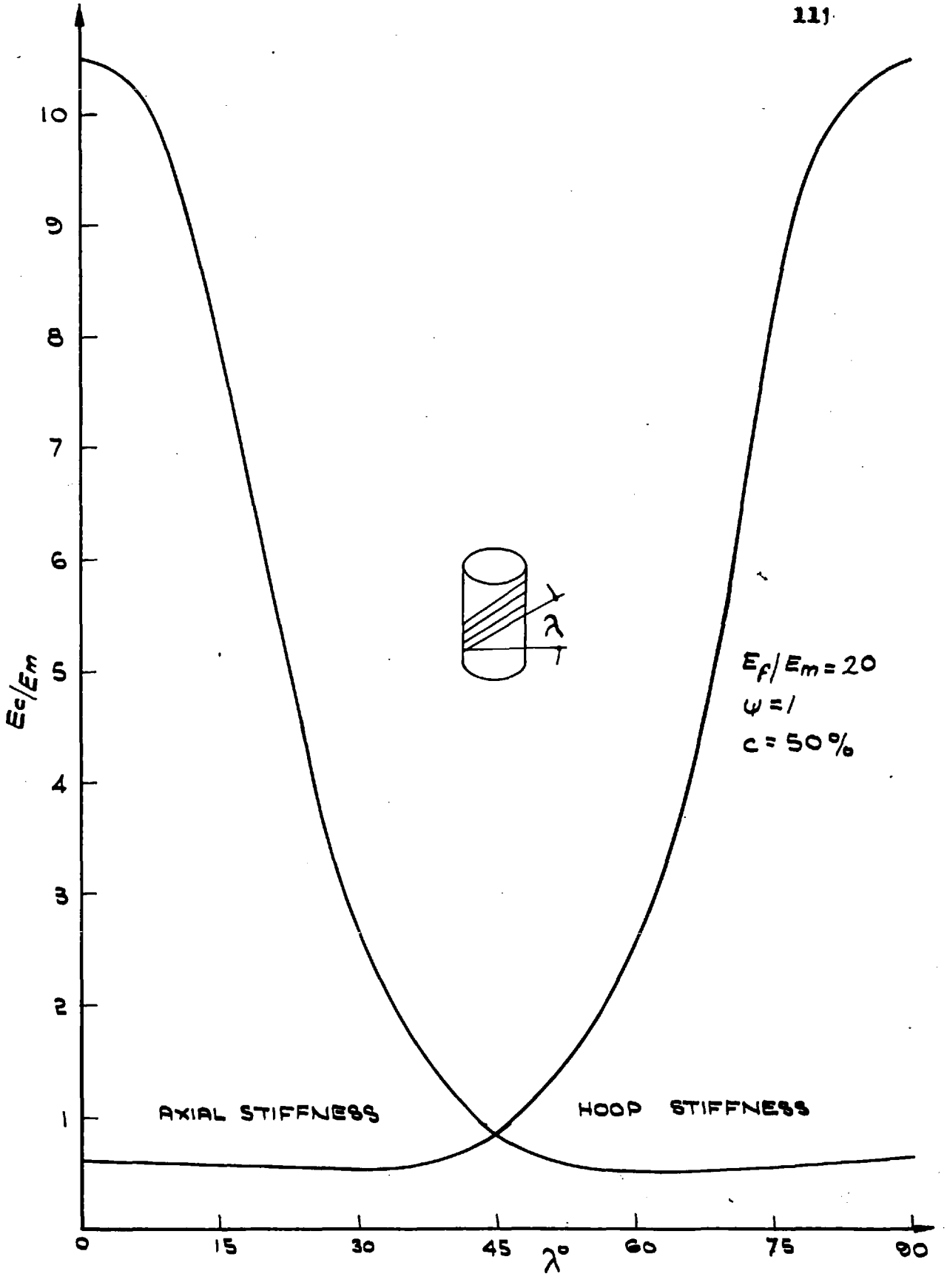

G.1.7a Variation of stiffnesses with respect to fibre orientation.

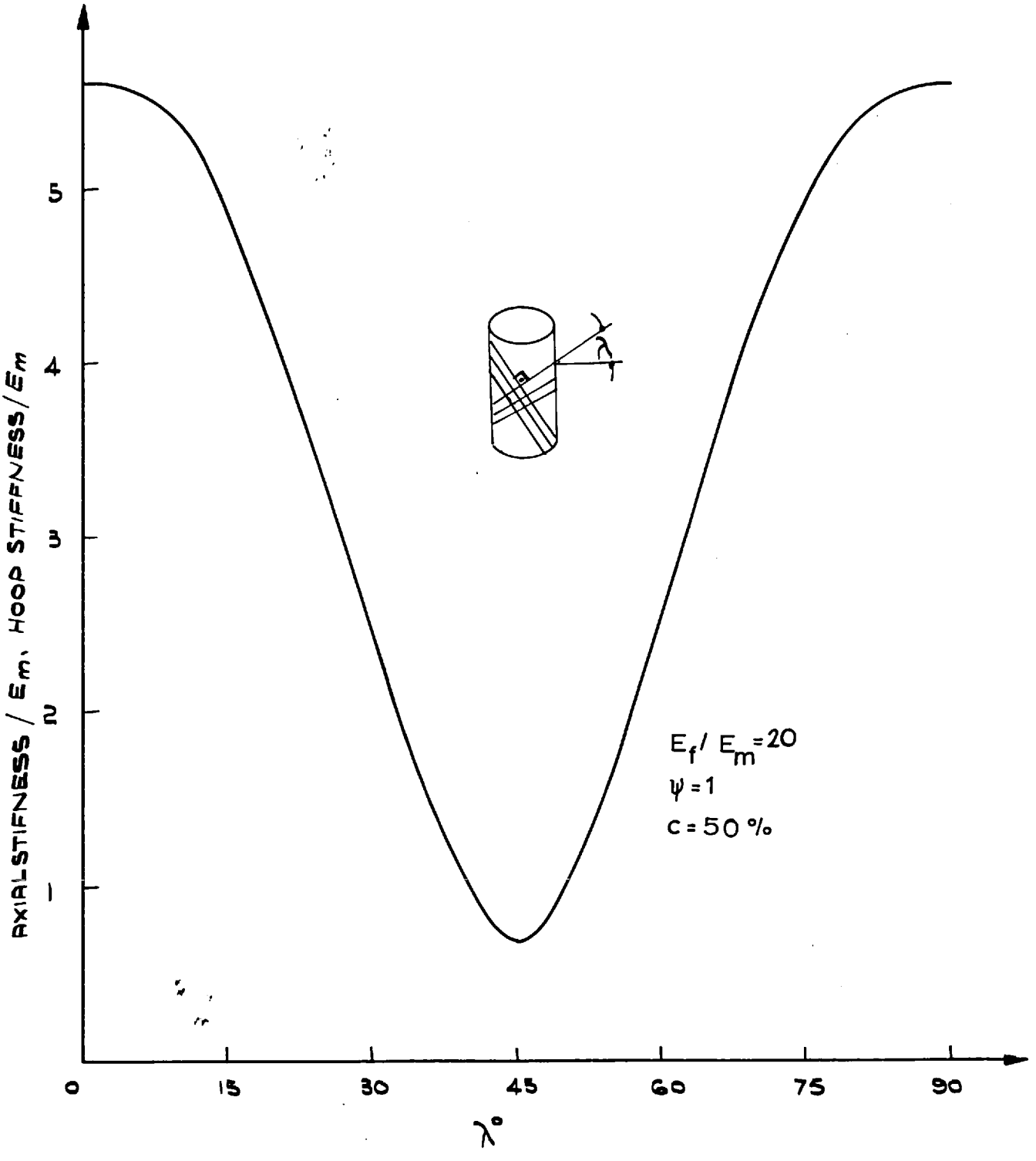

G.1.7b Variation of stiffnesses with respect to fibre orientation.

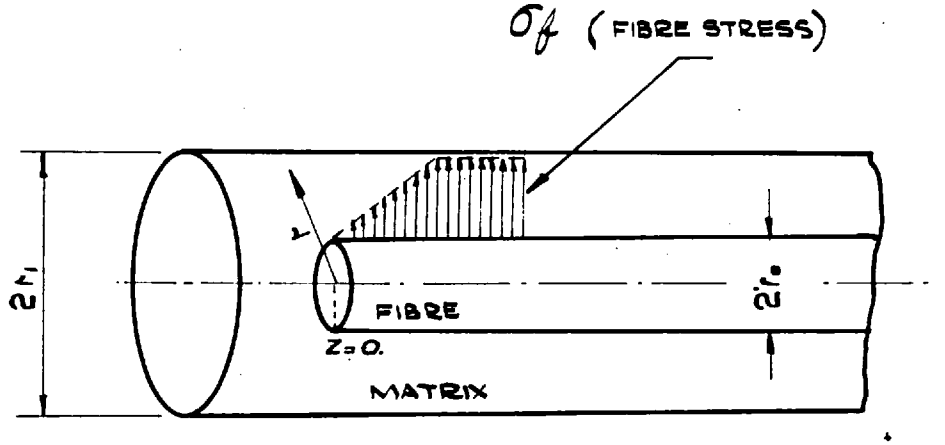

FIG I.6 Stress build-up at the end of a fibre matrix interphase.

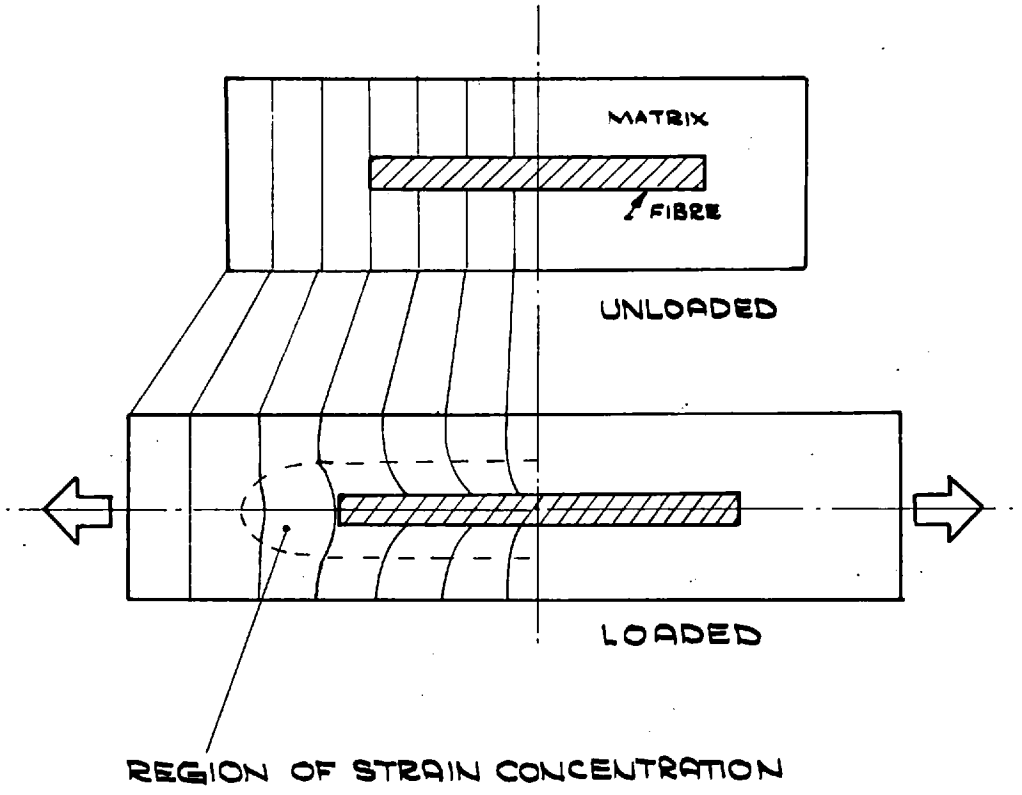

FIG. 1.7 Schematic representation of micro strain differences between two phases.

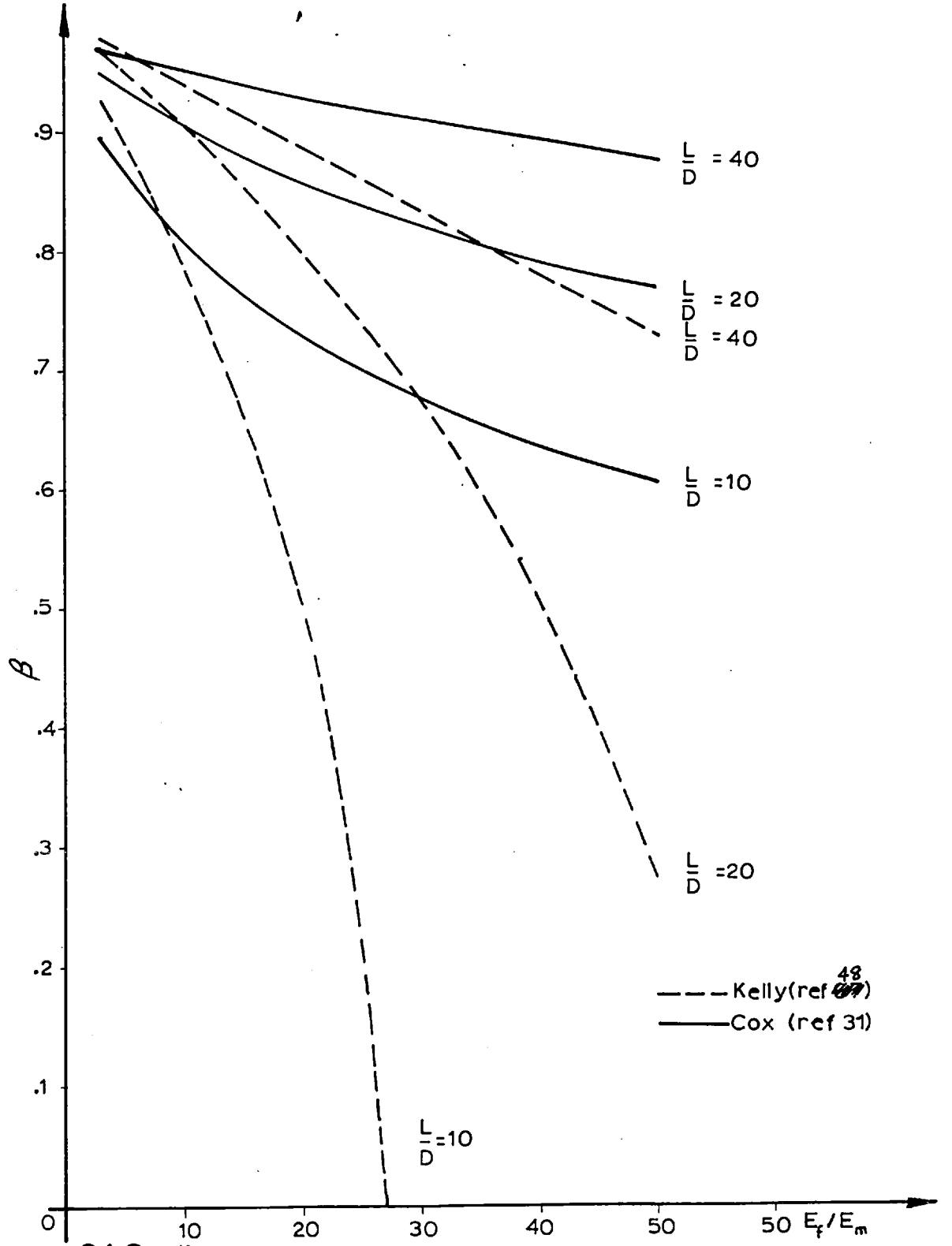

G.1.8 Theoretical Variation of β

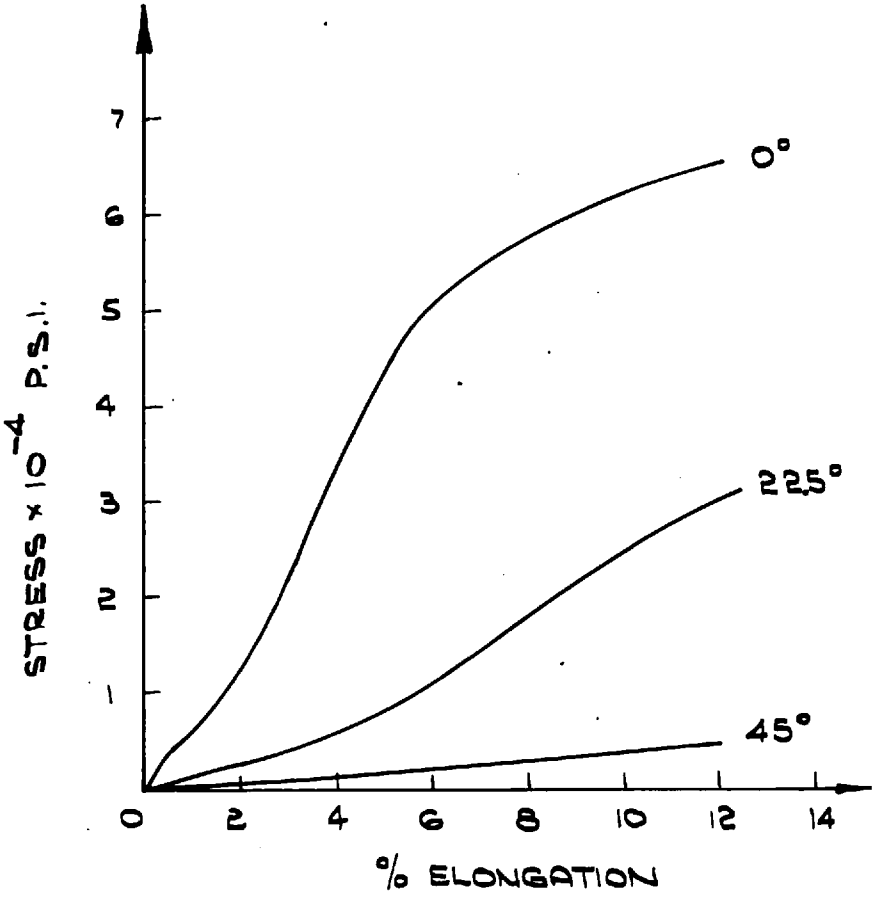

G.2.1 Stress/strain relationships for iron gauze

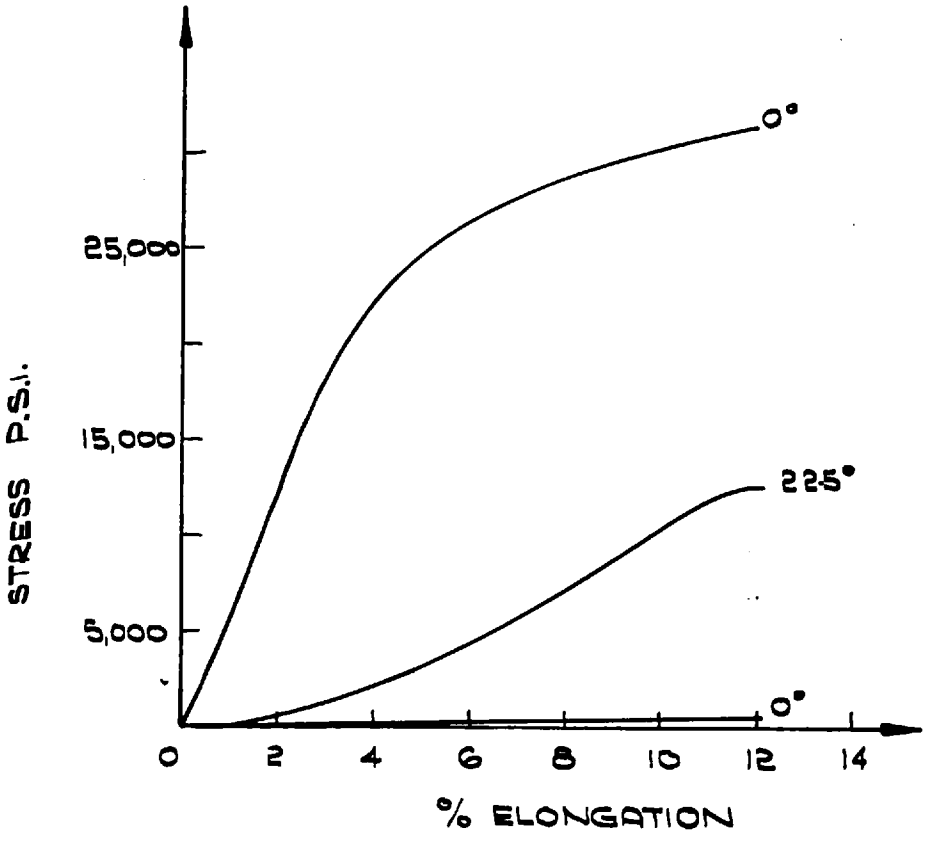

G.2.2 Stress/strain relationships for copper gauze

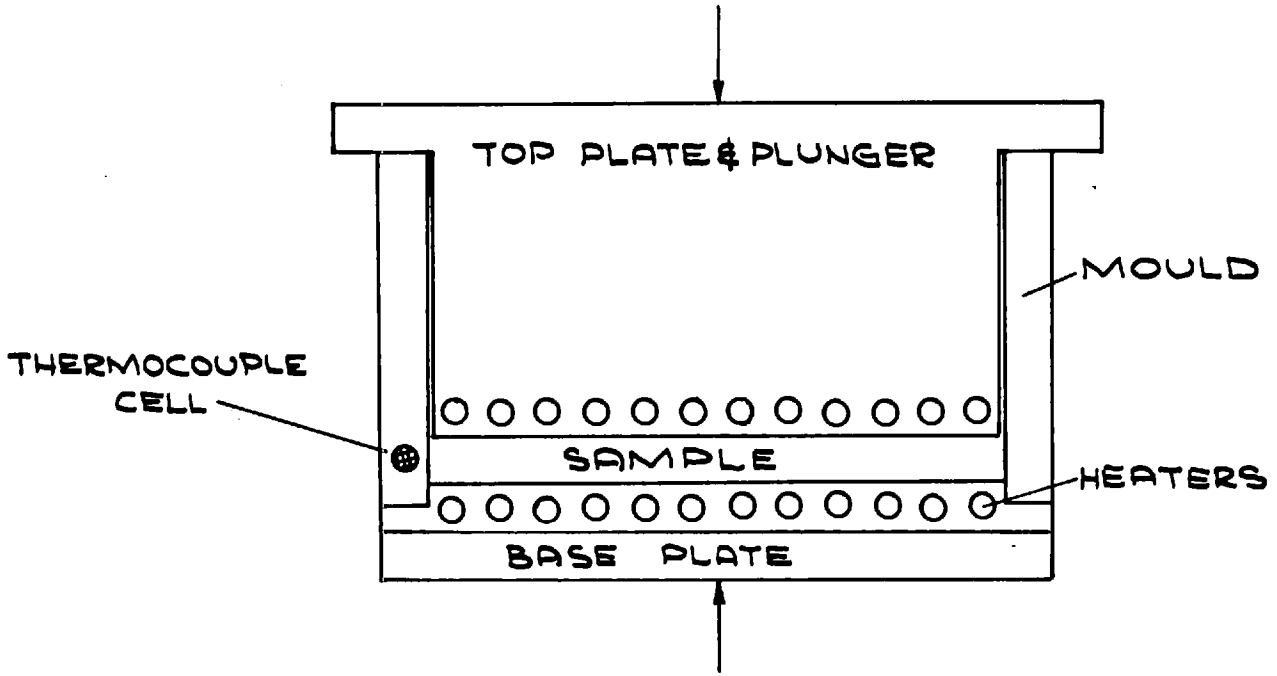

FIG. 2.1 Diagrammatical representation of compression moulding

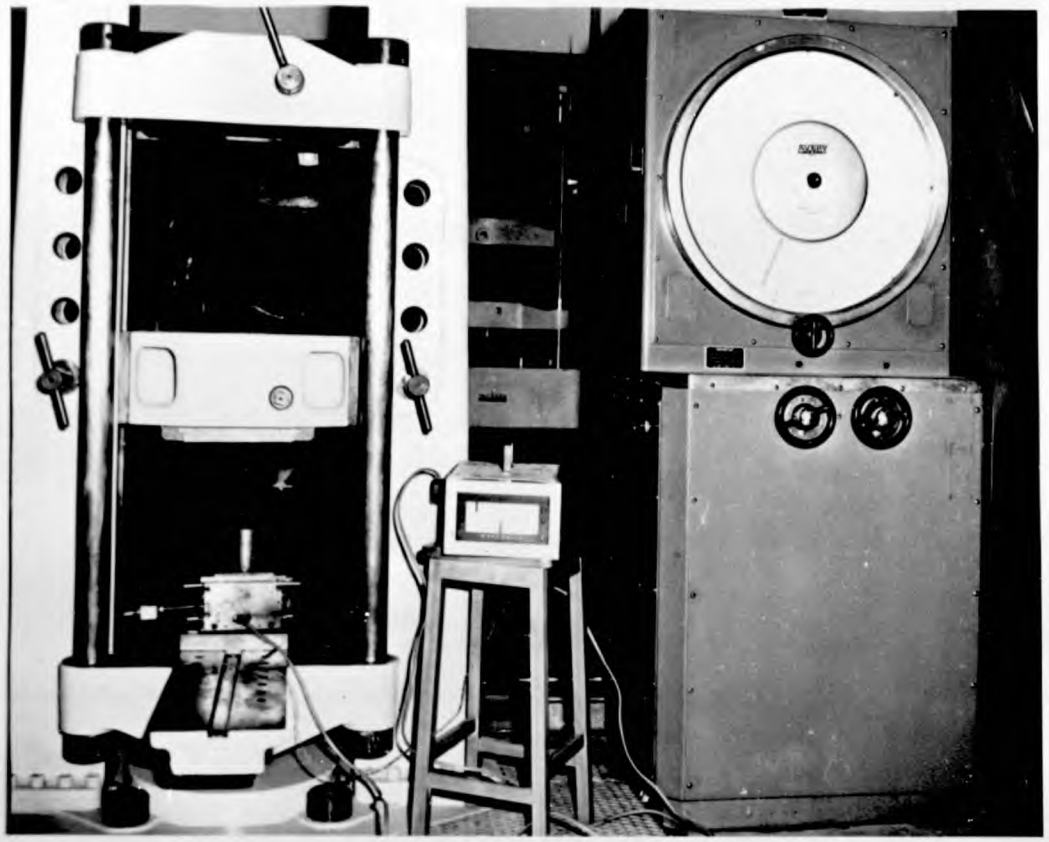

FIG.2.1 Set up for moulding uni directional and cross reinforced

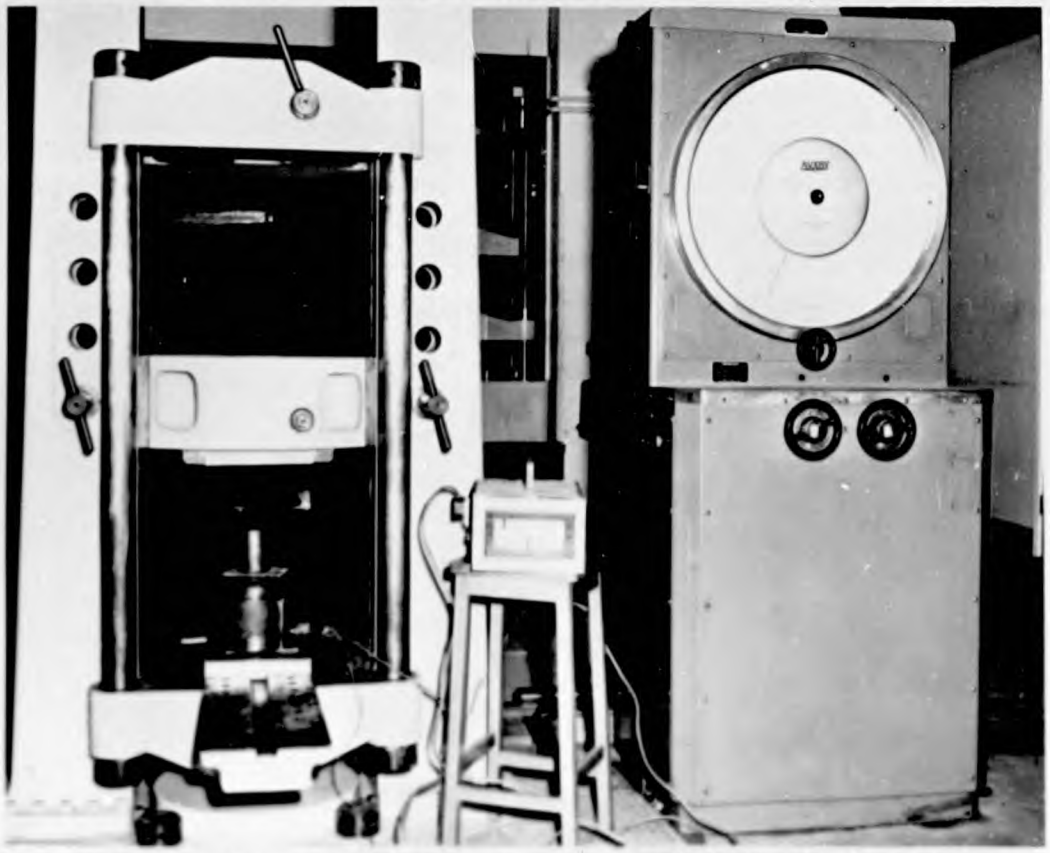

FIG.2.2 Set up for moulding randomly distributed composites

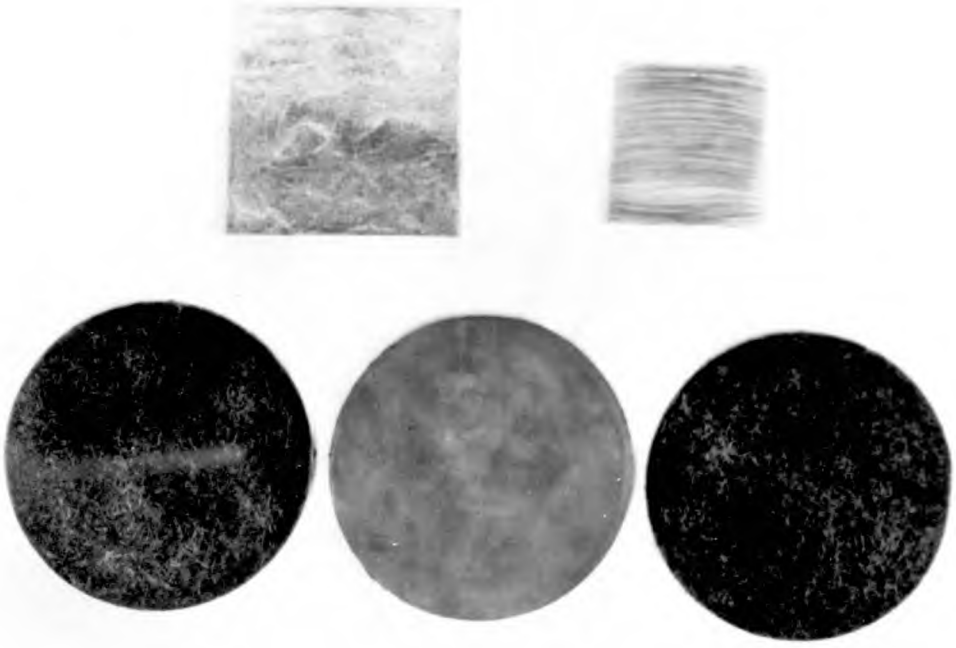

FIG.2.3 Composites removed from the mould

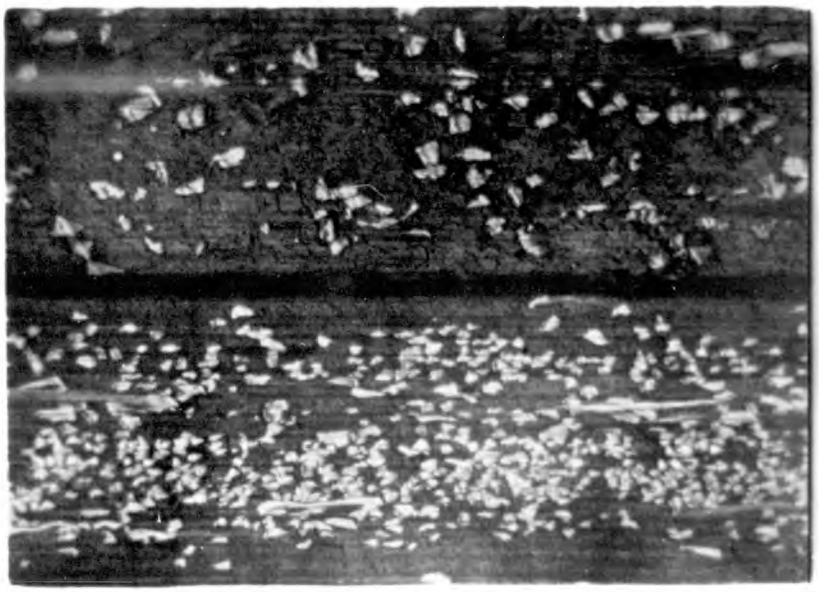

FIG.2.4 Cross-sections of alum. and bronze reinforced propathene

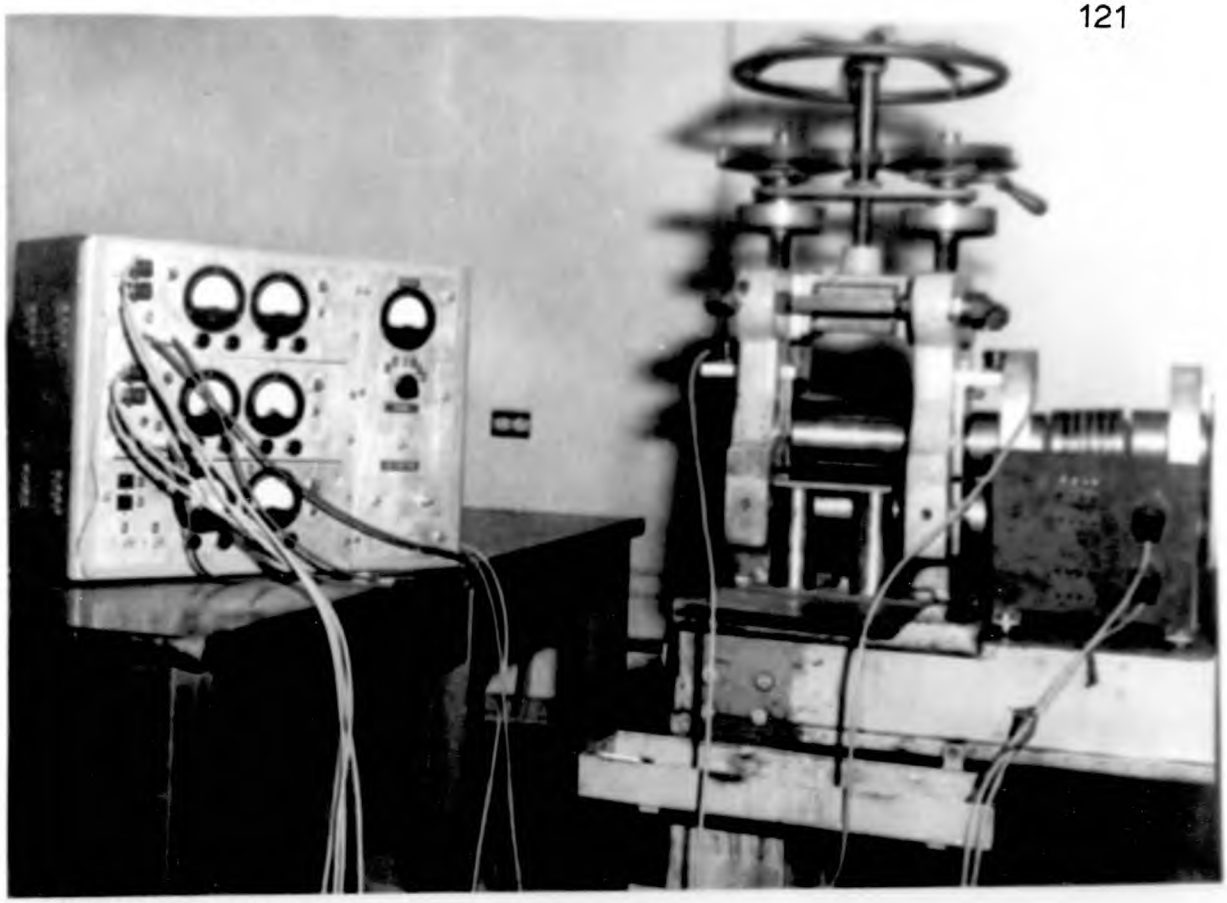

FIG.2.5 Rolling Mill

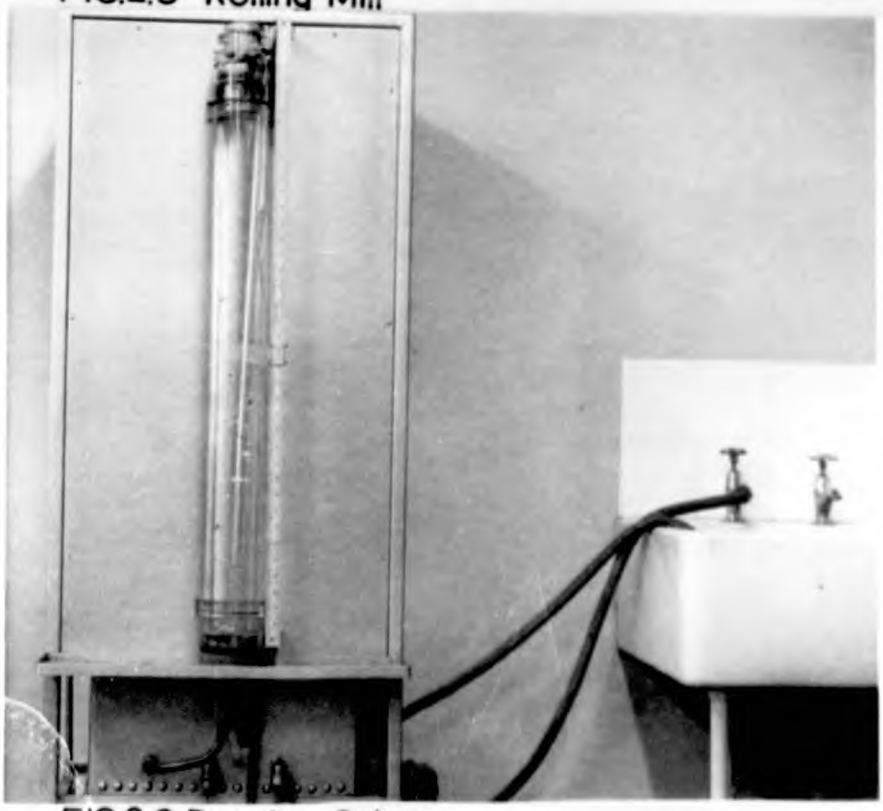

FIG.2.6 Density Column

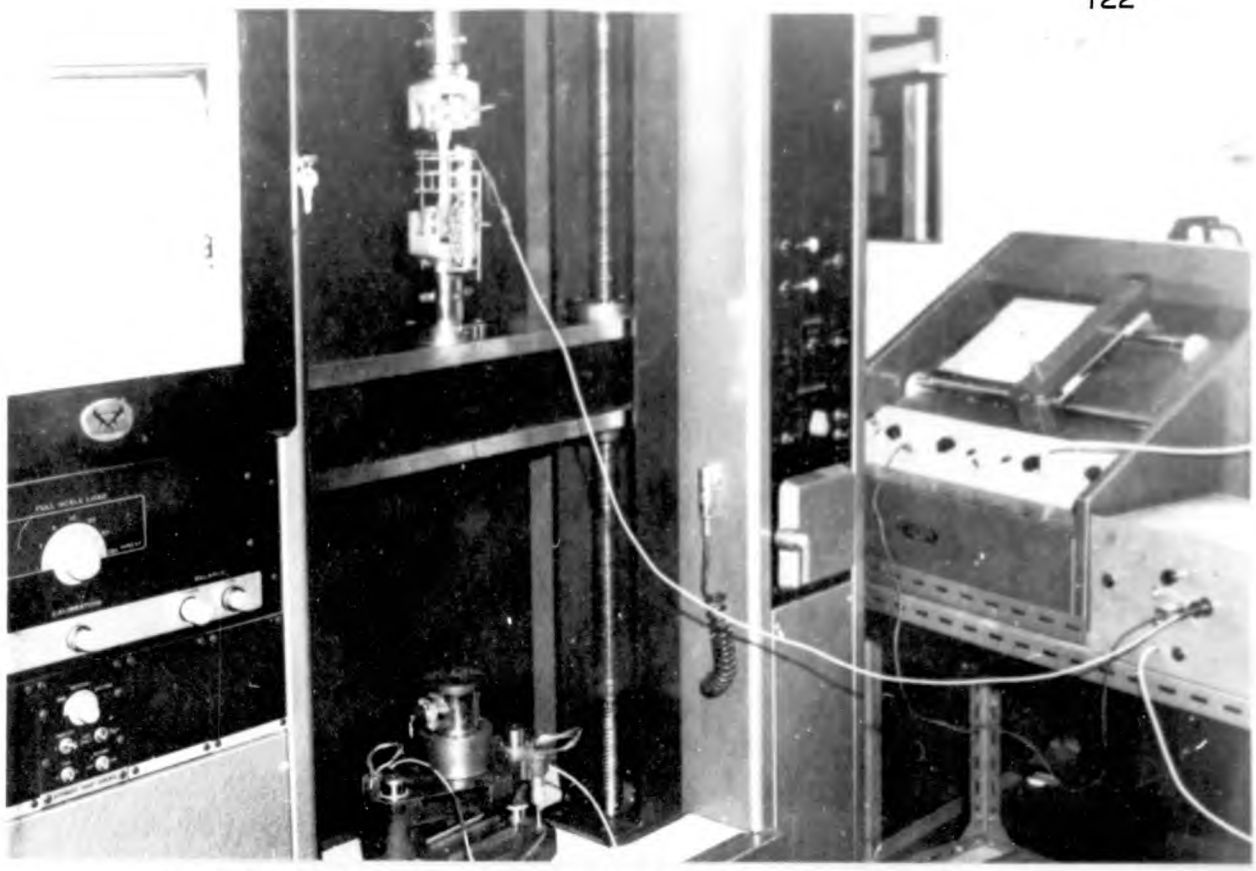

FIG. 2.7. Set up for tensile tests

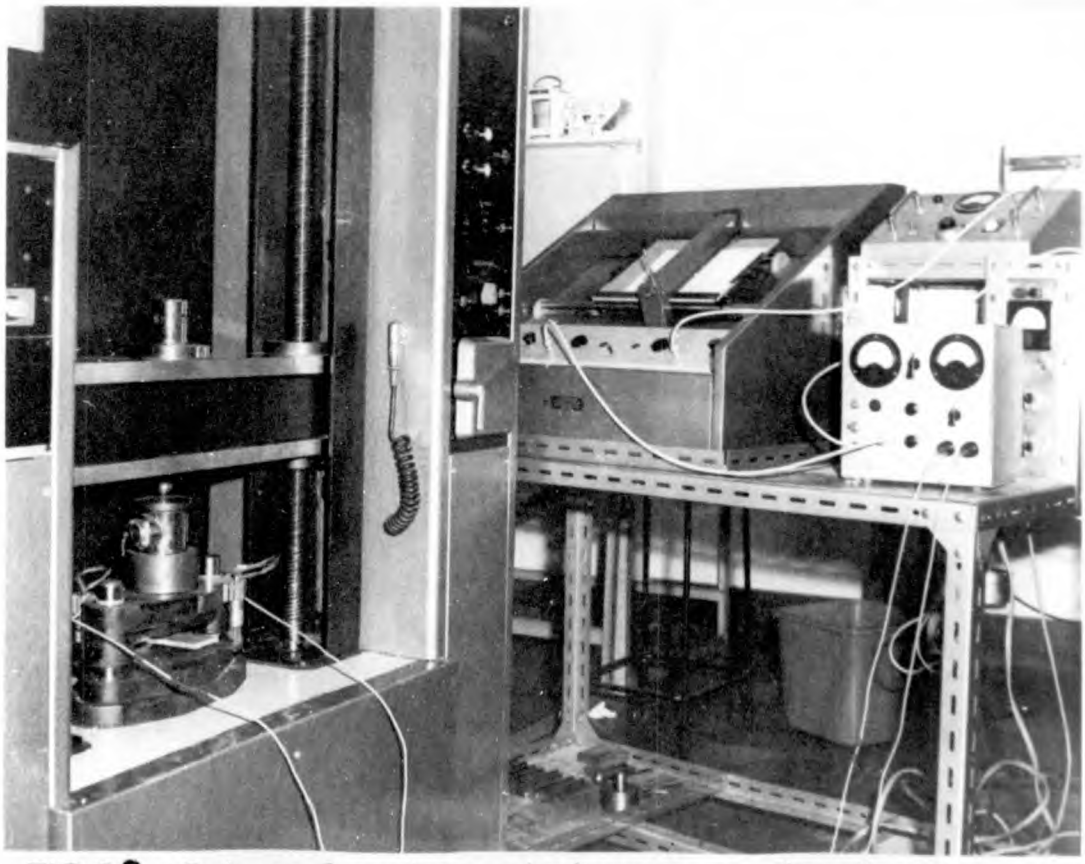

FIG. 2.8.a Set up for plane strain compression tests

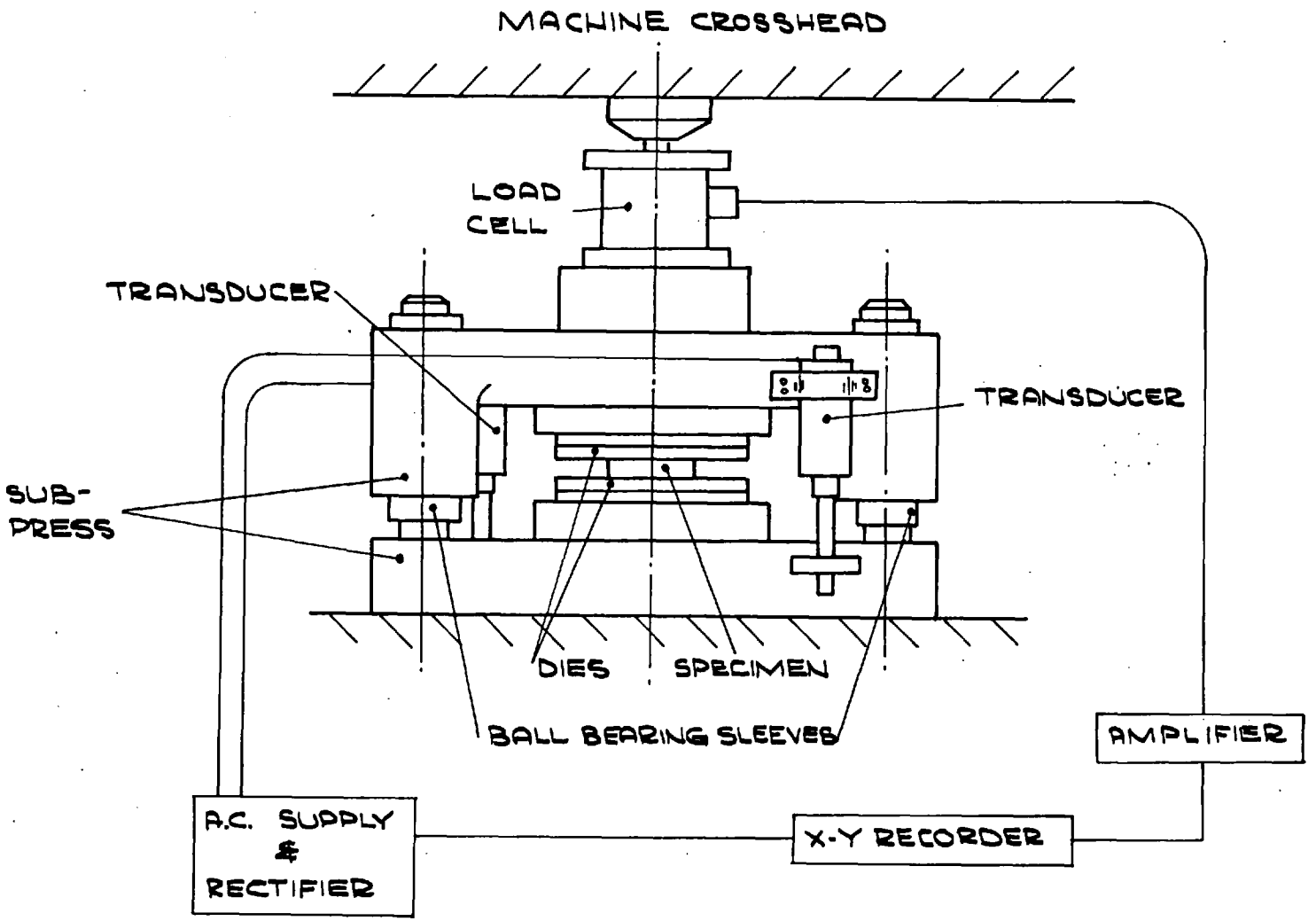

FIG. 2.8.b Instrumented sub-press

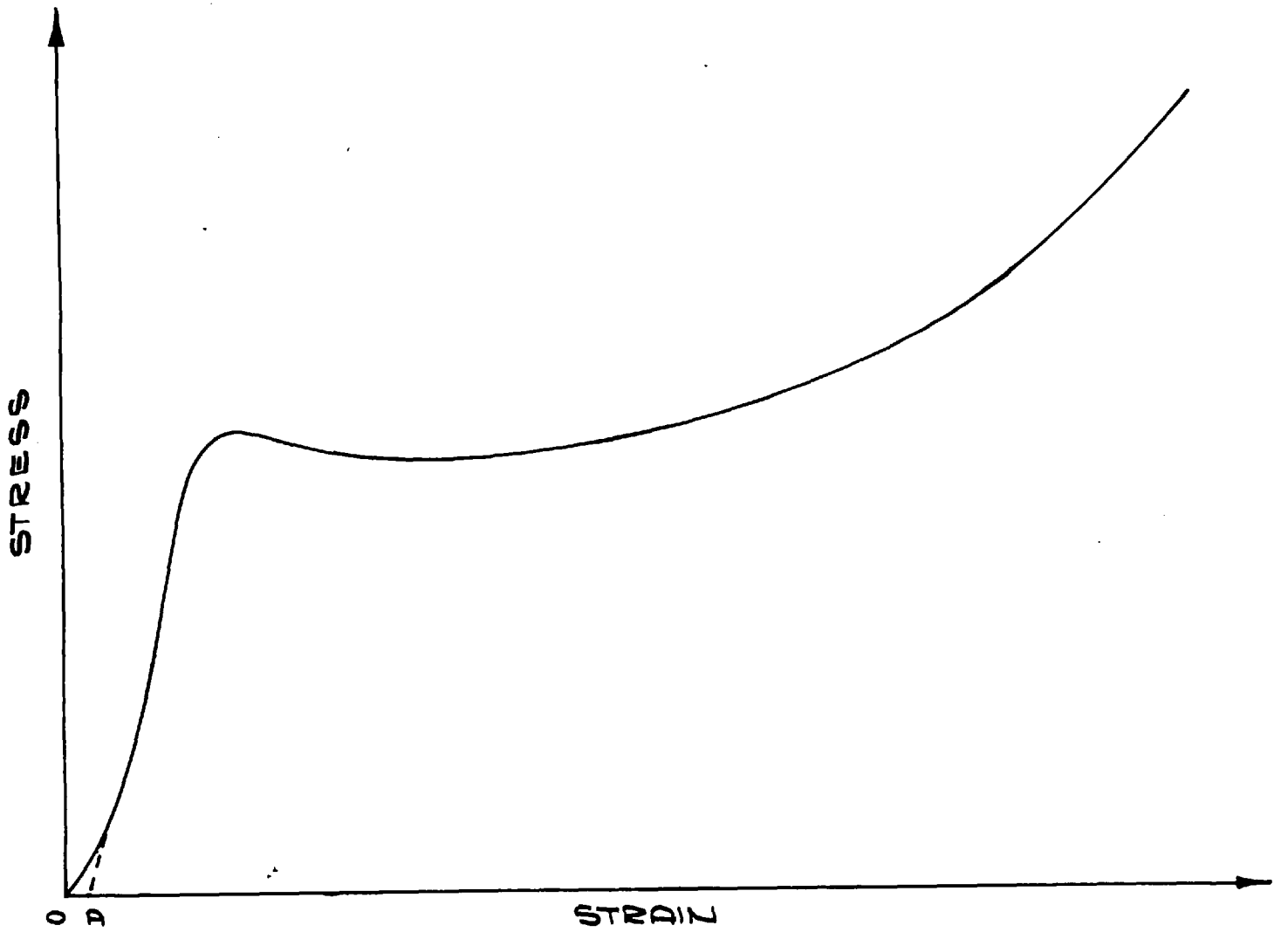

G.2.3 Stress/strain curve for P.V.C. obtained from plane strain compression test

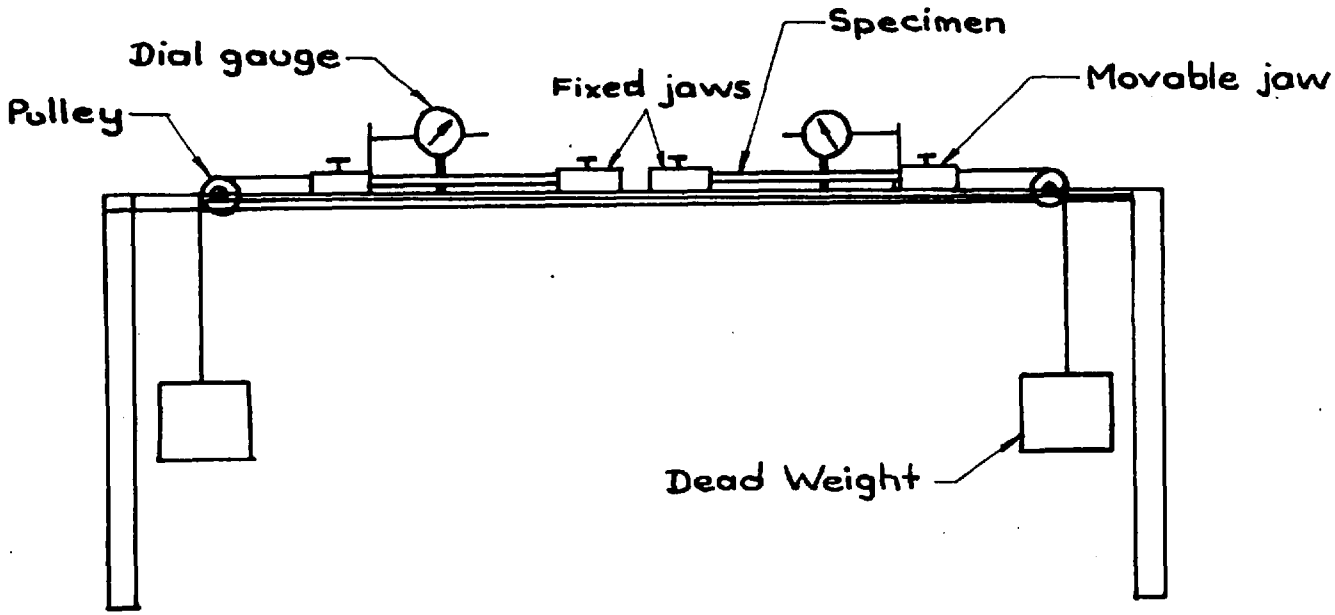

FIG.29 **Diagrammatical representation of creep tests**

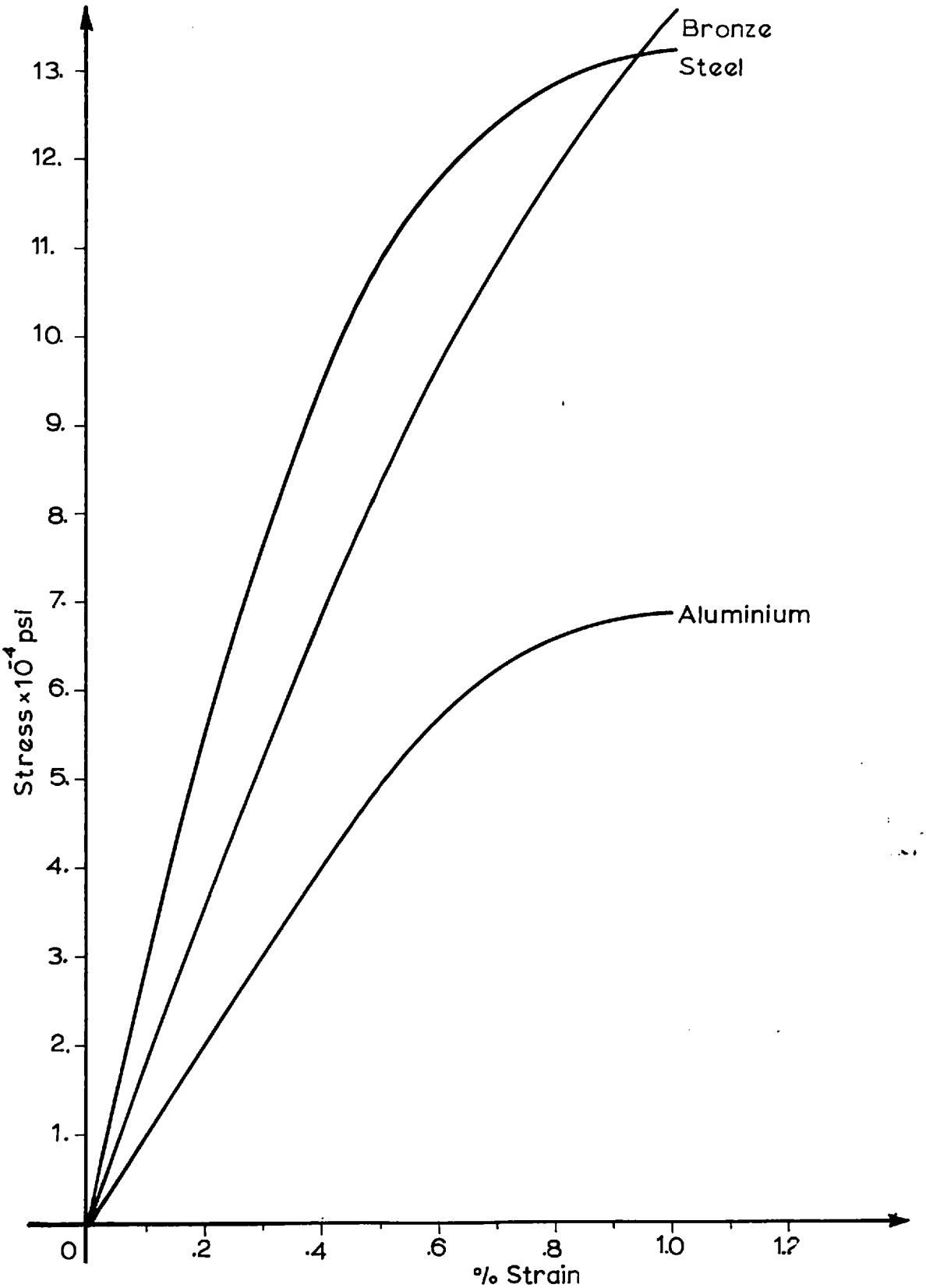

G.2.4 **Stress/strain relationships for the metal f .bres**

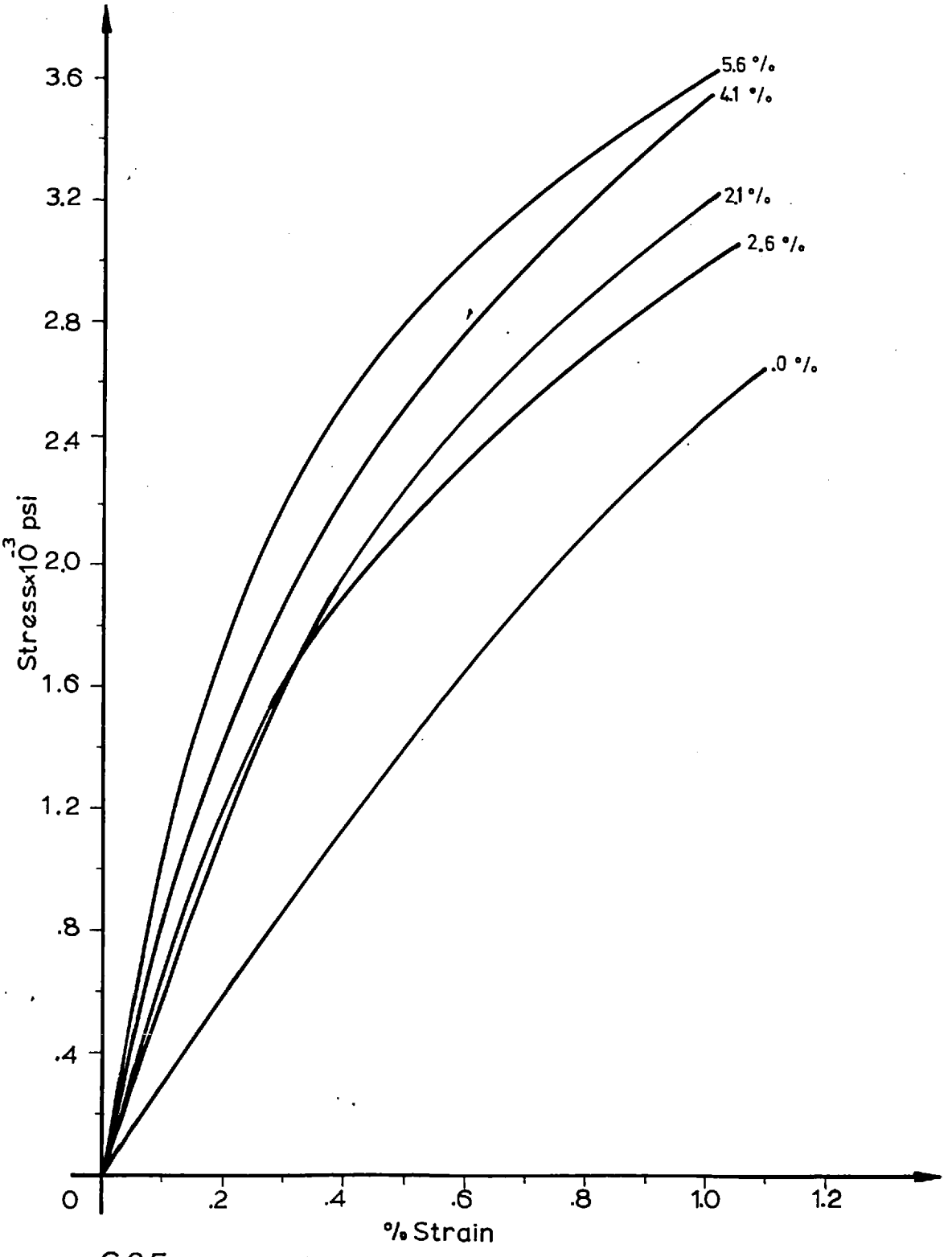

G.2.5 **Stress/strain relationships for unidirectional reinforced copper/propathene composite**

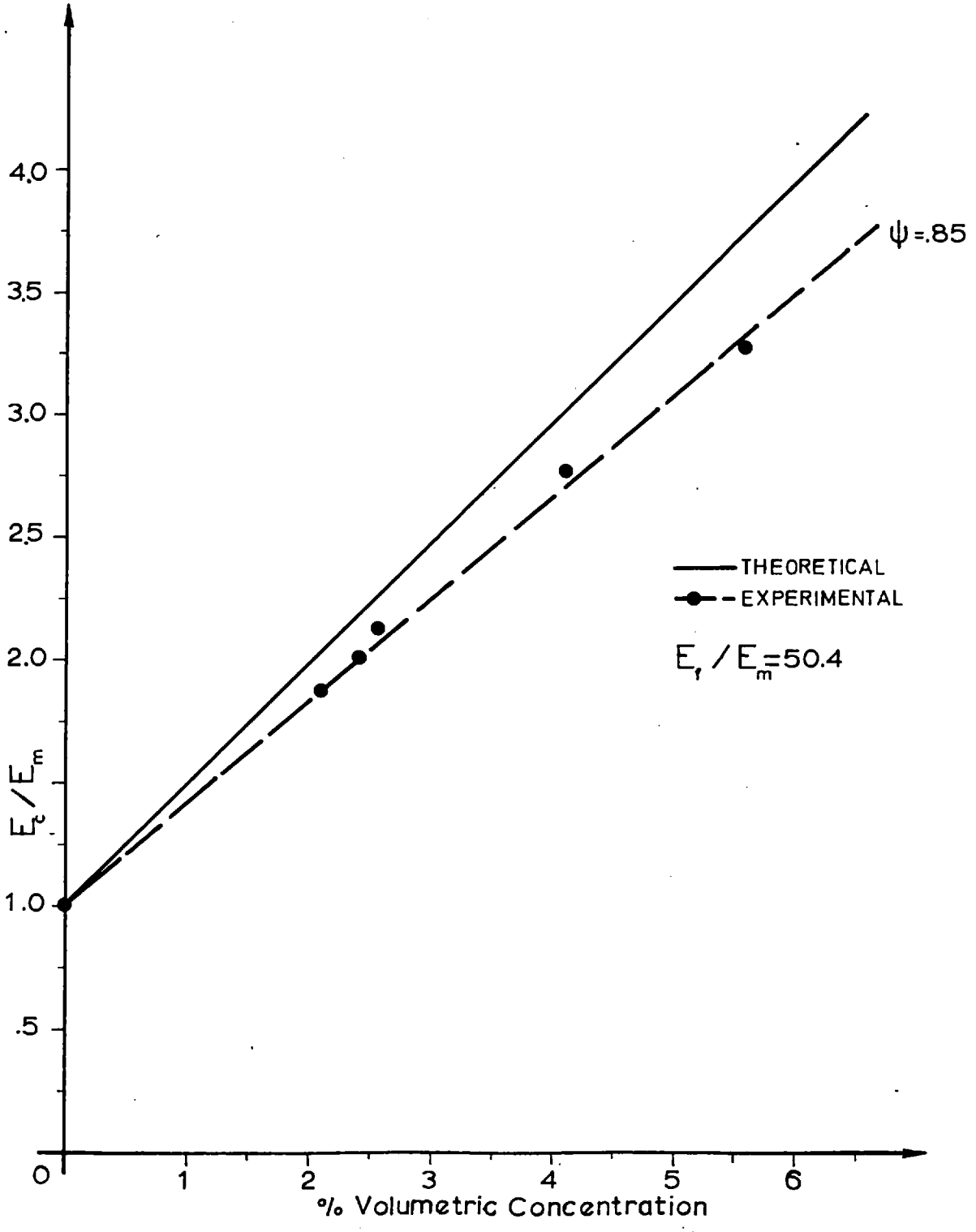

G.2.6 **Unidirectional reinforced copper/Propathene composite**

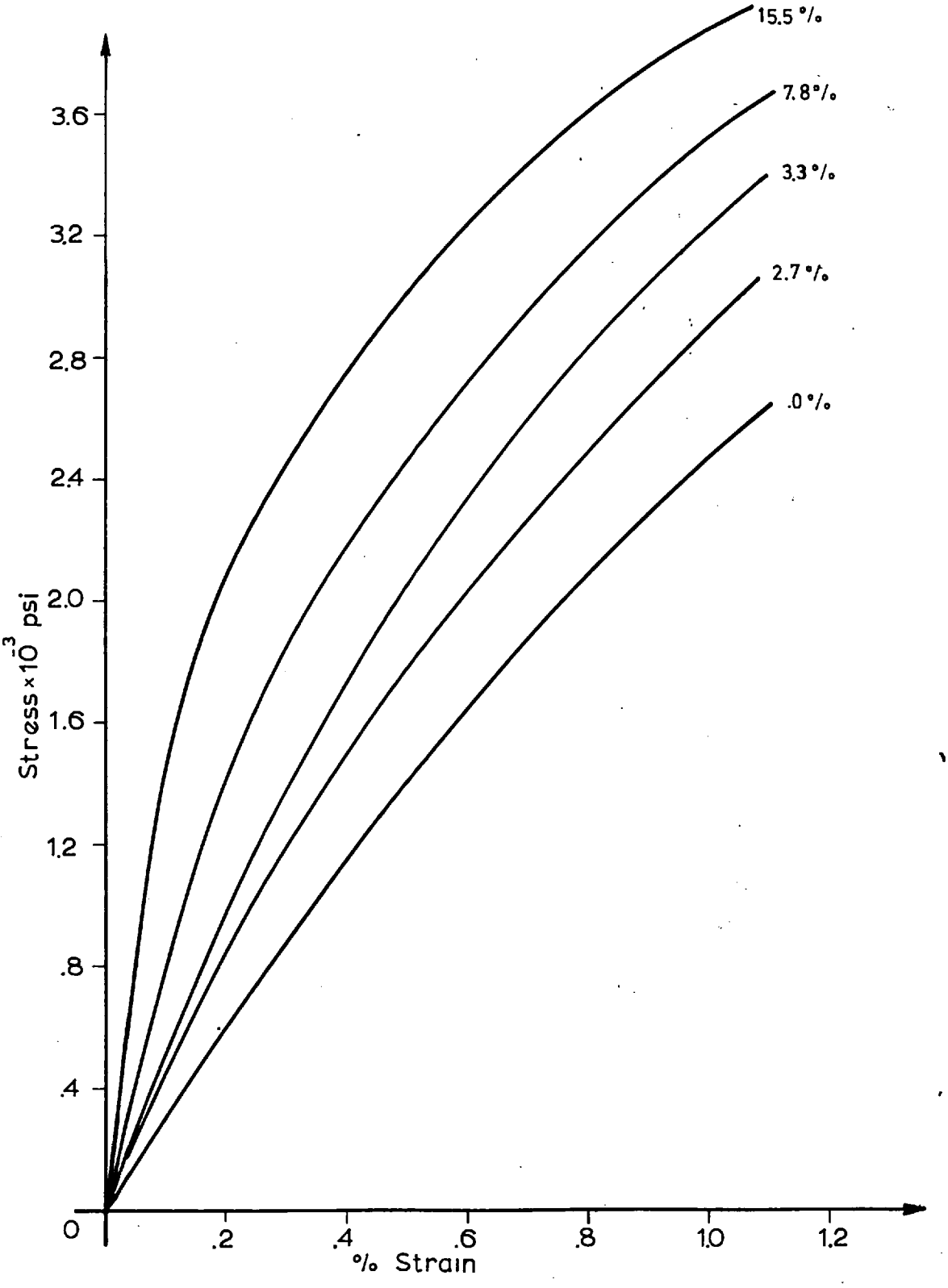

G.2.7 **Stress/strain relationships for copper gauze reinforced Propathene**

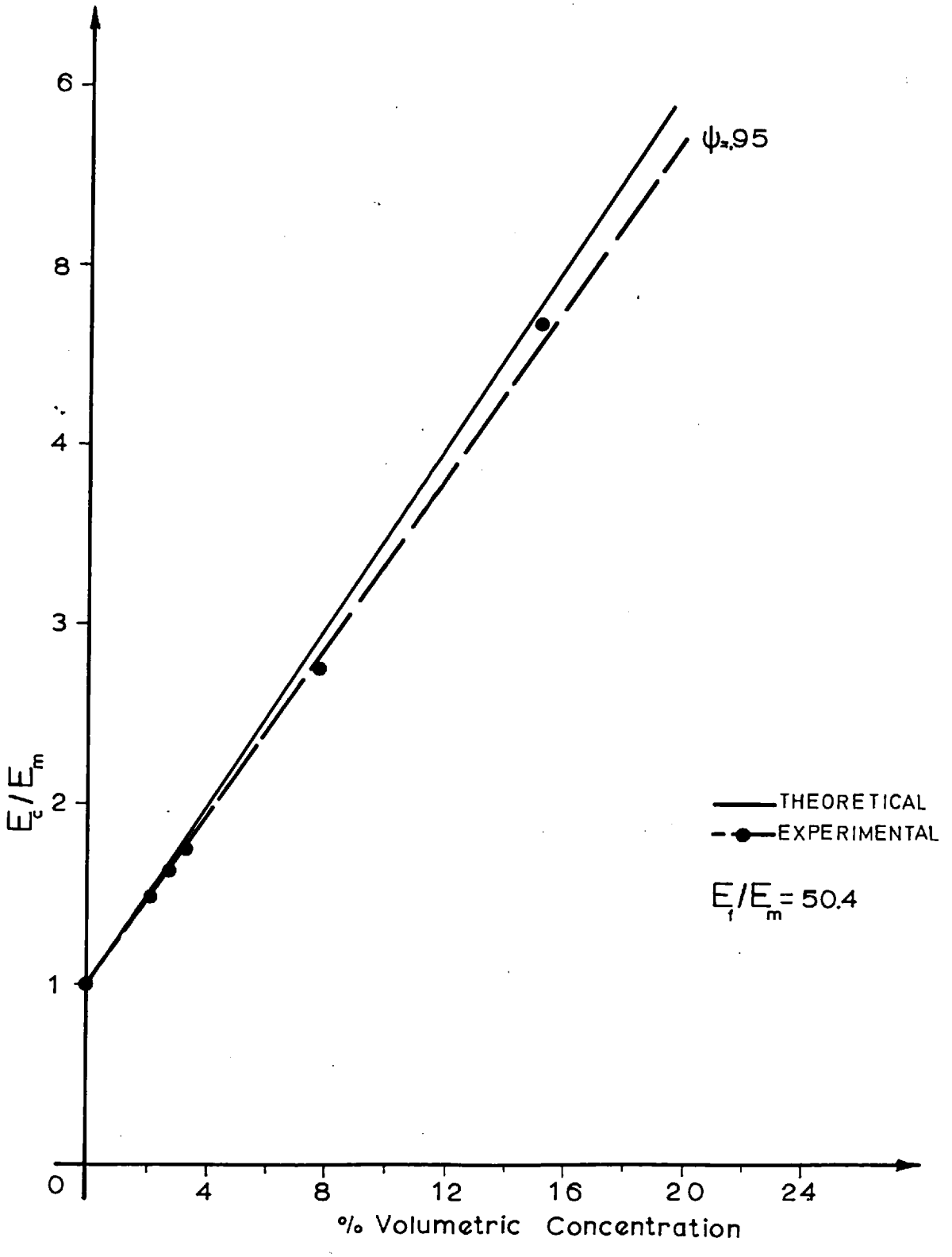

G.2.8 **Copper gauze reinforced Propathene**

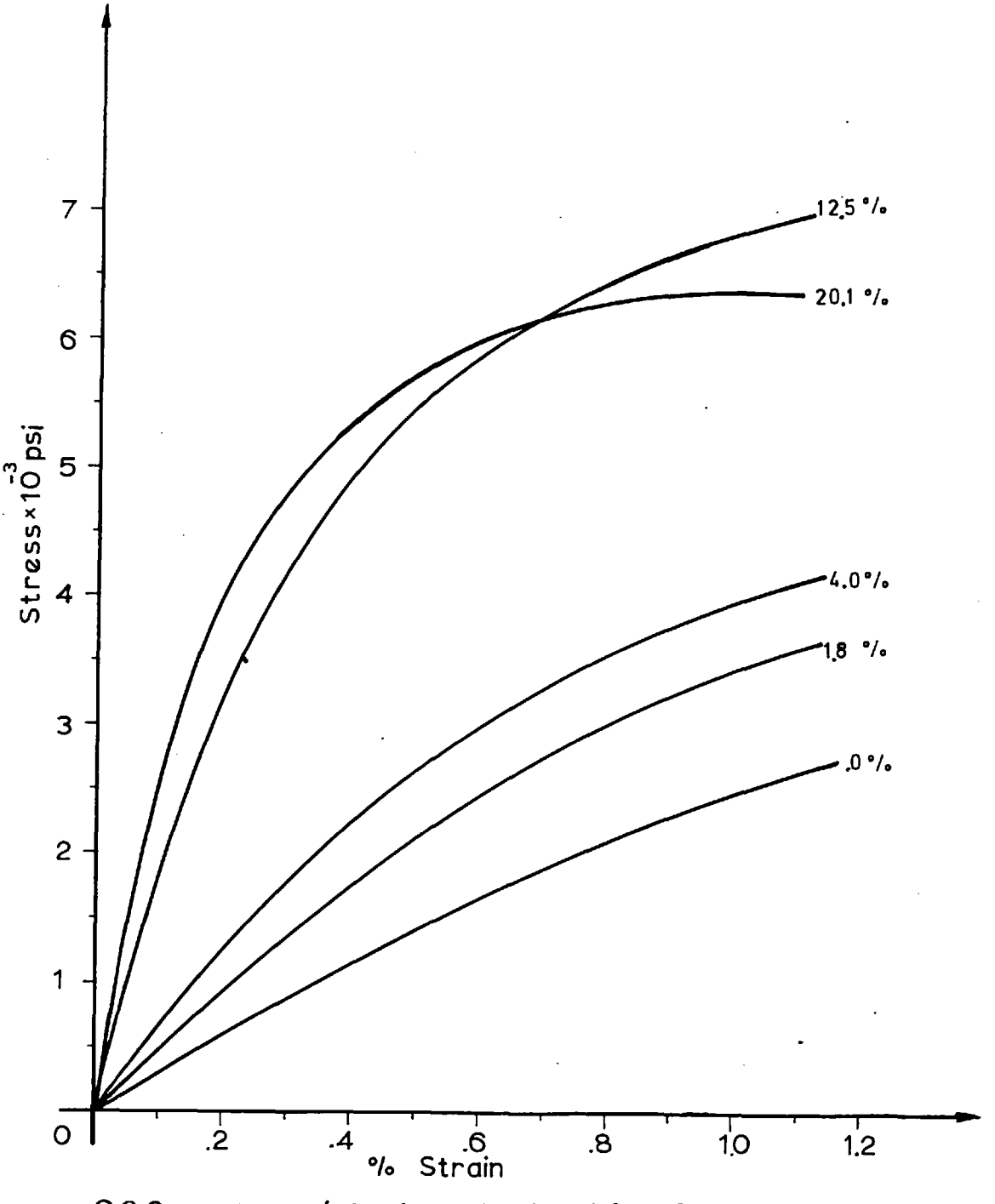

G.2.9 **Stress/strain relationships for iron gauze reinforced Propathene**

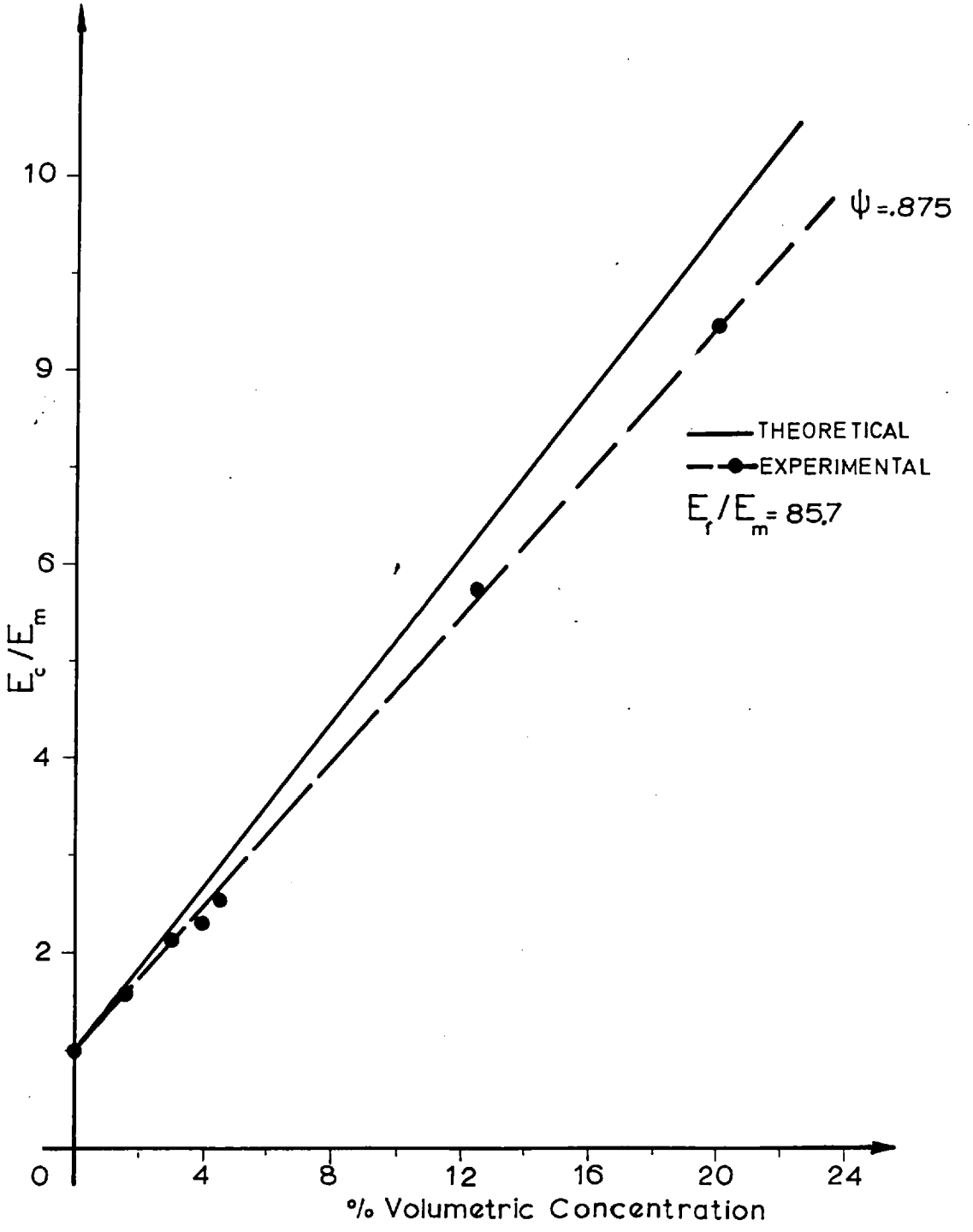

G.2.10 **Iron gauze reinforced Propathene**

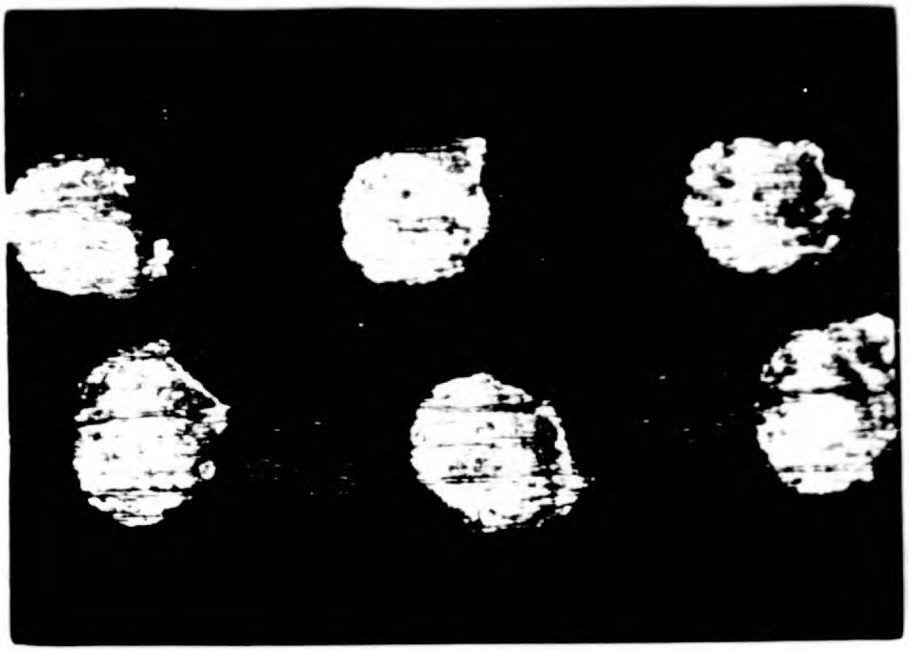

FIG.2.10. Cross-section of unidirectional reinforced composites

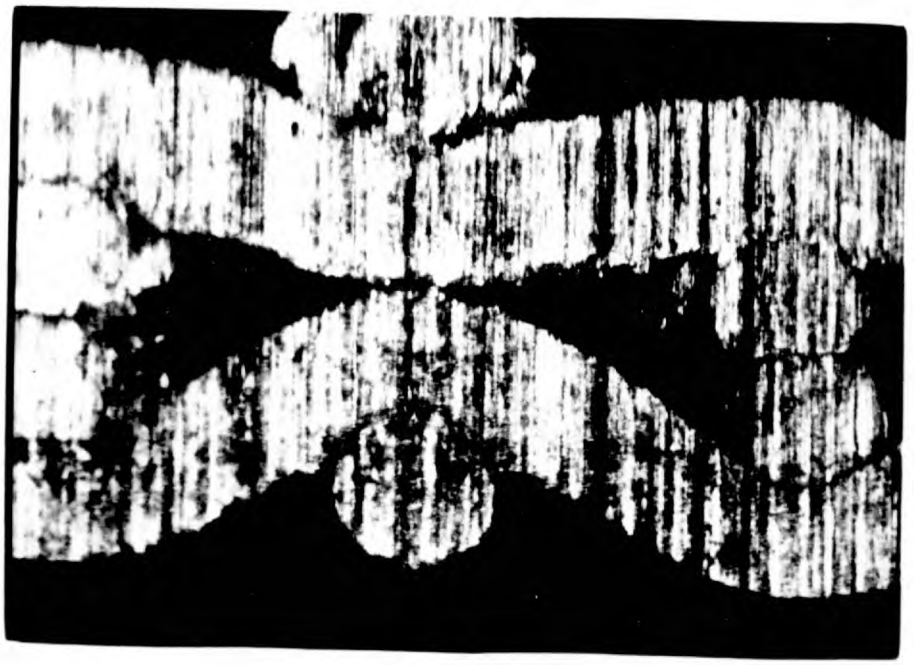

FIG.2.11. Cross-section of cross-reinforced composites

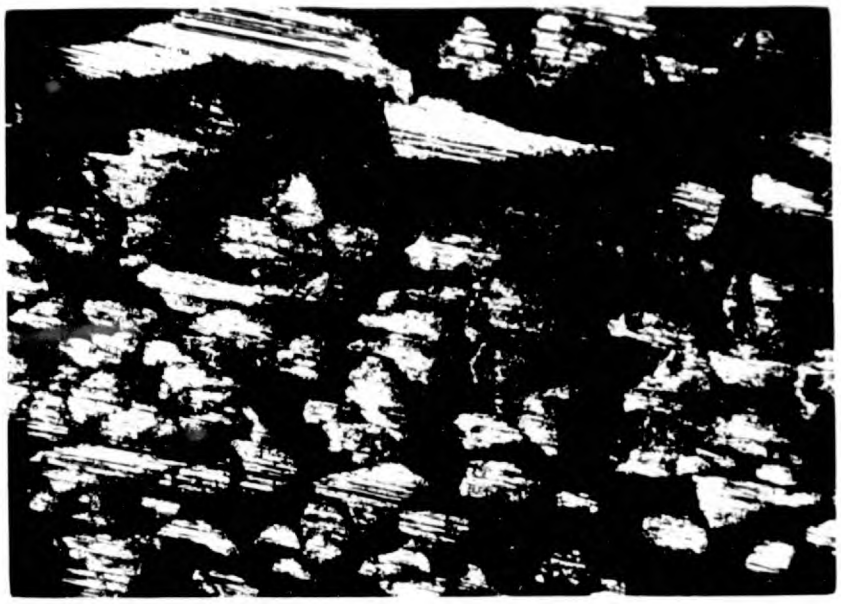

FIG.2.12. Cross-section of randomly distributed Al/ Propathene

FIG.2.13. Cross-section of randomly distributed s.steel/propathene

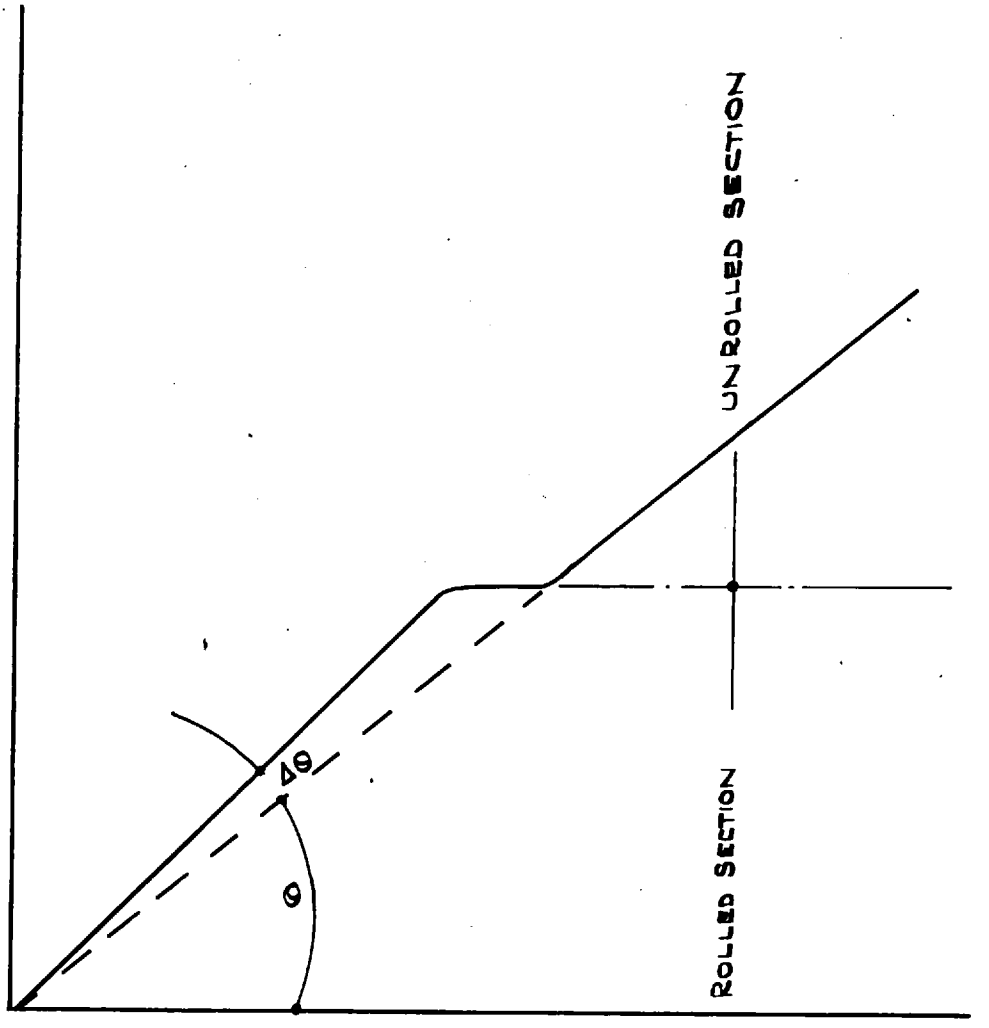

FIG 2.14. Exaggerated view of the rotation of a fibre in matrix during rolling

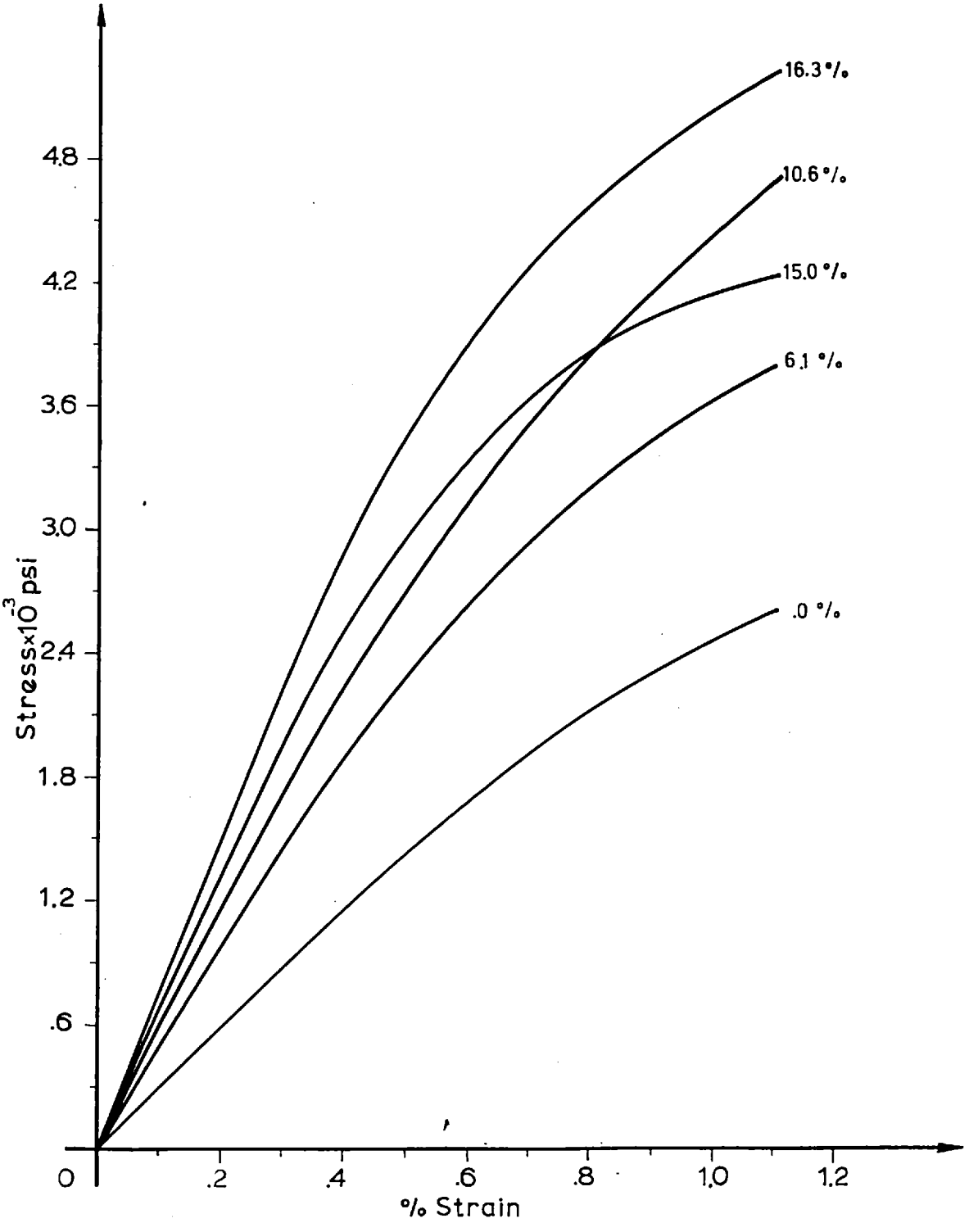

G.2.11 **Stress/strain relationships for randomly distributed aluminium/Propathene composite**

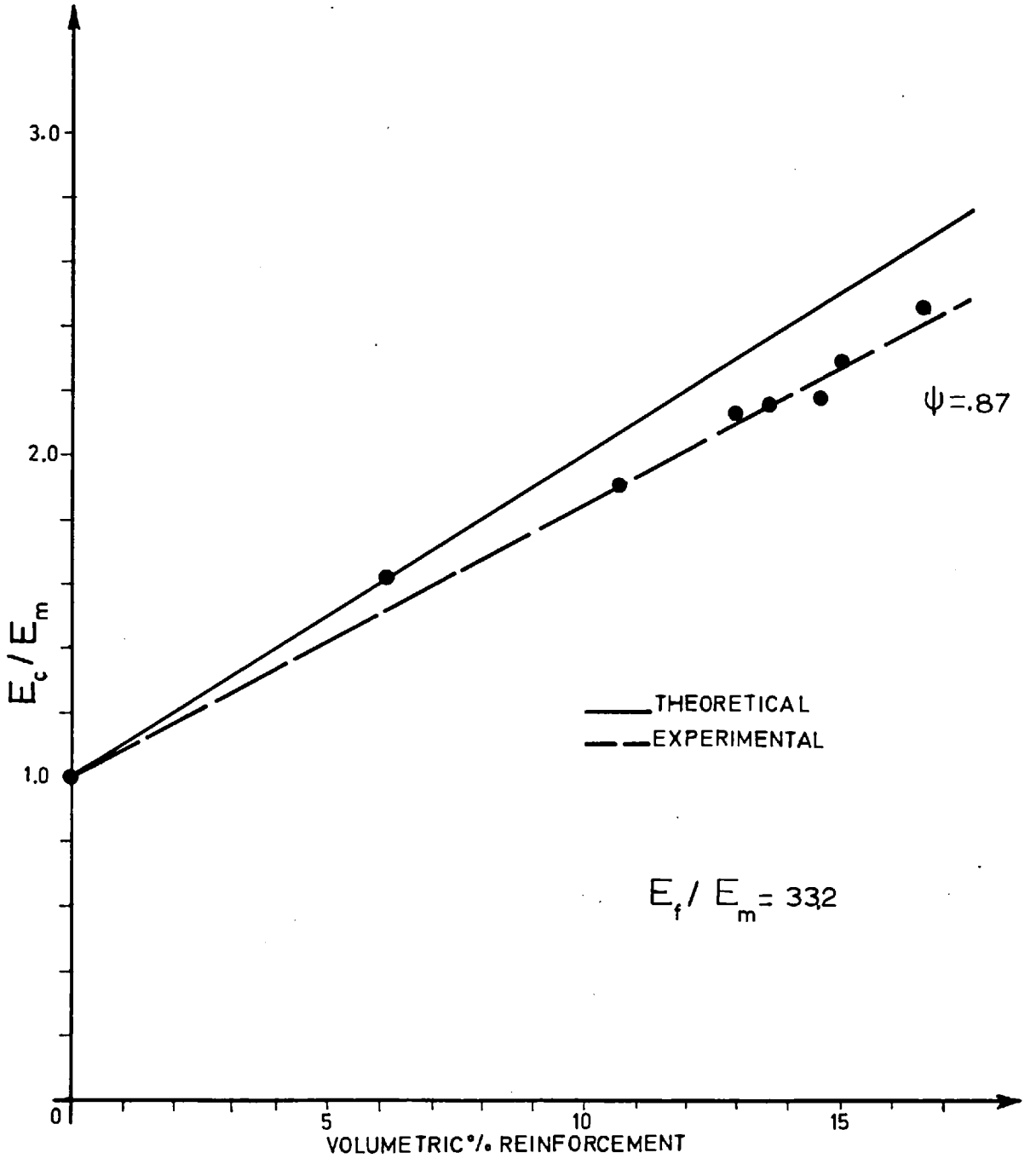

G.2.12 **Randomly distributed Aluminium/Propathene composite**

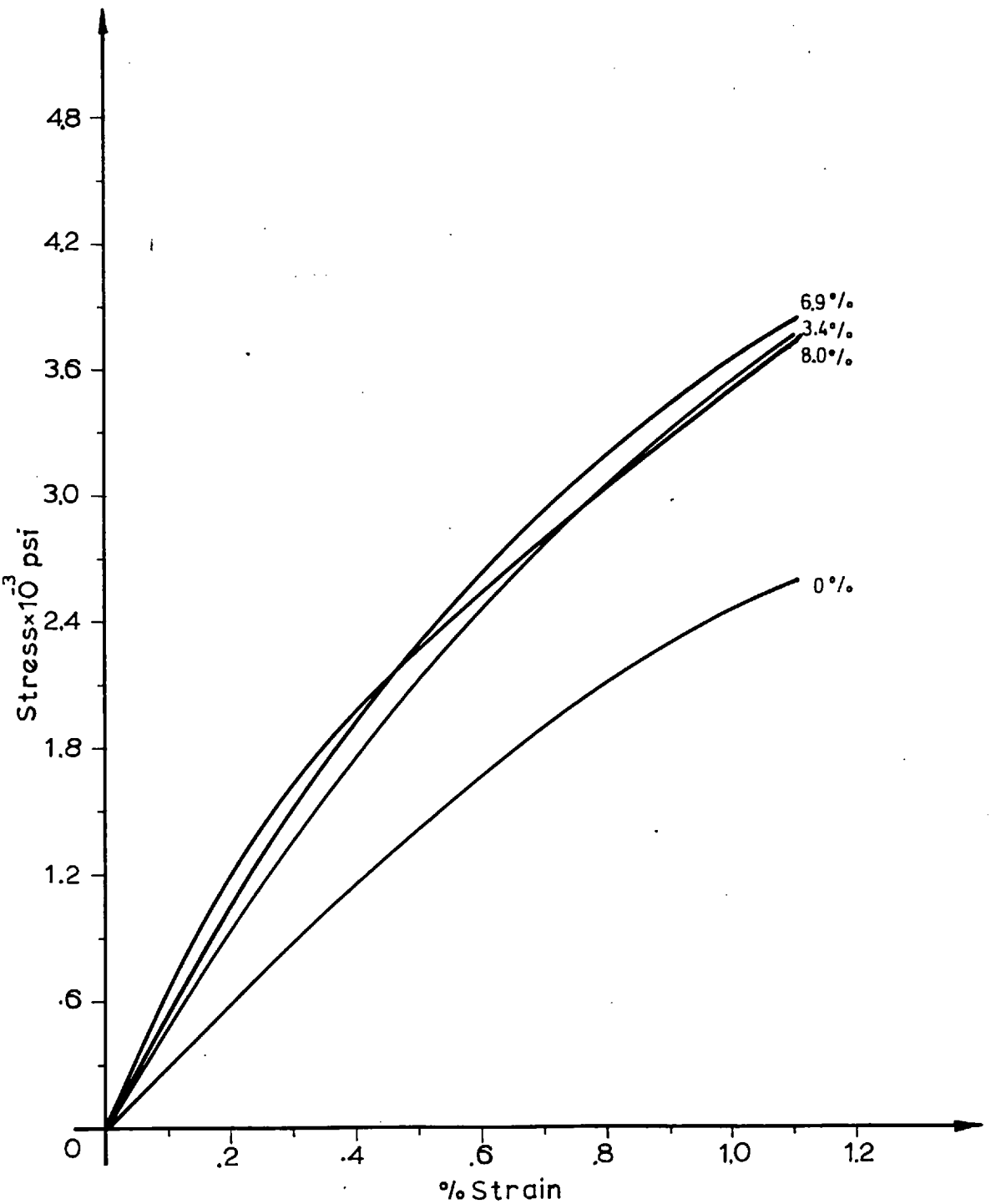

G.2.13 **Stress/strain relationships for randomly distributed bronze/Propathene composite**

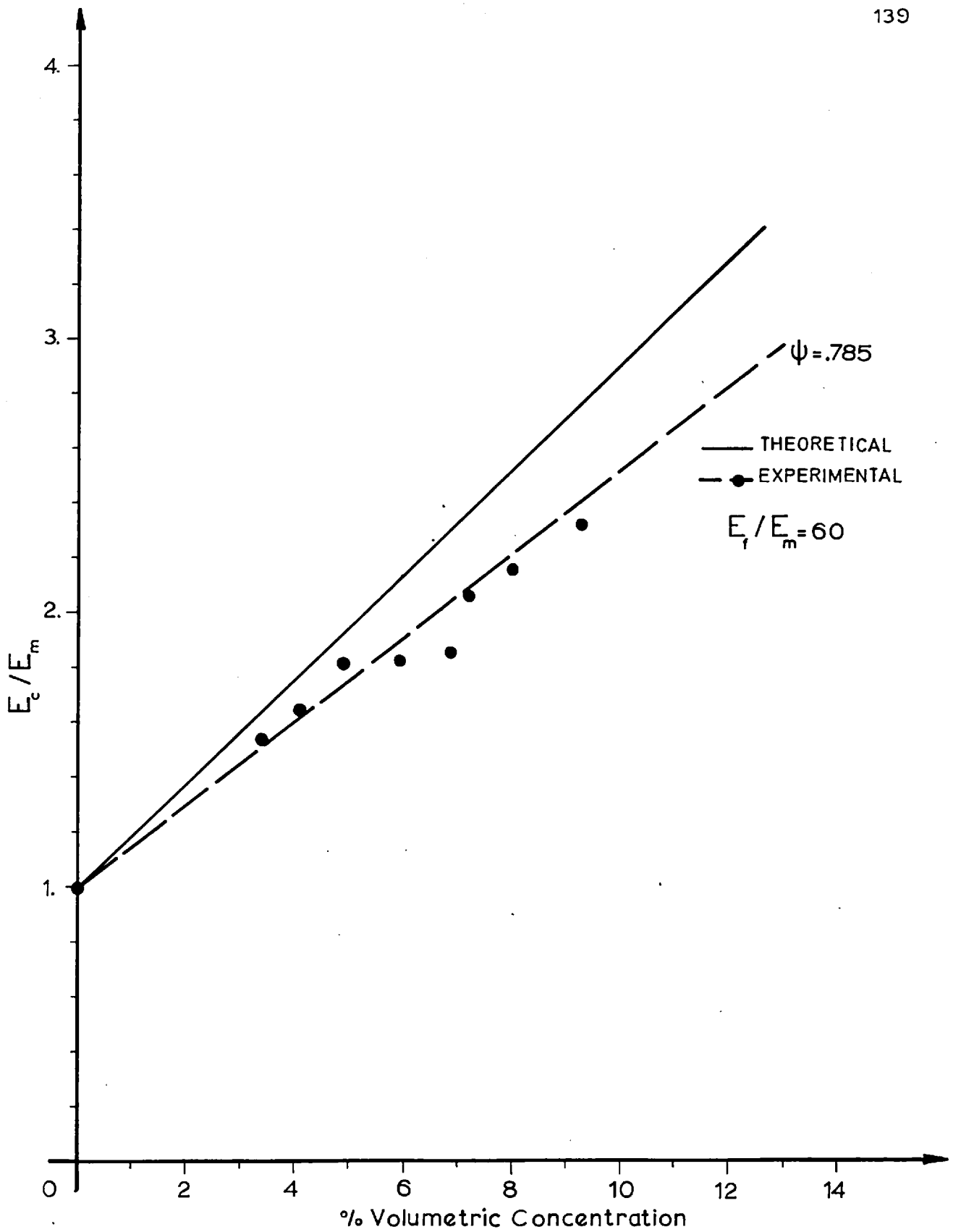

G.2.14 **Randomly distributed bronze/Propathene composite**

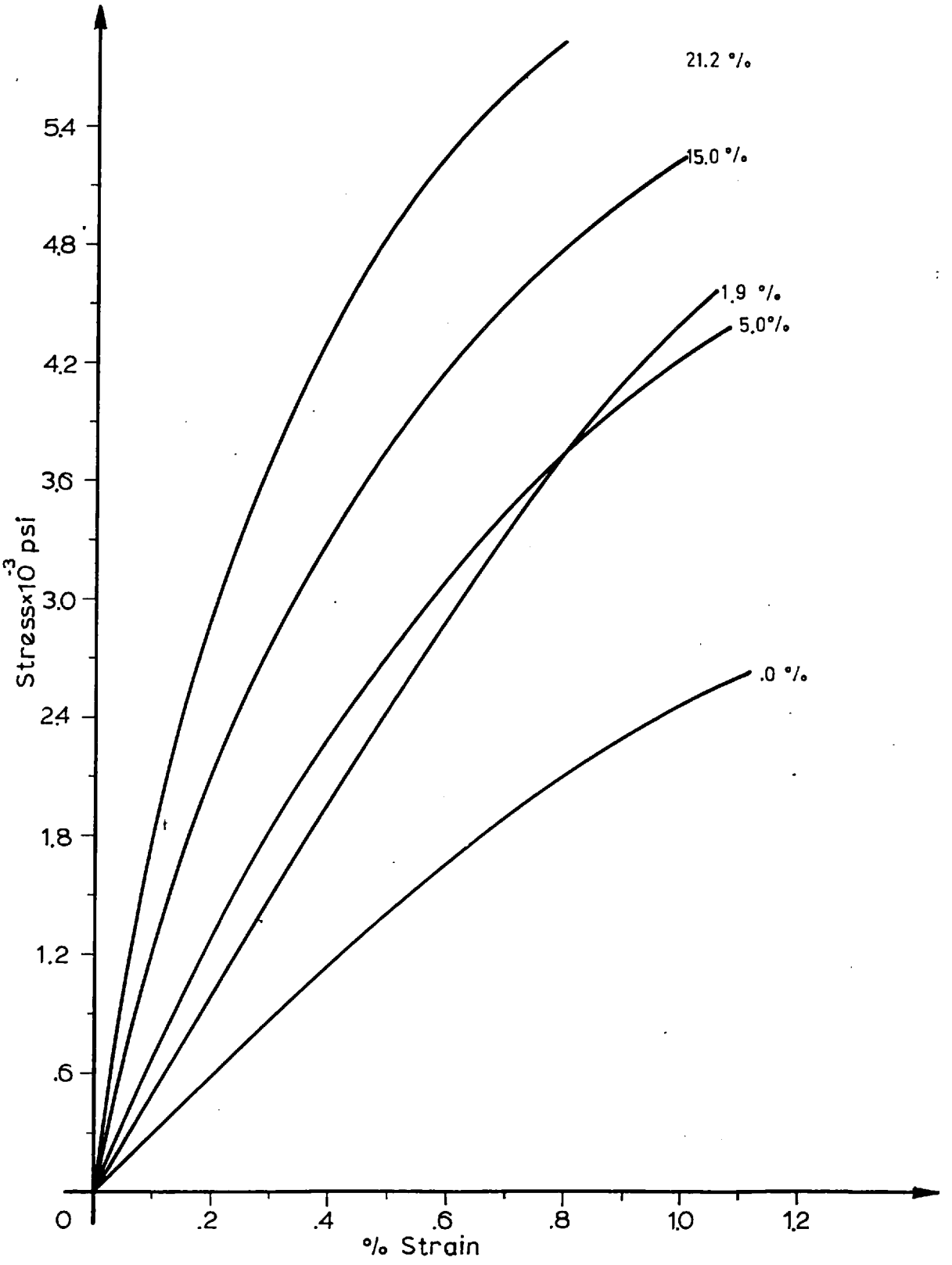

G.2.15 **Stress/strain relationships for randomly distributed steel/Propathene composite**

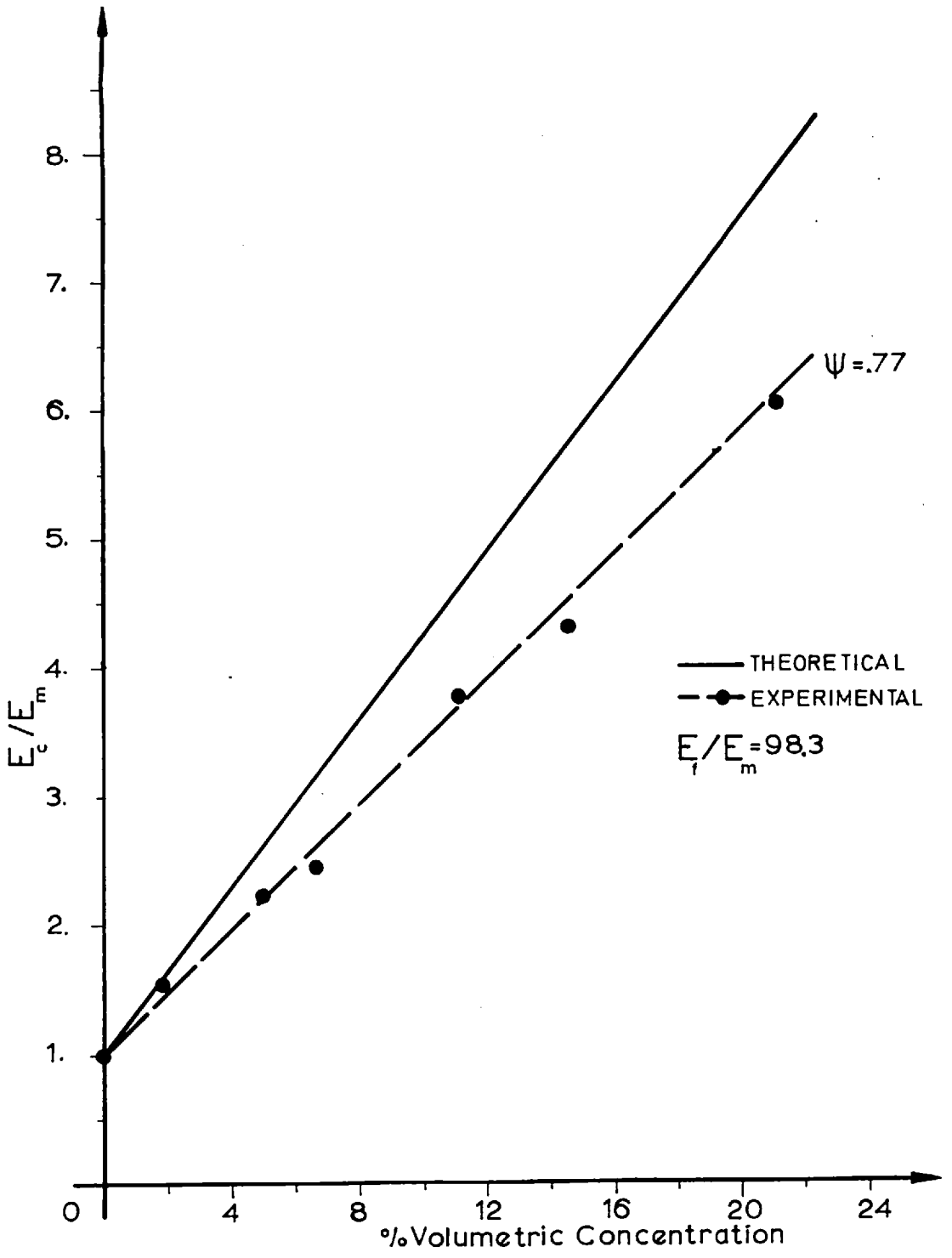

G.2.16 **Randomly distributed steel/propathene composite**

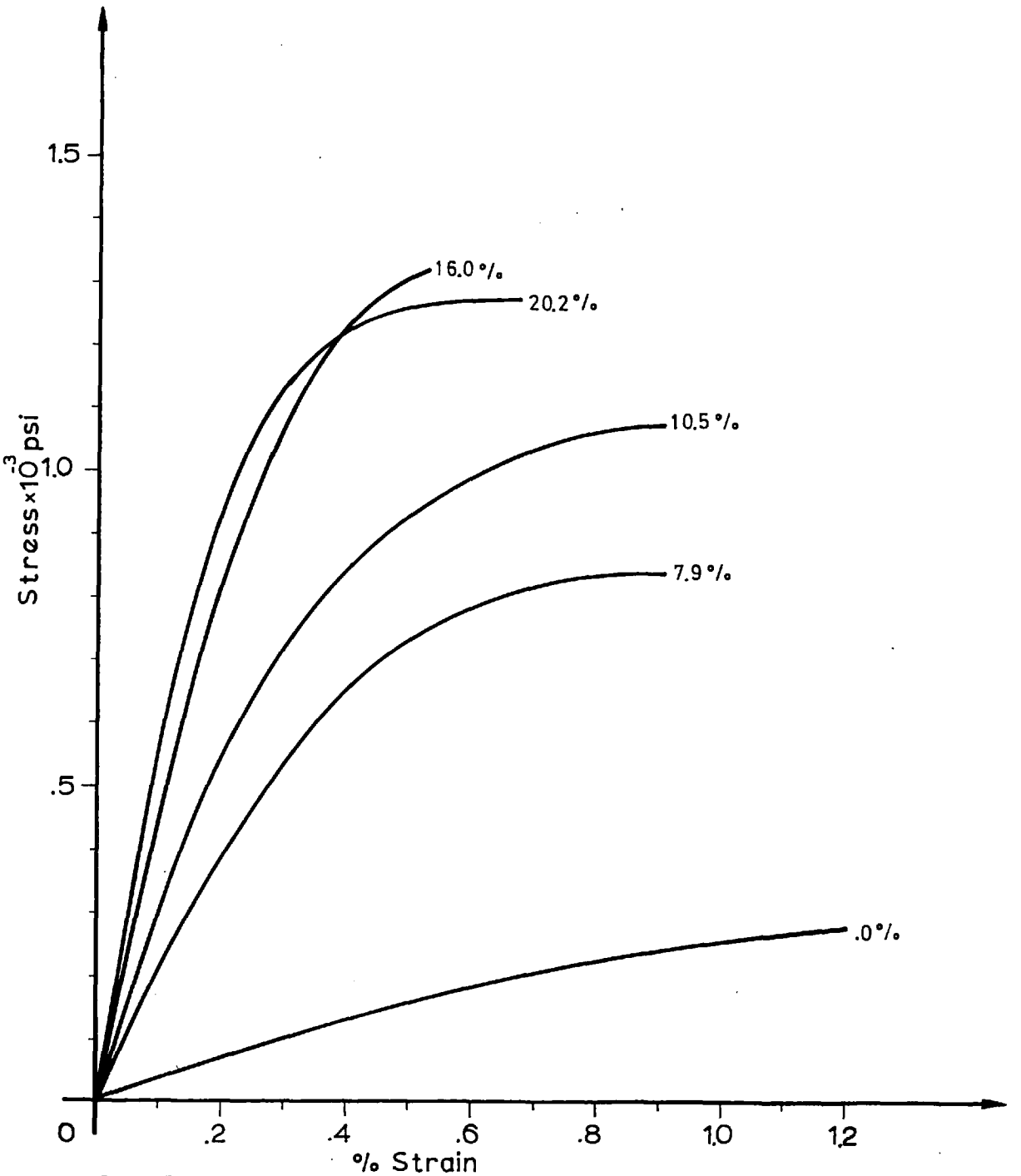

G.2.17 **Stress/strain relationships for randomly distributed aluminium/L.D. Polyethylene composite**

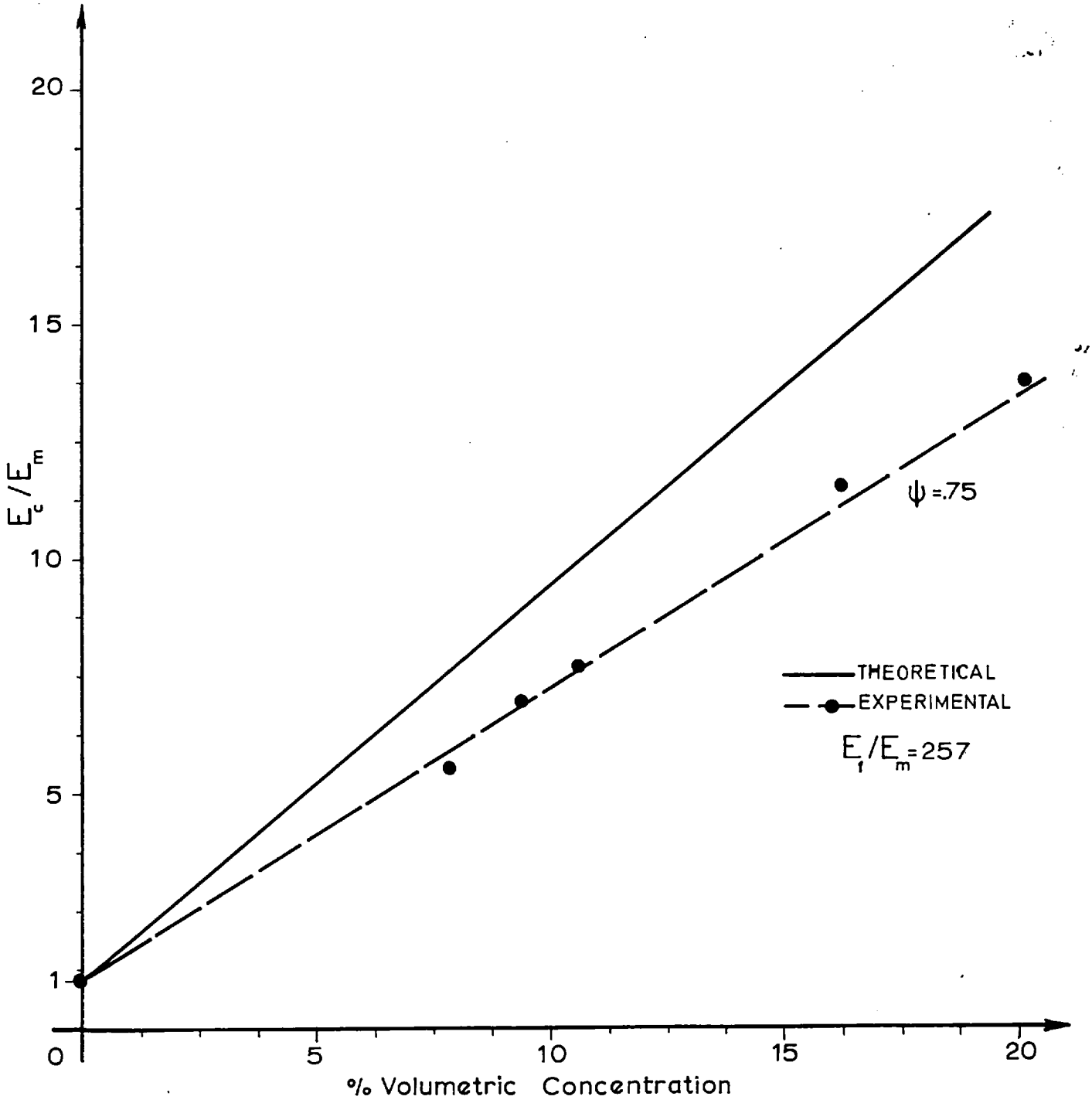

G.2.18 **Randomly distributed aluminium/L.D. Polyethylene composite**

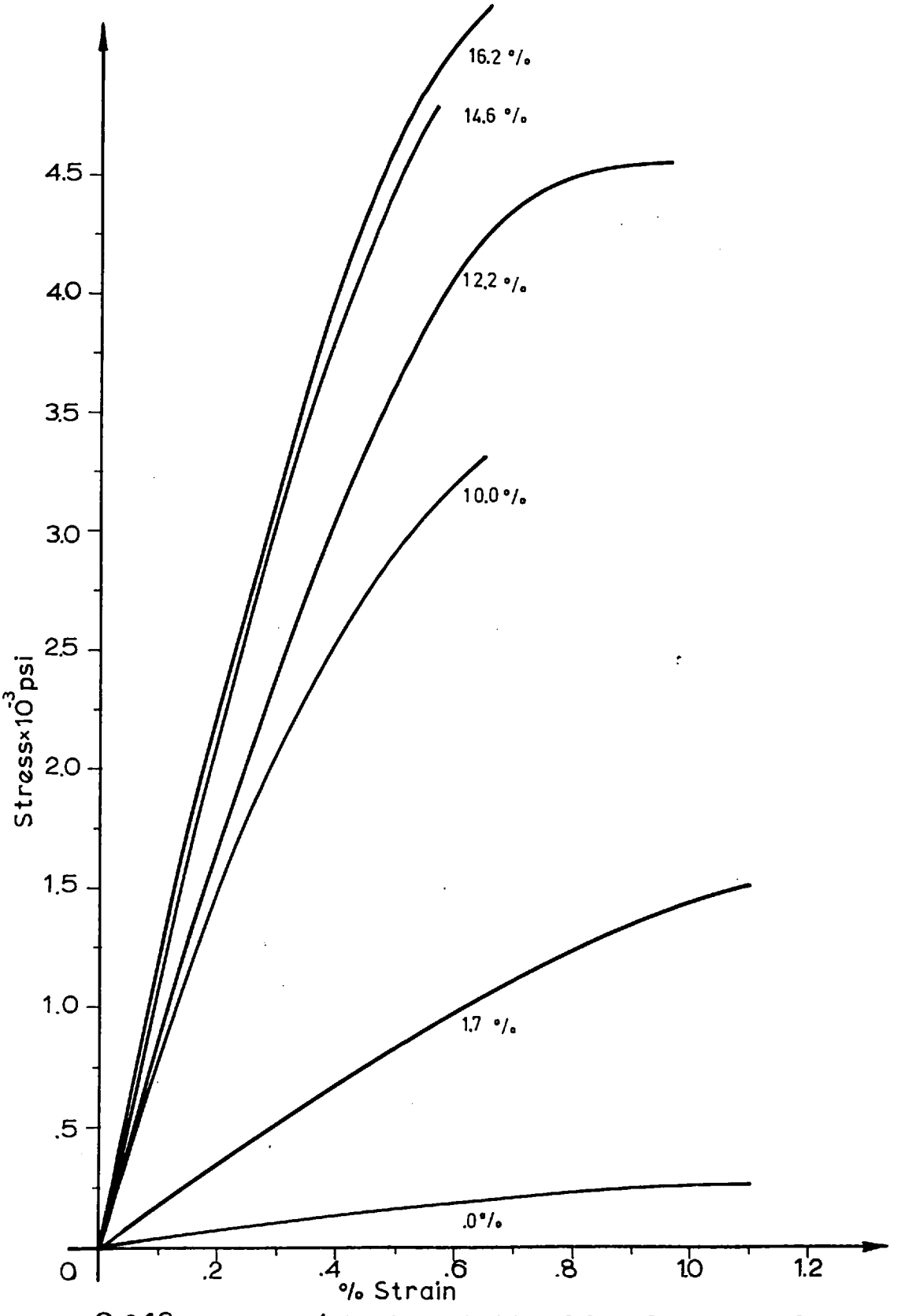

G.2.19 **Stress/strain relationships for randomly distributed steel/L.D. Polyethylene composite**

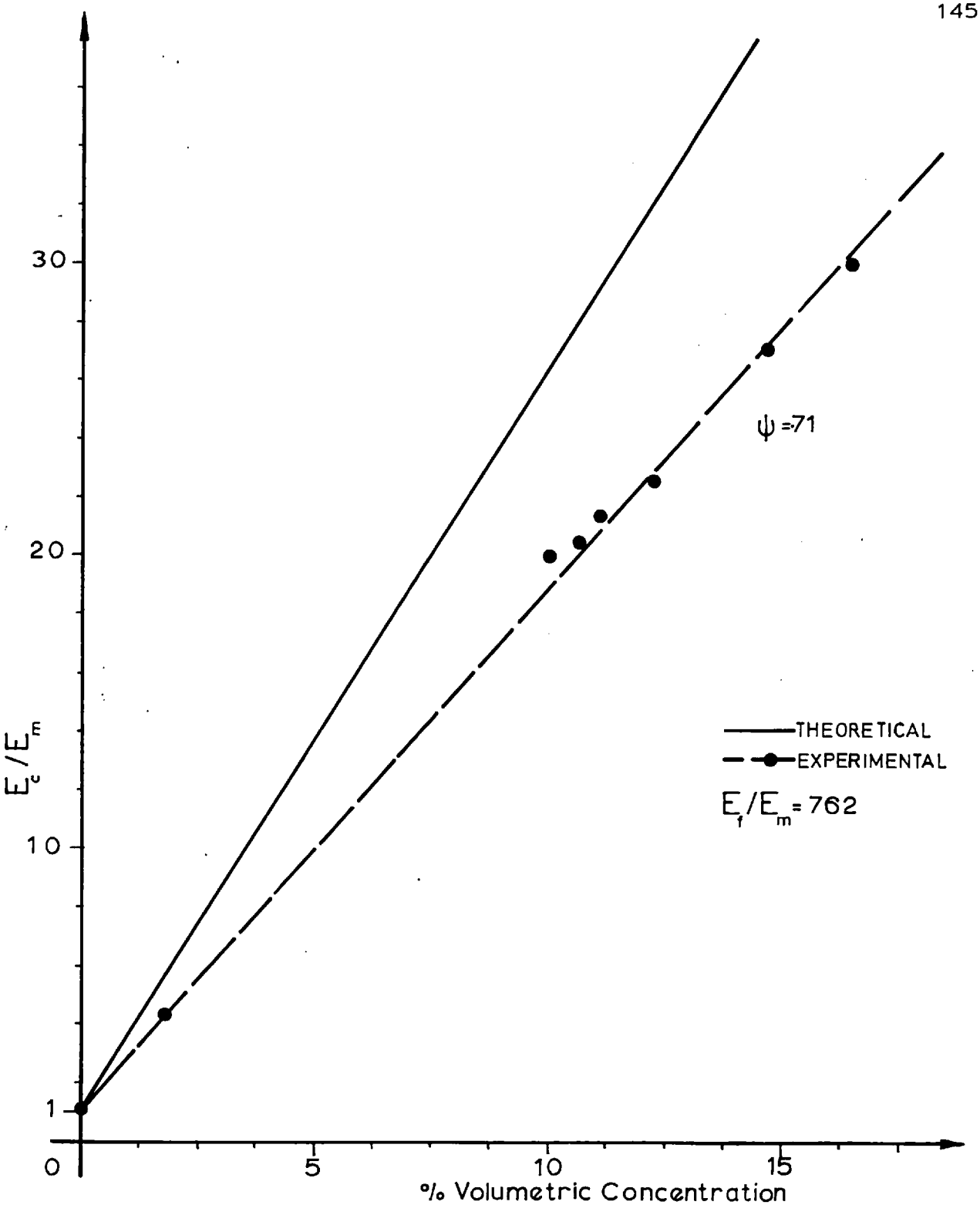

G.2.20 **Randomly distributed steel/L.D. Polyethylene composite**

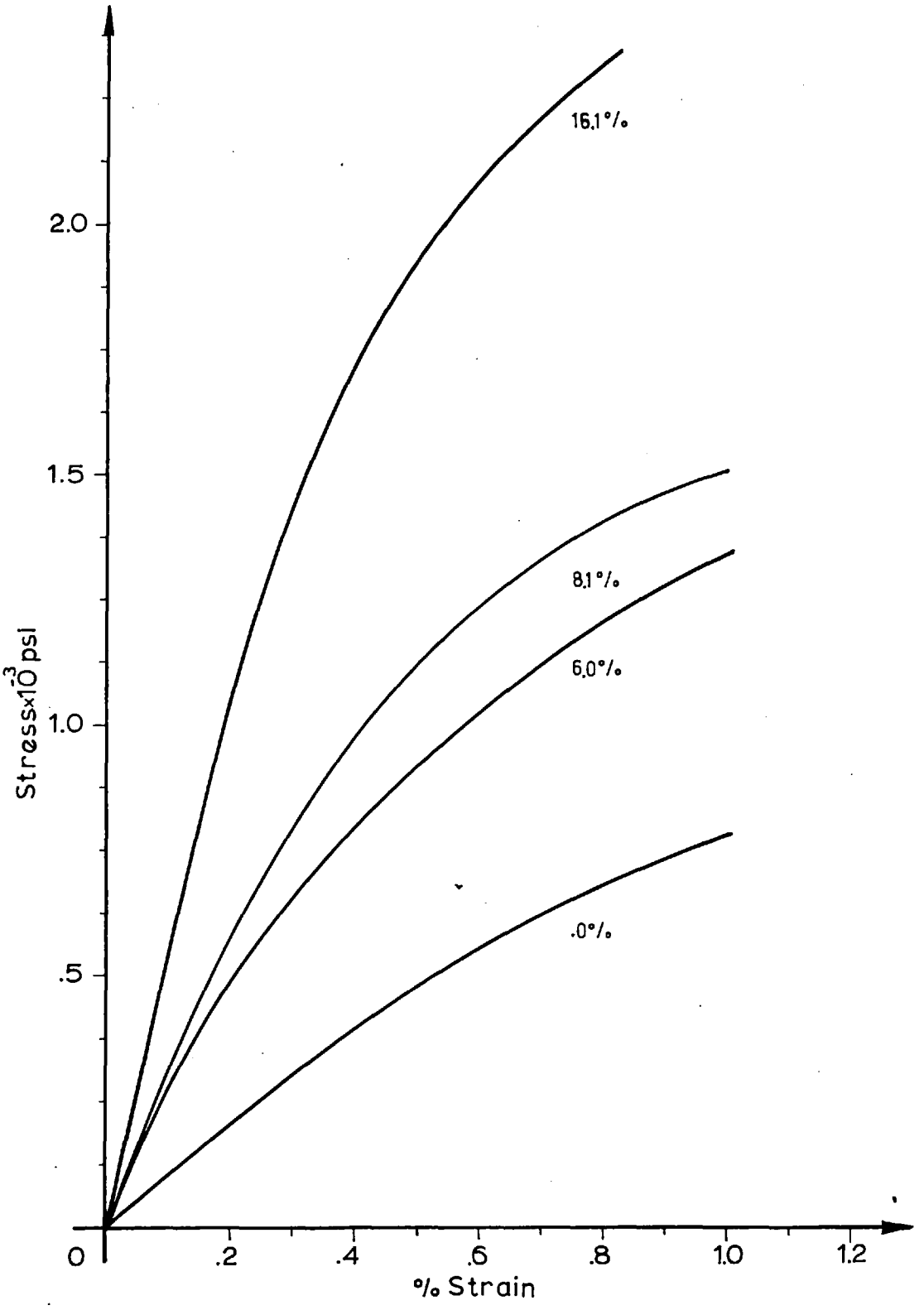

G.2.21 **Stress/strain relationships for randomly distributed aluminium/H.D. Polyethylene composite**

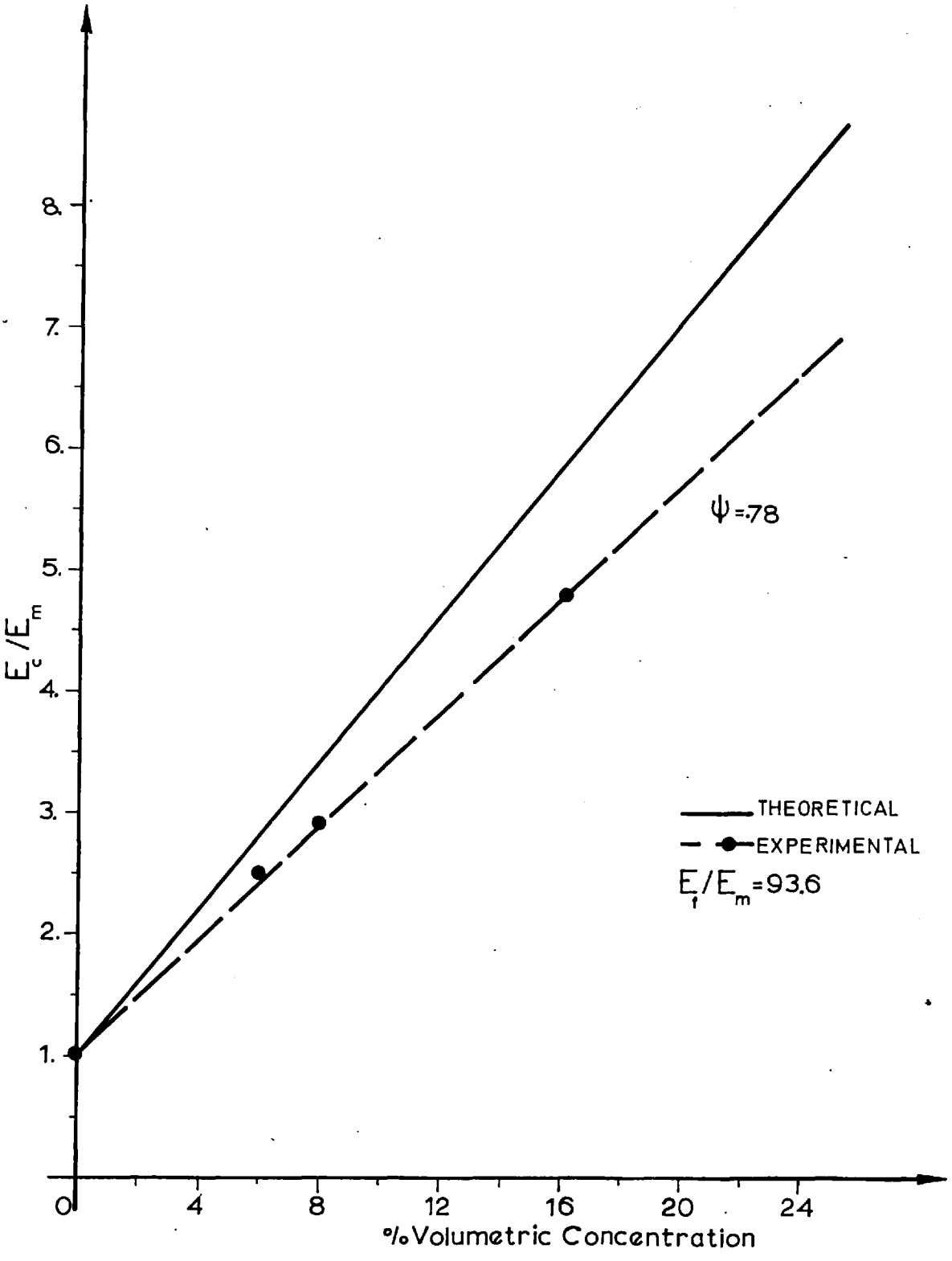

G.2.22 **Randomly distributed aluminium/H.D. Polyethylene composite**

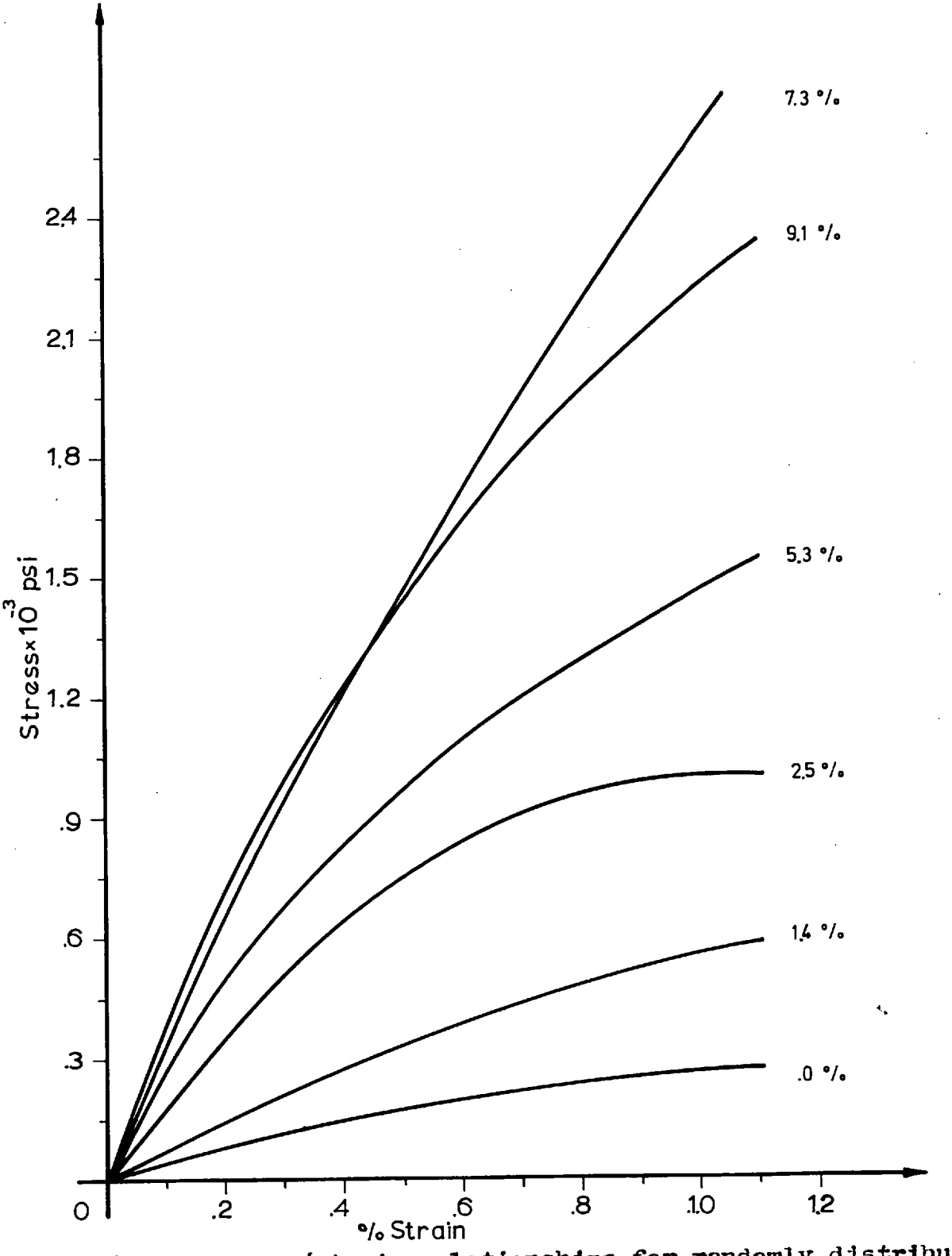

G.2.23 Stress/strain relationships for randomly distributed bronze/M.D. Polyethylene composite

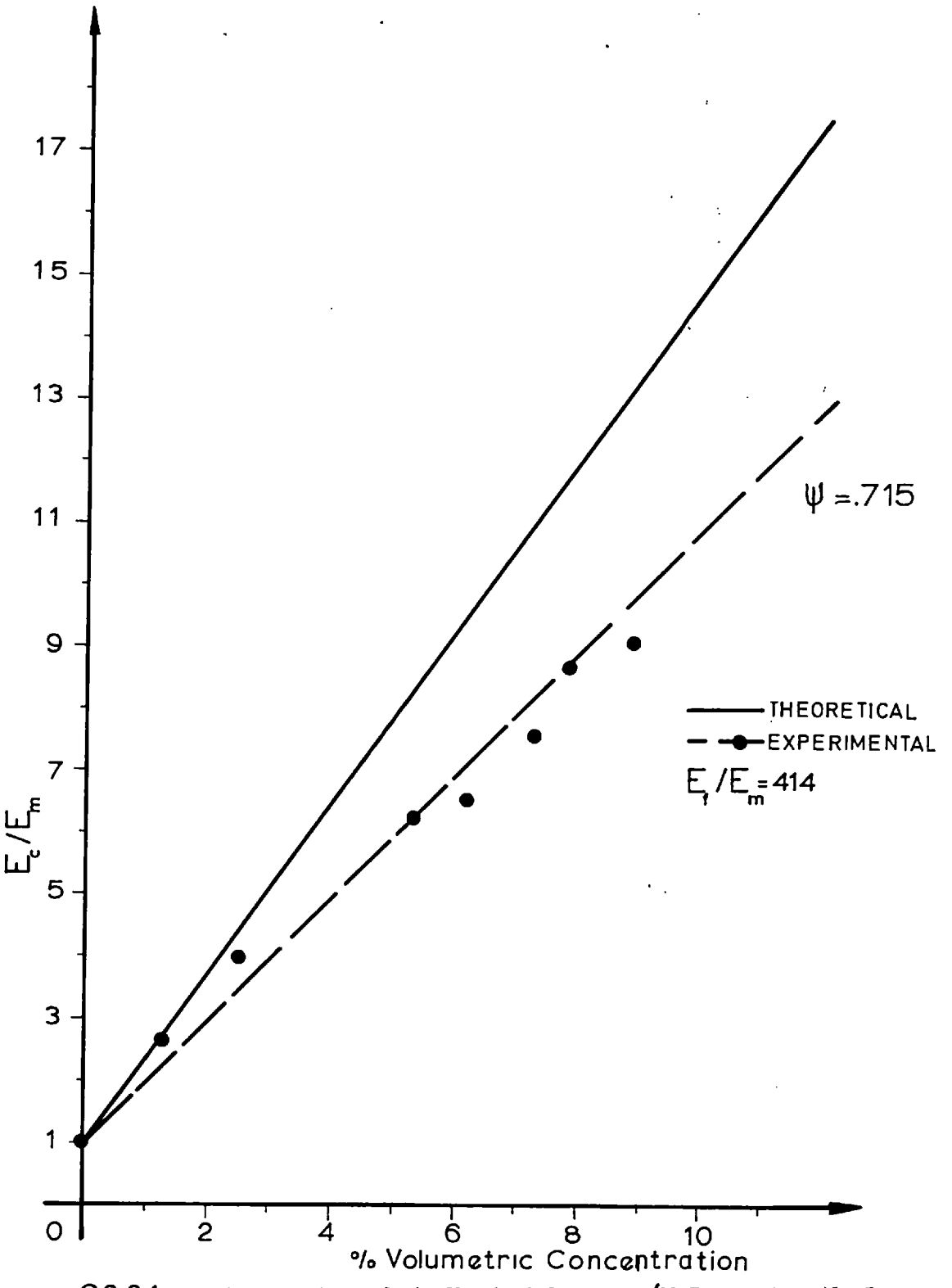

G2.24 Randomly distributed bronze/M.D. Polyethylene composite

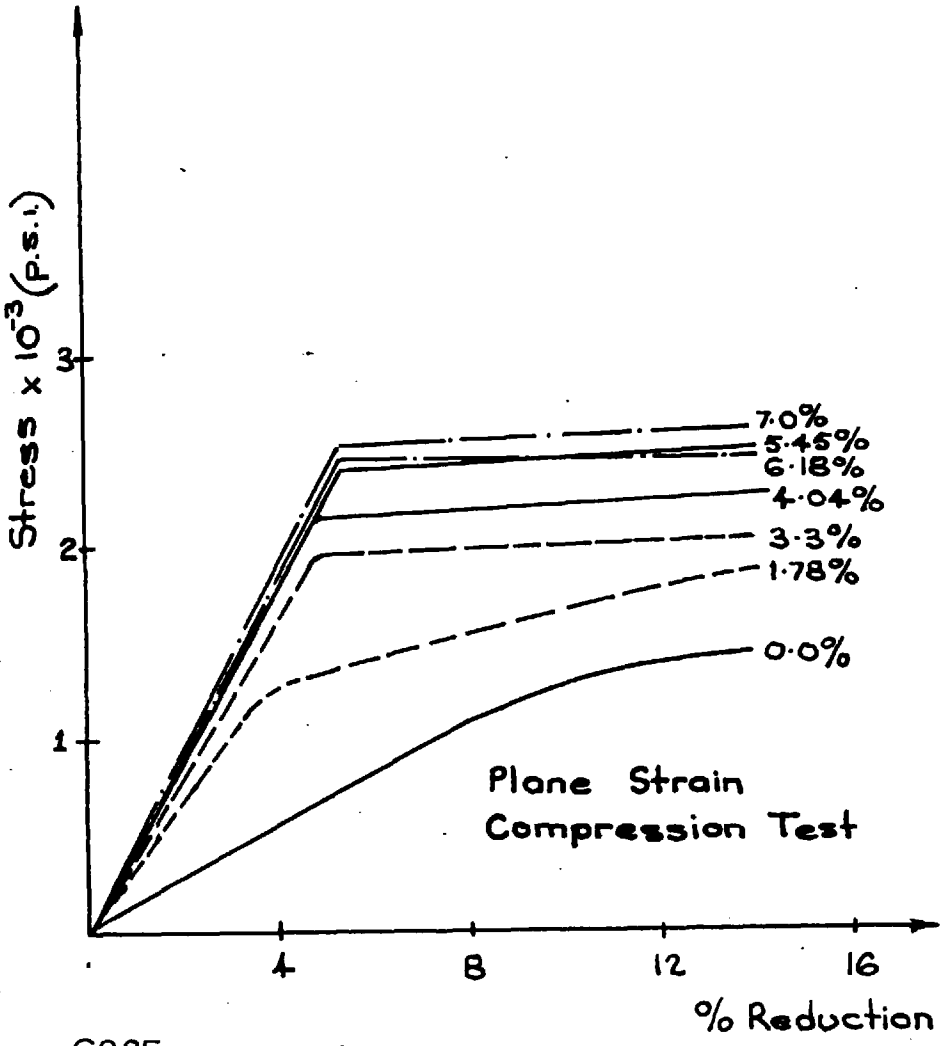

G225 **Stress/strain relationships for randomly distributed bronze fibre reinforced medium density Polyethylene**

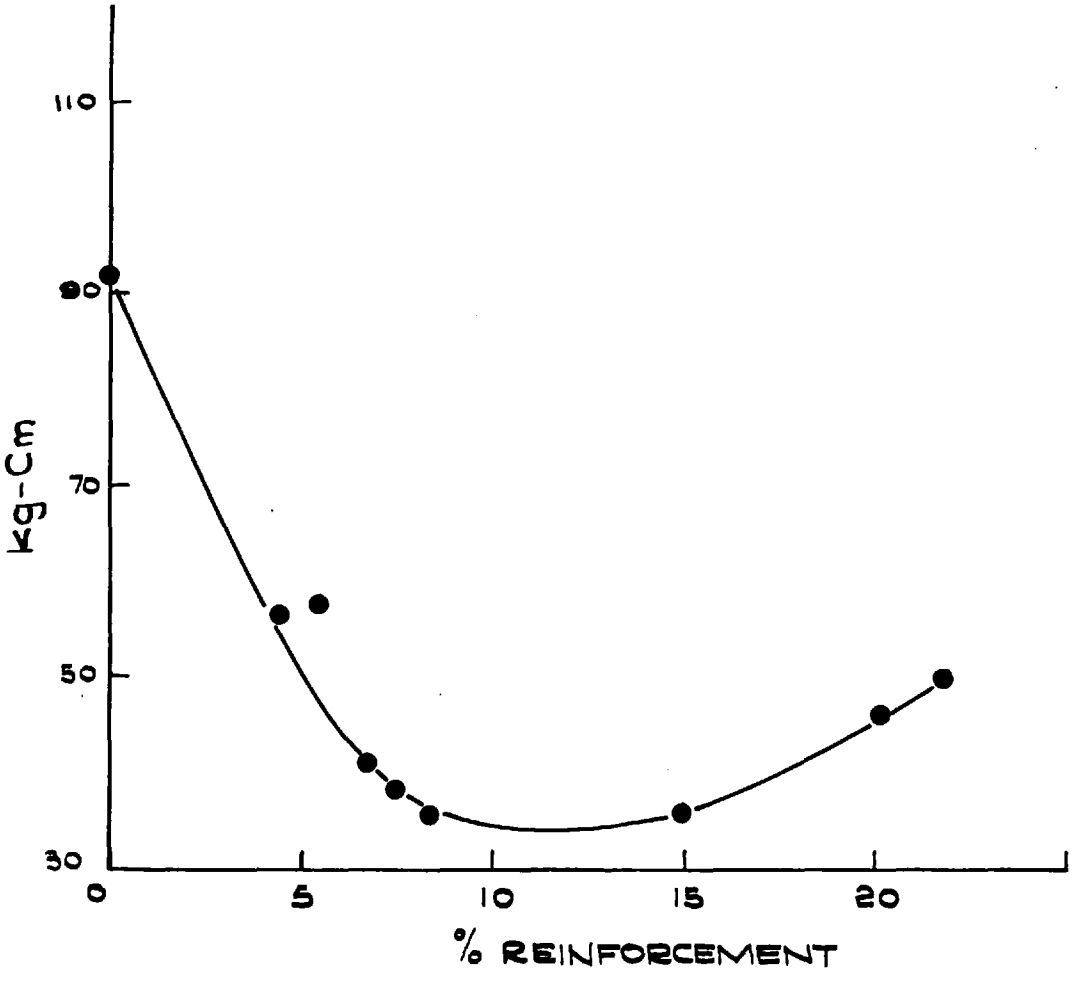

G.2.26 **Randomly distributed steel fibre reinforced low density Polyethylene (Charpy Test)**

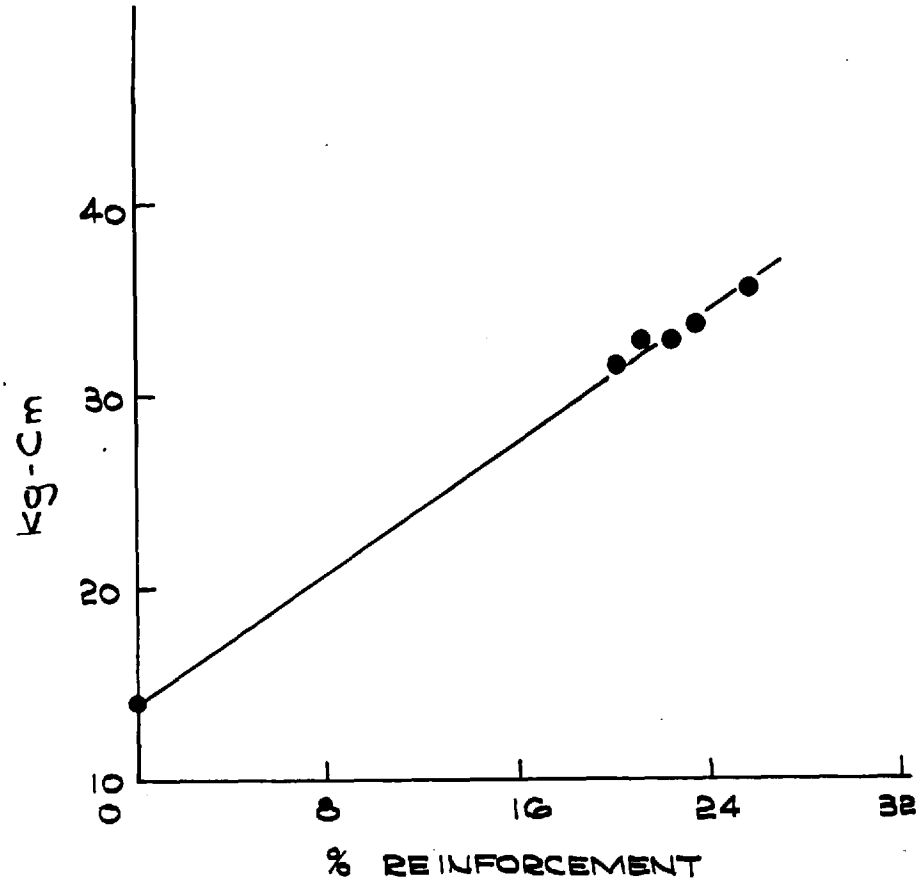

G227 Randomly distributed aluminium fibre reinforced high density Polyethylene (Charpy Test)

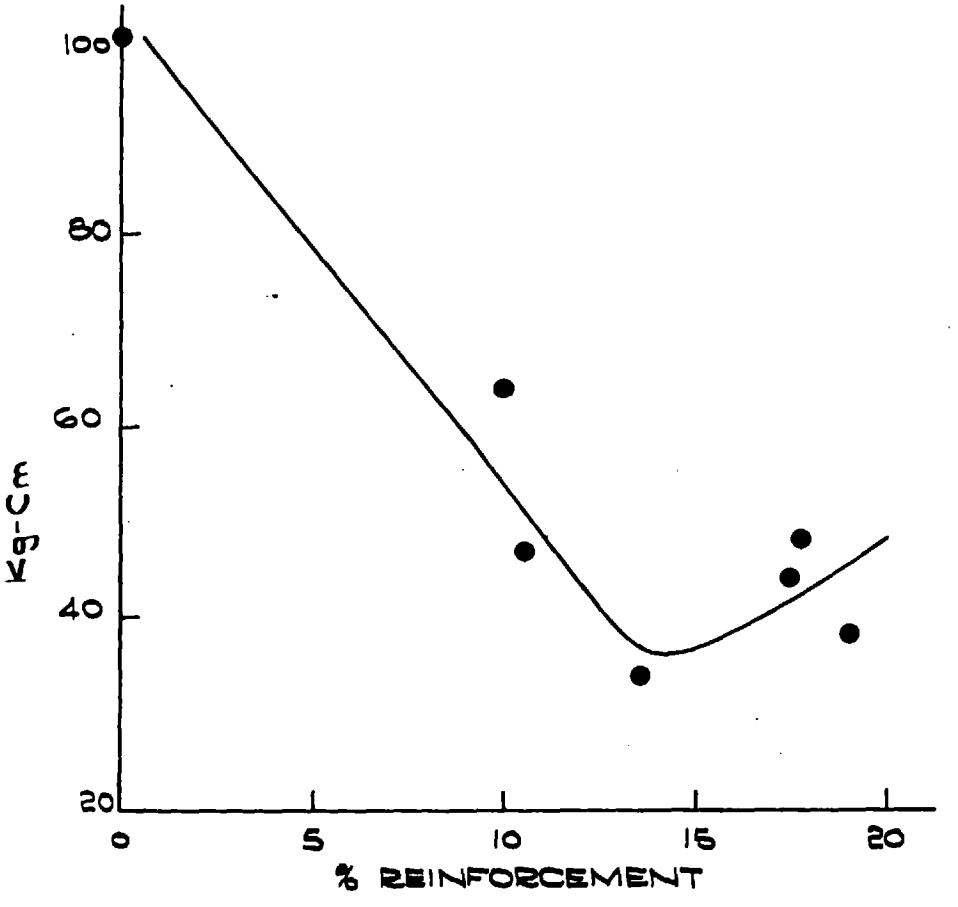

G2.28 **Randomly distributed aluminium fibre reinforced low density Polyethylene** (Charpy Test)

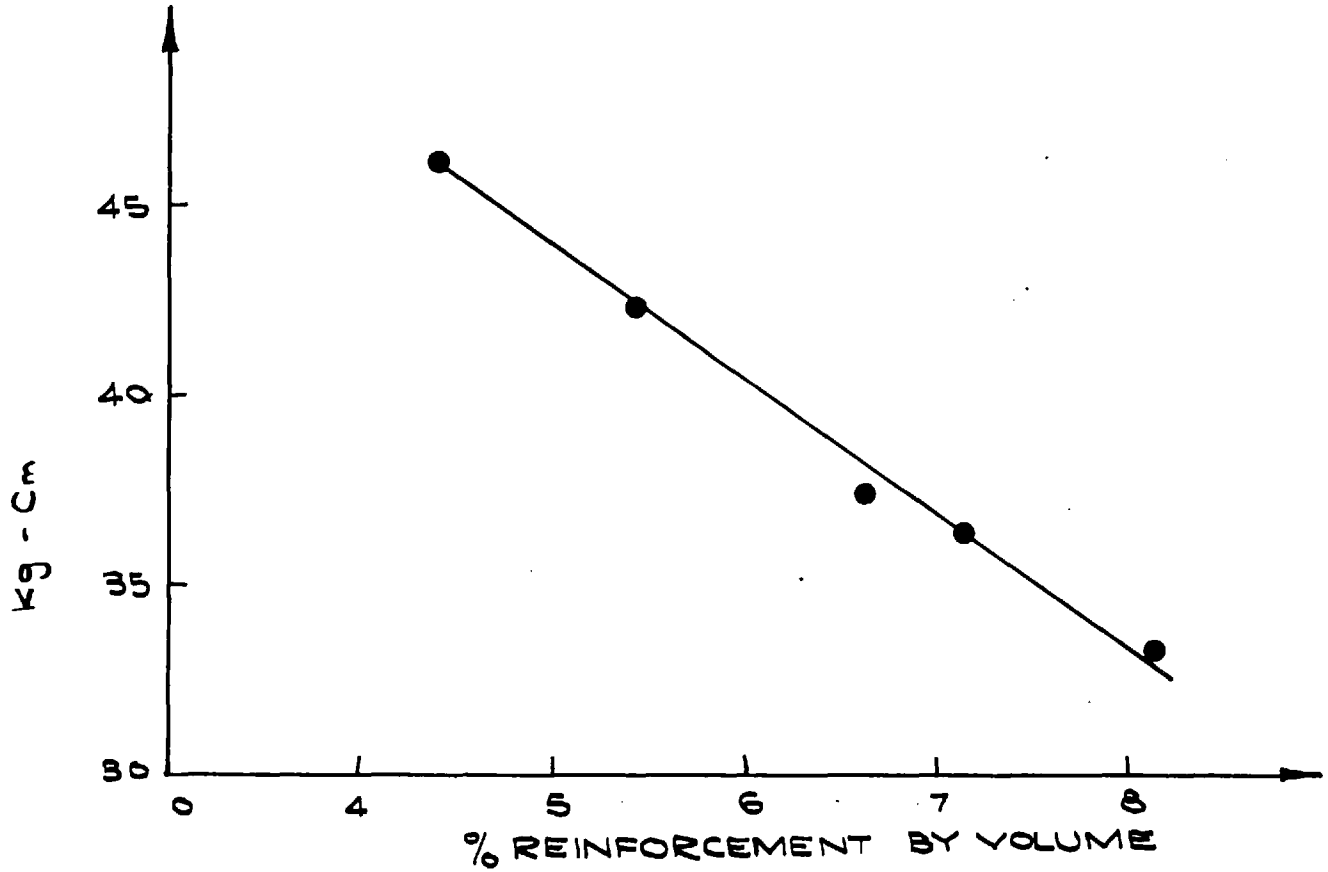

G.2.29 Randomly distributed steel fibre reinforced medium density Polythene (Charpy test)

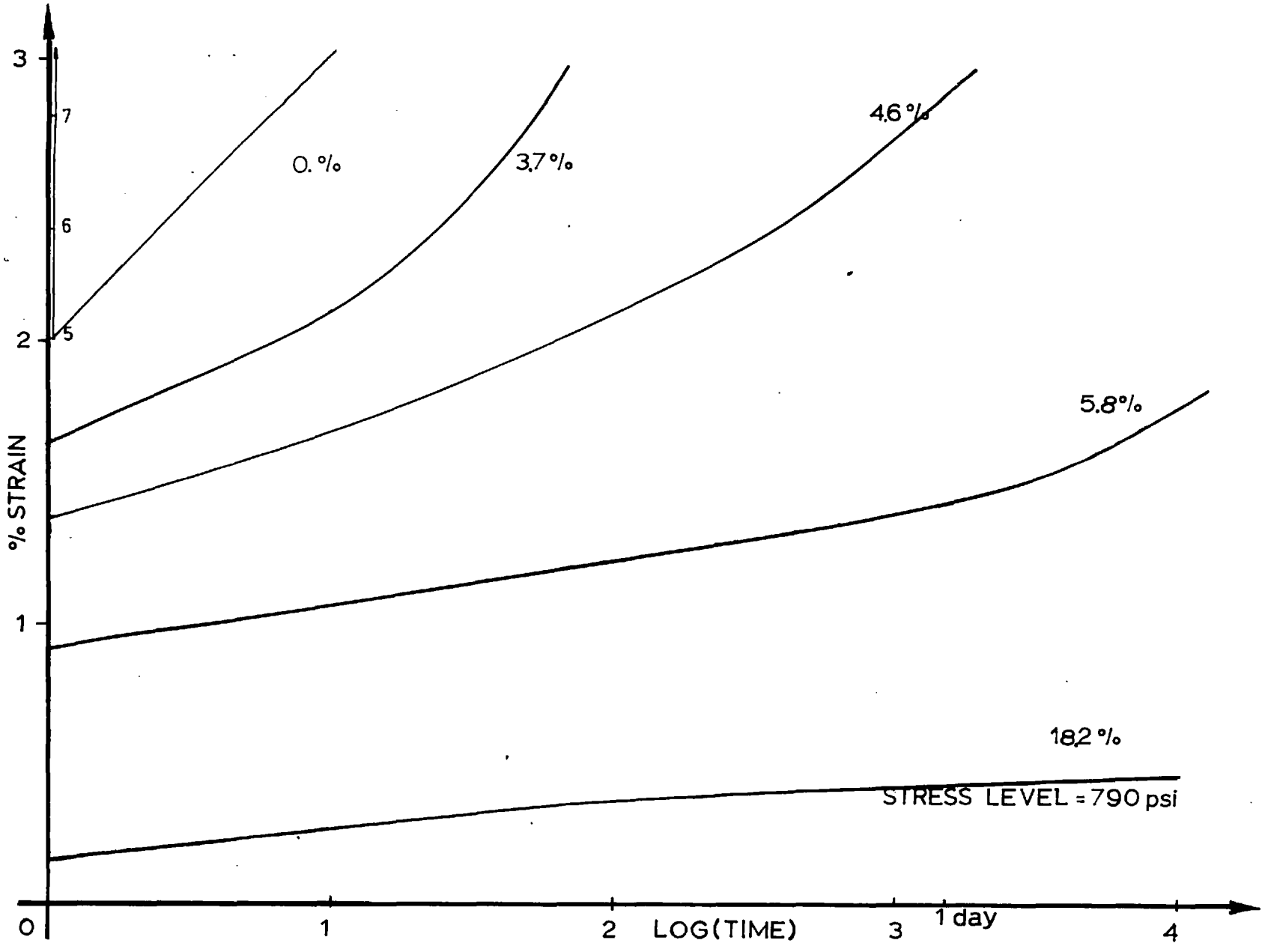

G2.30 **Creep tests for randomly distributed bronze/M.D. Polyethylene composite**

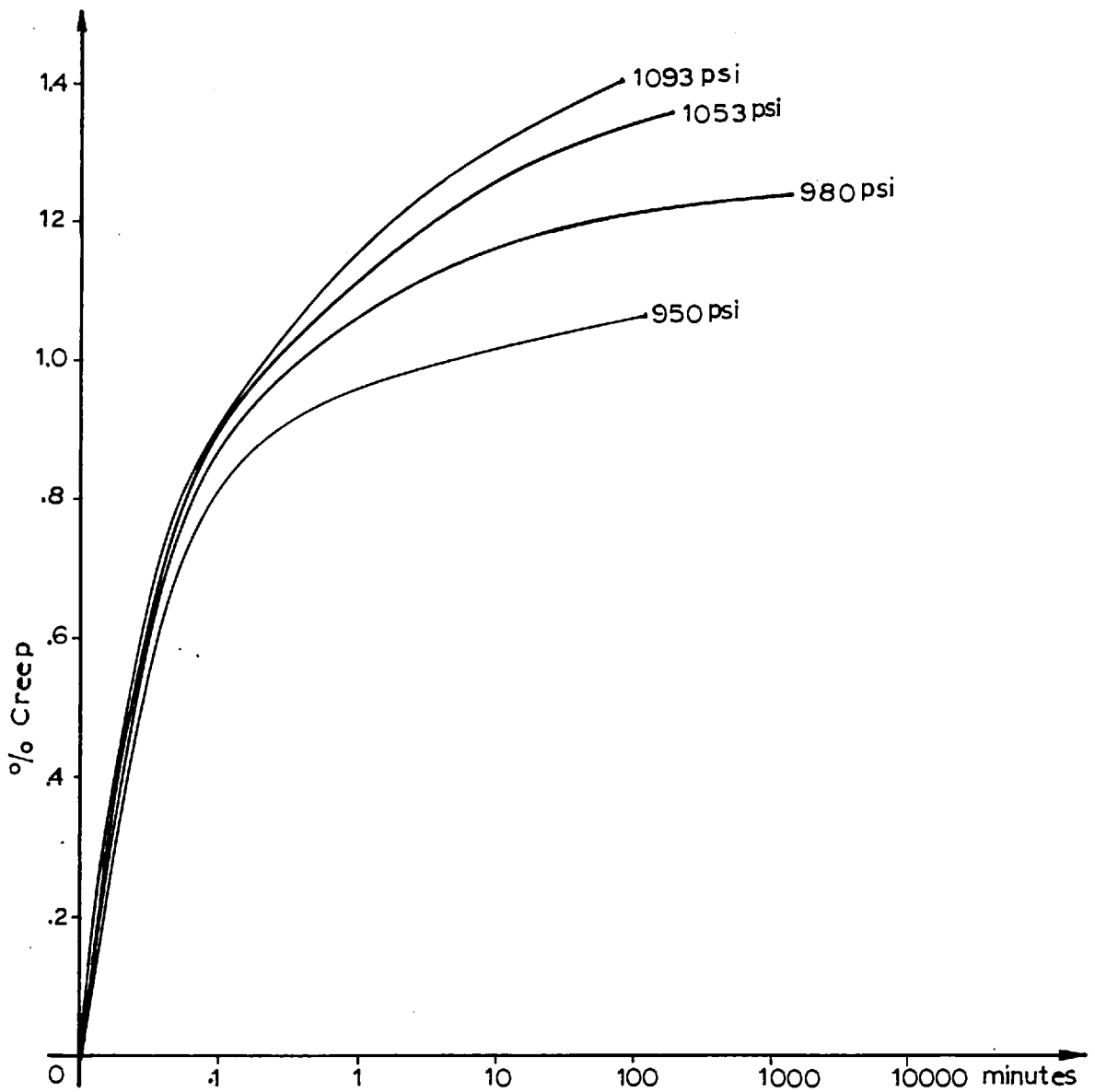

G.2 .31 Creep Behaviour for 10.1% randomly distributed Steel fibre Reinforced M.D.Polyethylene

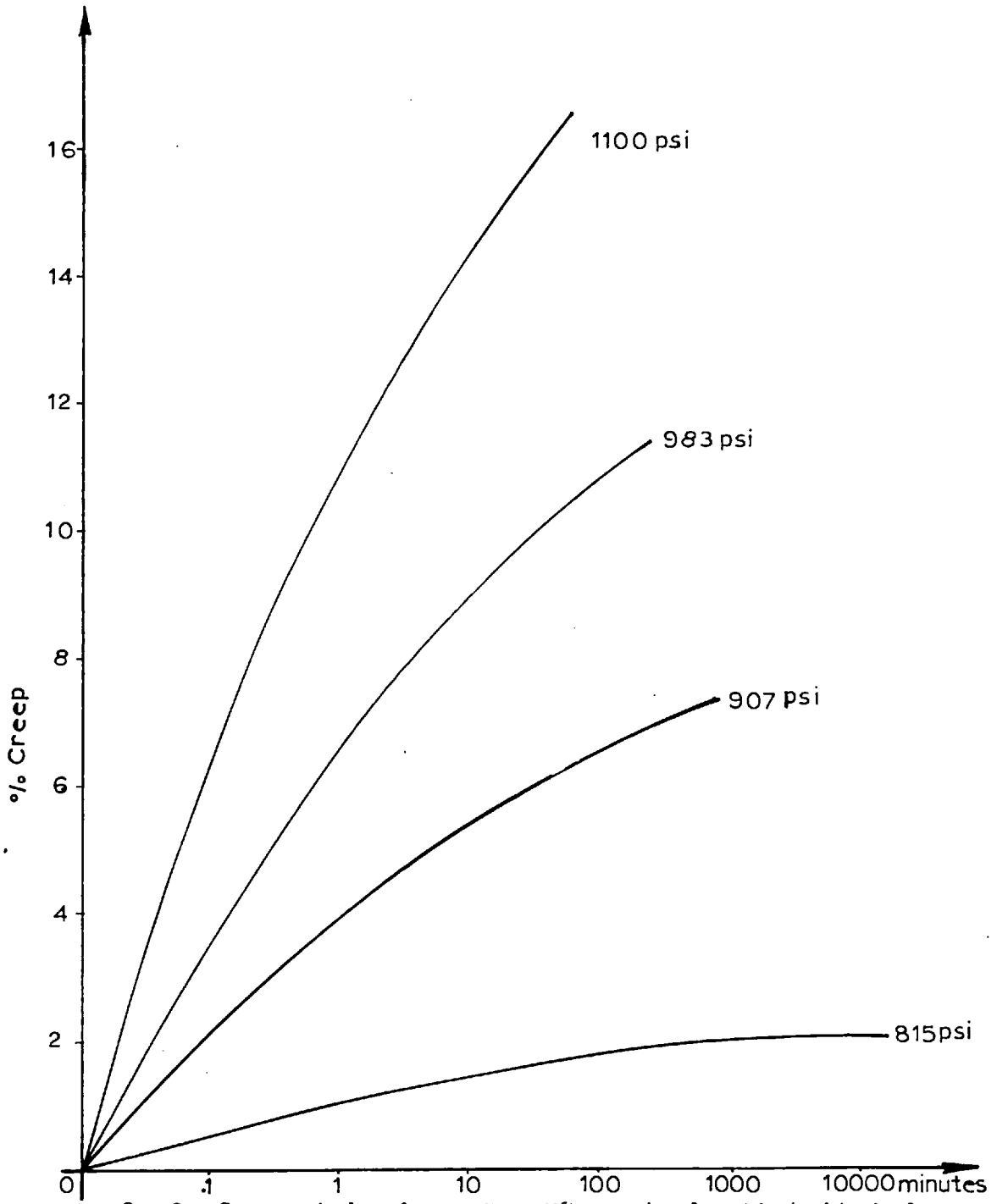

C.2.32 Creep behaviour for 5% randomly distributed bronze fibre reinforced H.D.Polyethylene.

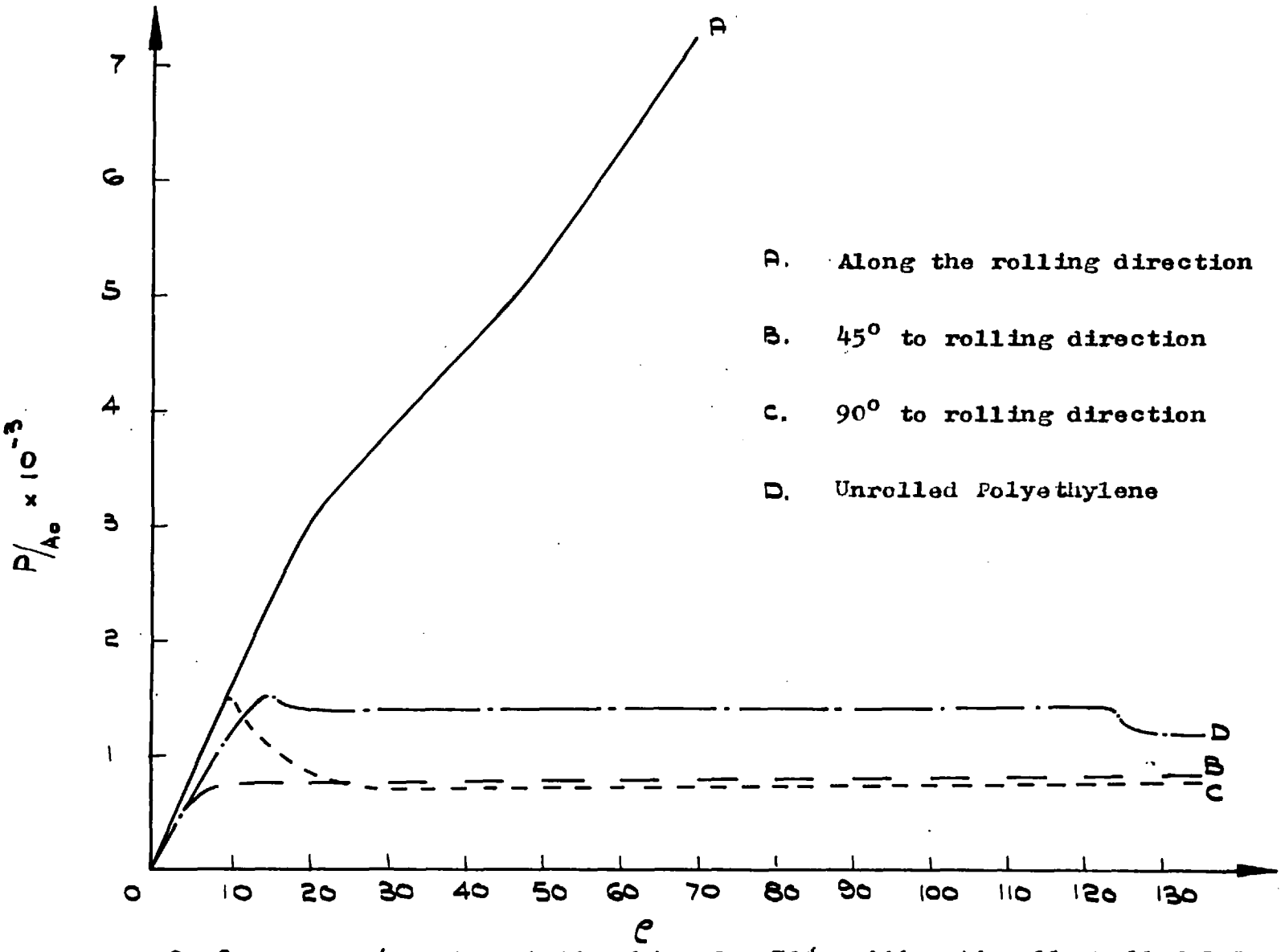

G. 2.33 Stress/strain relationships for 70% unidirectionally rolled L.D. Polyethylene (cast)

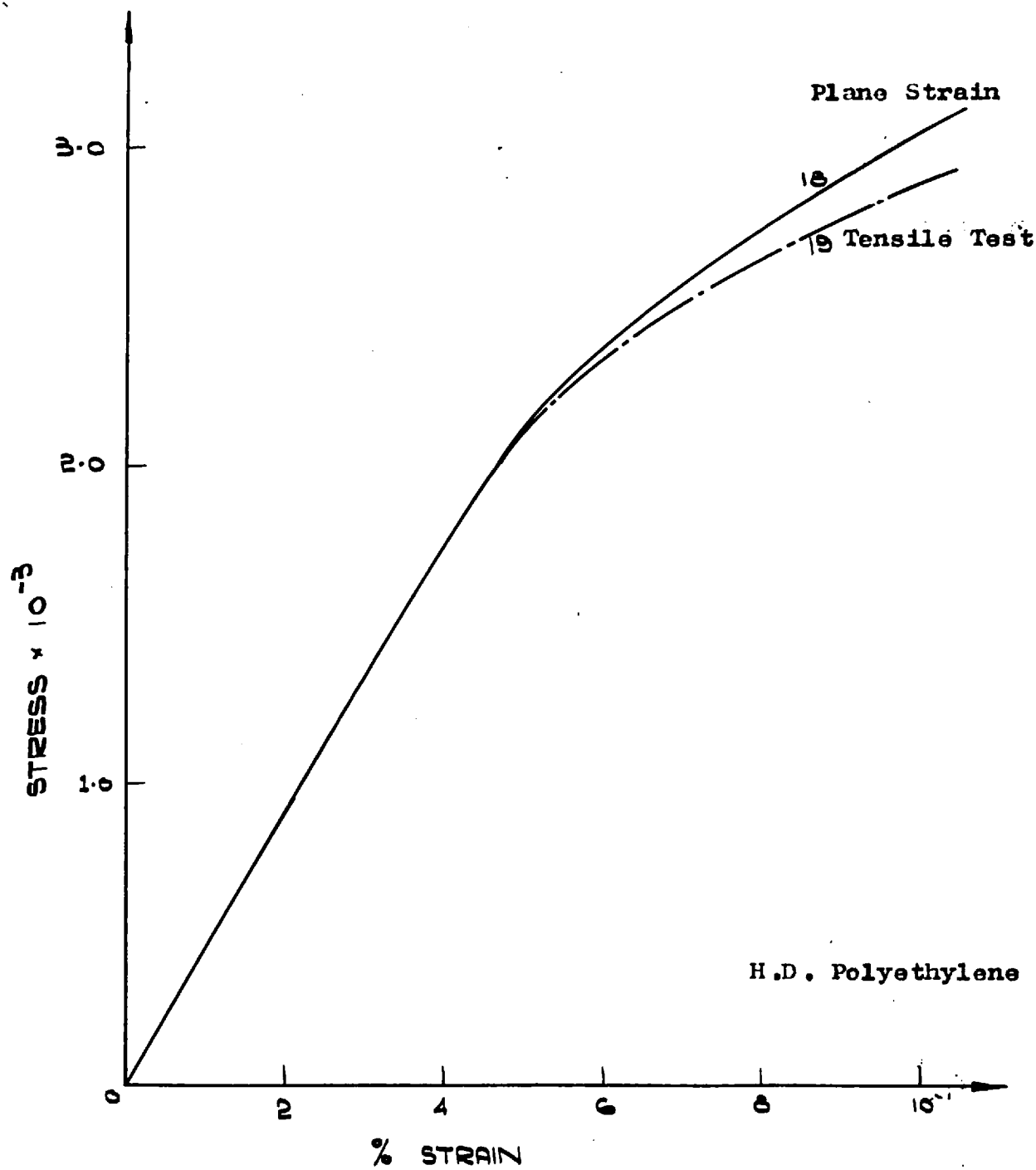

G.2.34 Comparison of tensile and plane strain compression test on the basis of large strain definition

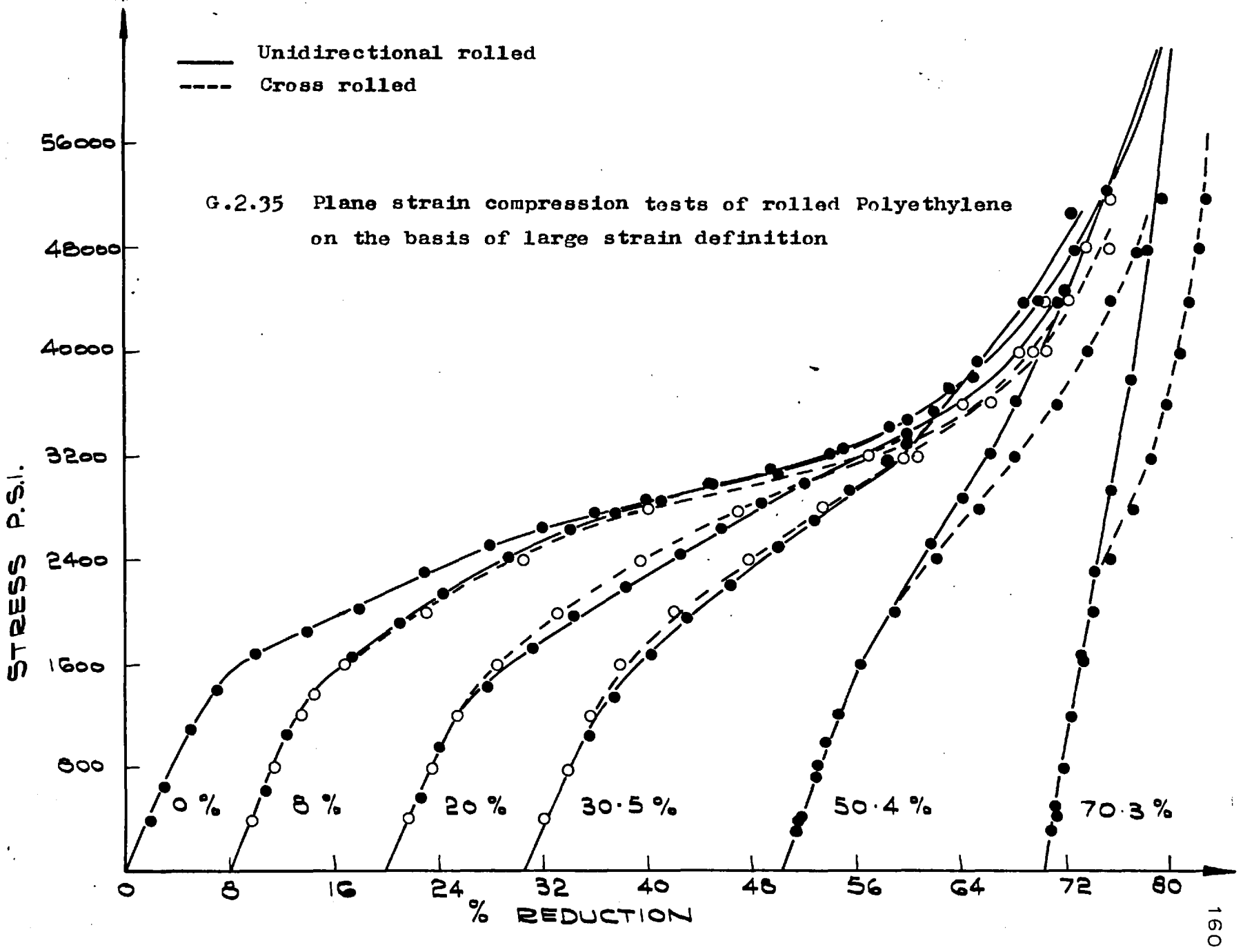

G.2.35 Plane strain compression tests of rolled Polyethylene on the basis of large strain definition

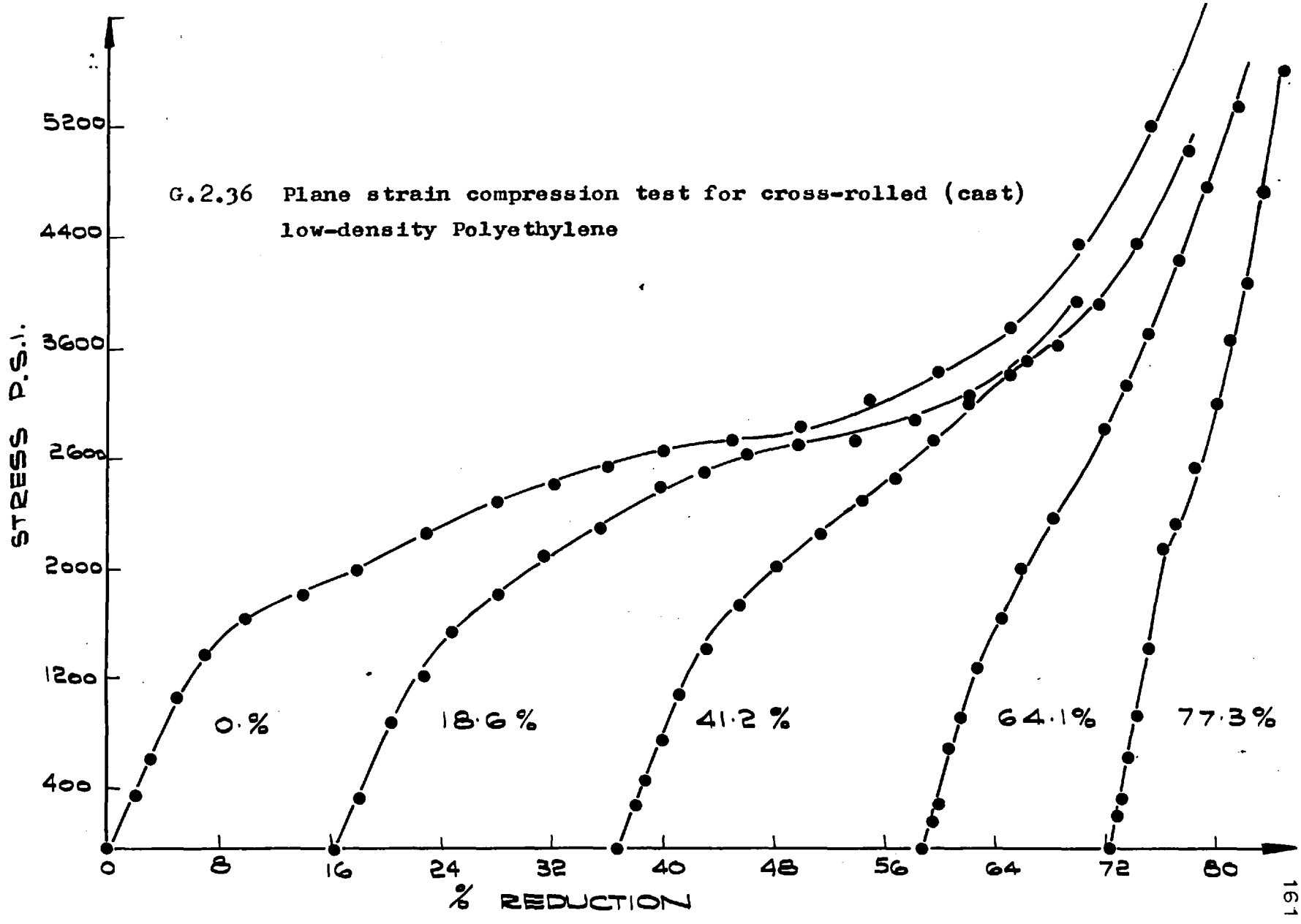

G.2.36 Plane strain compression test for cross-rolled (cast) low-density Polyethylene

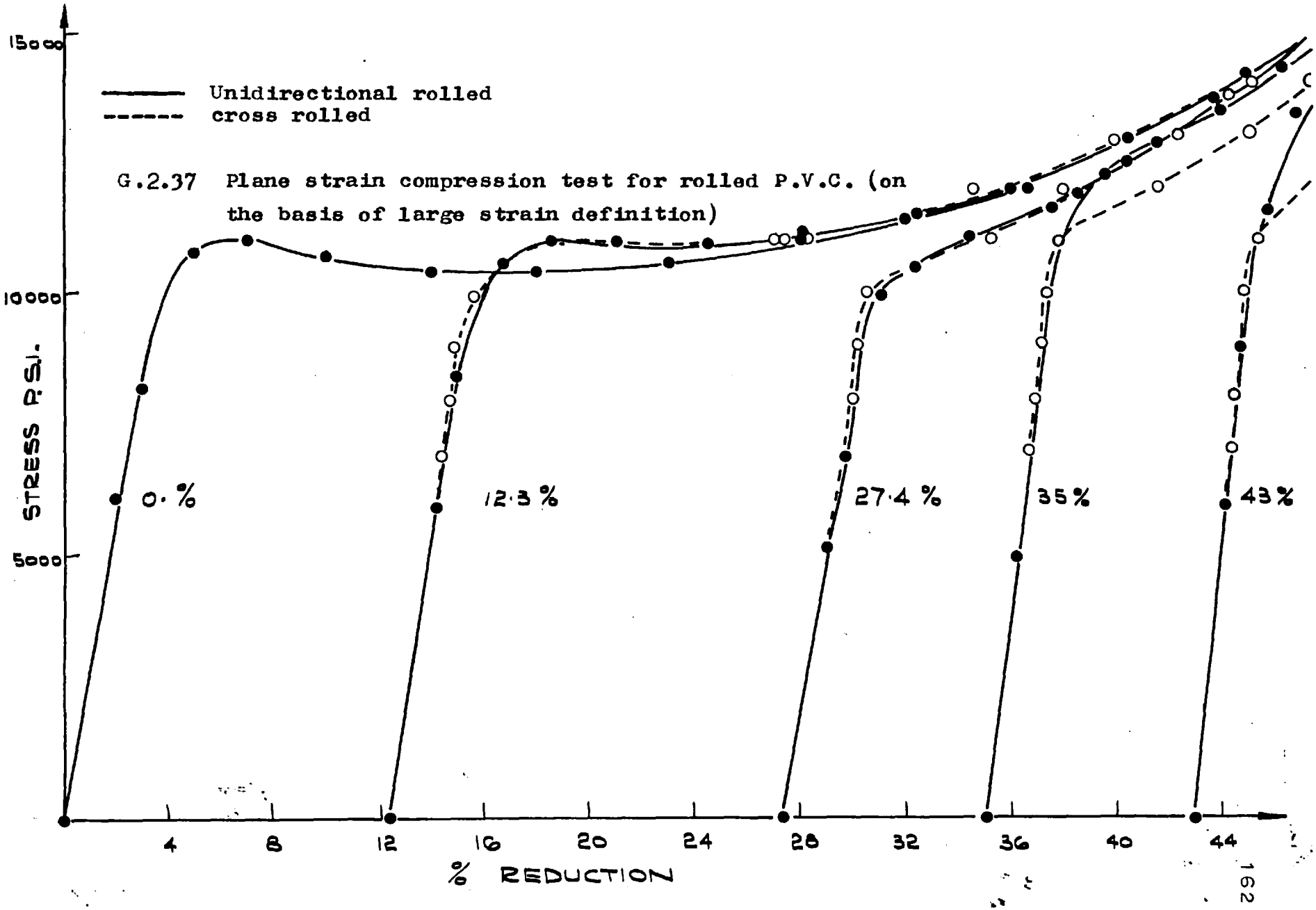

G.2.37 Plane strain compression test for rolled P.V.C. (on the basis of large strain definition)

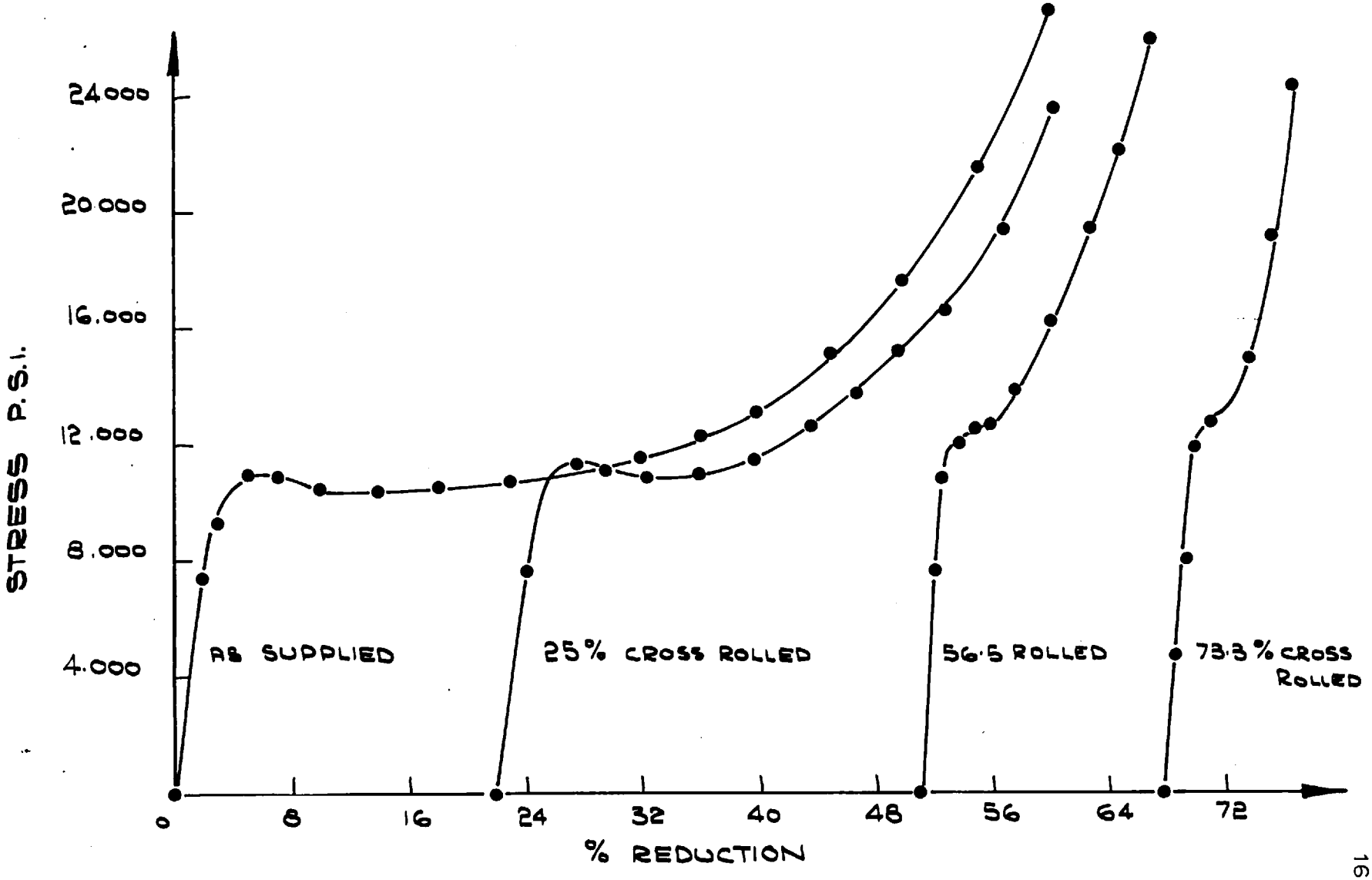

G.2.38. Plane strain compression test of cross-rolled P.V.C.

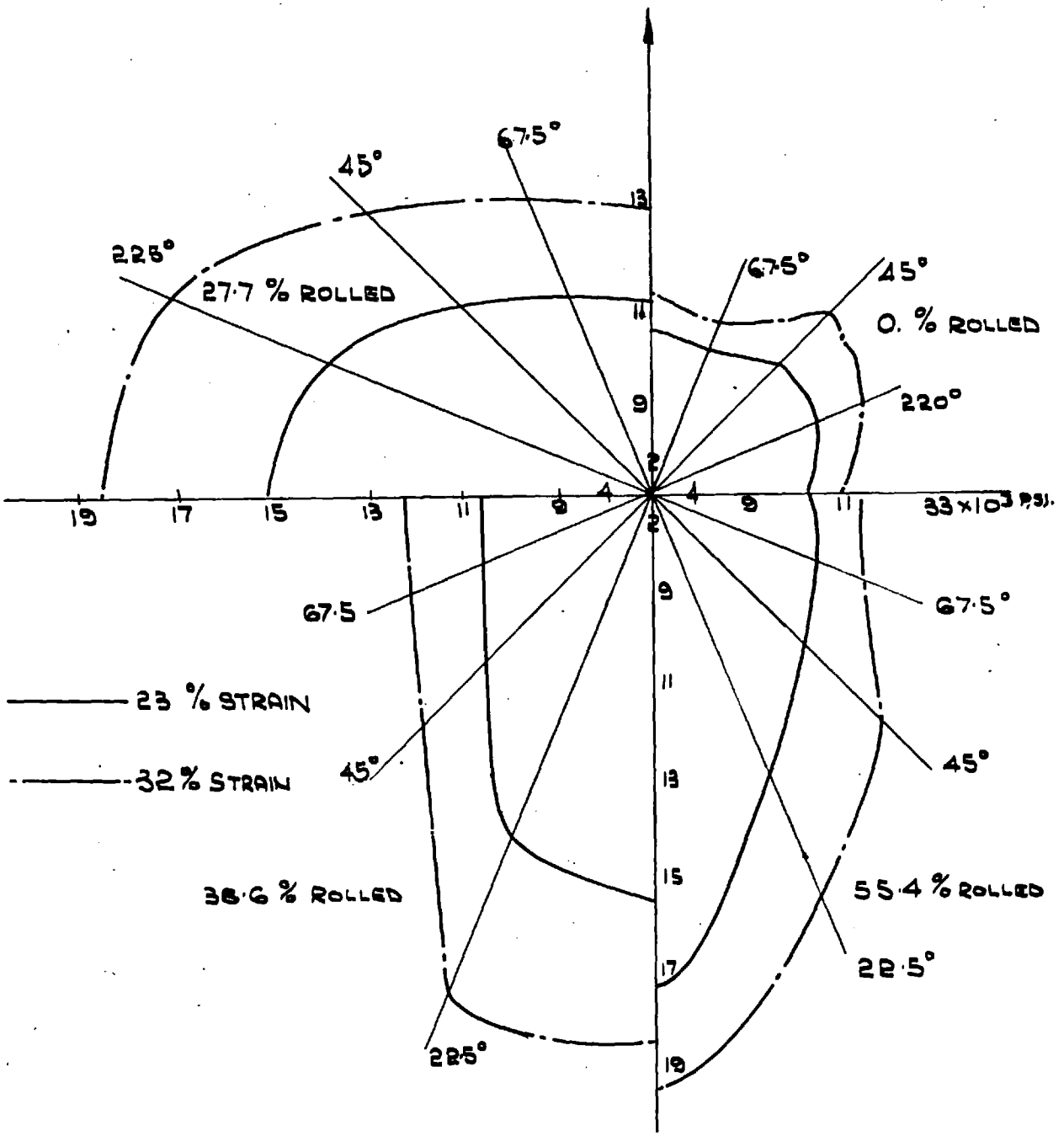

G.2.39 Plane strain compression test for unidirectional rolled P.V.C.

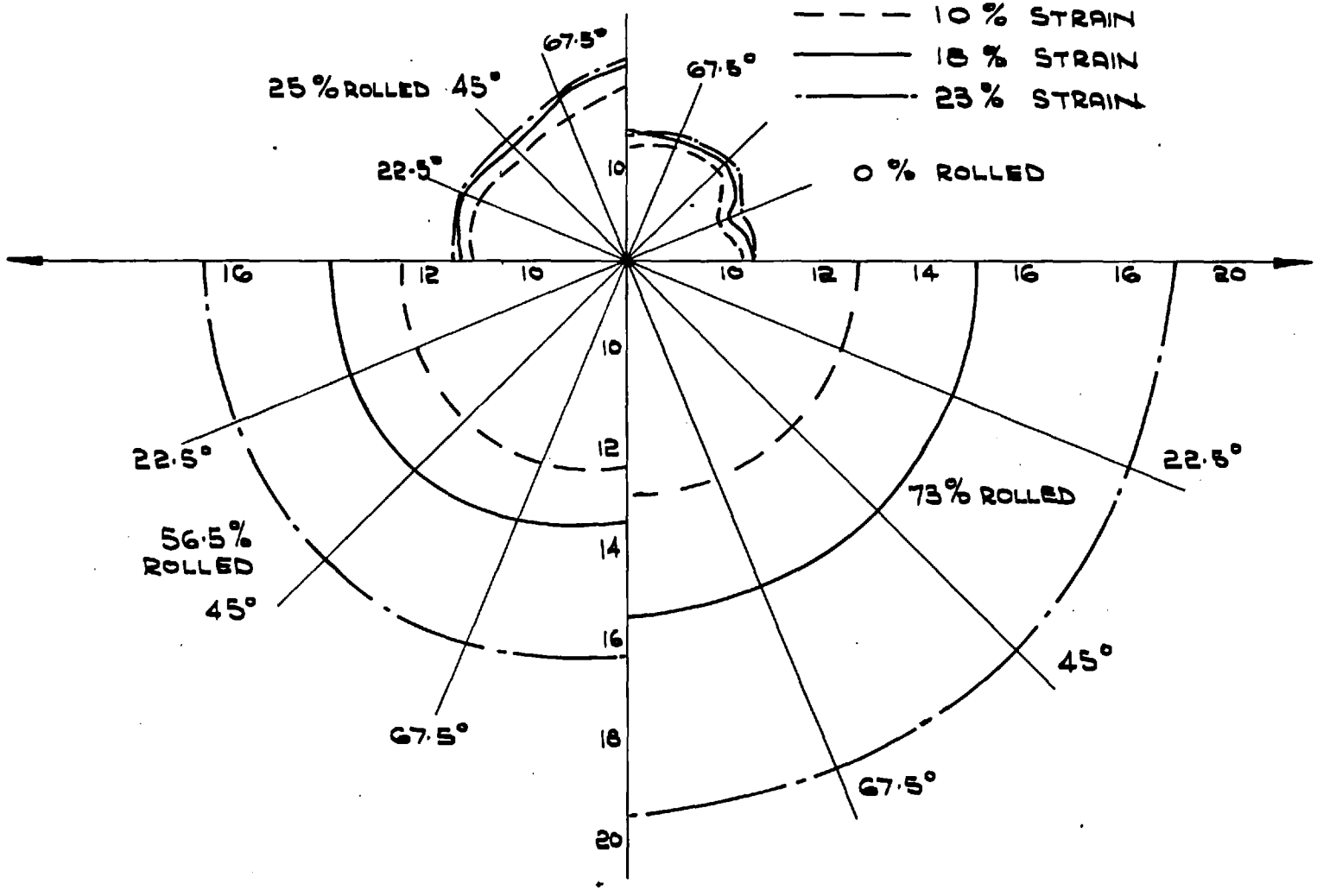

G.2.40 Plane strain compression test for cross-rolled P.V.C. (h_o = 1/4")

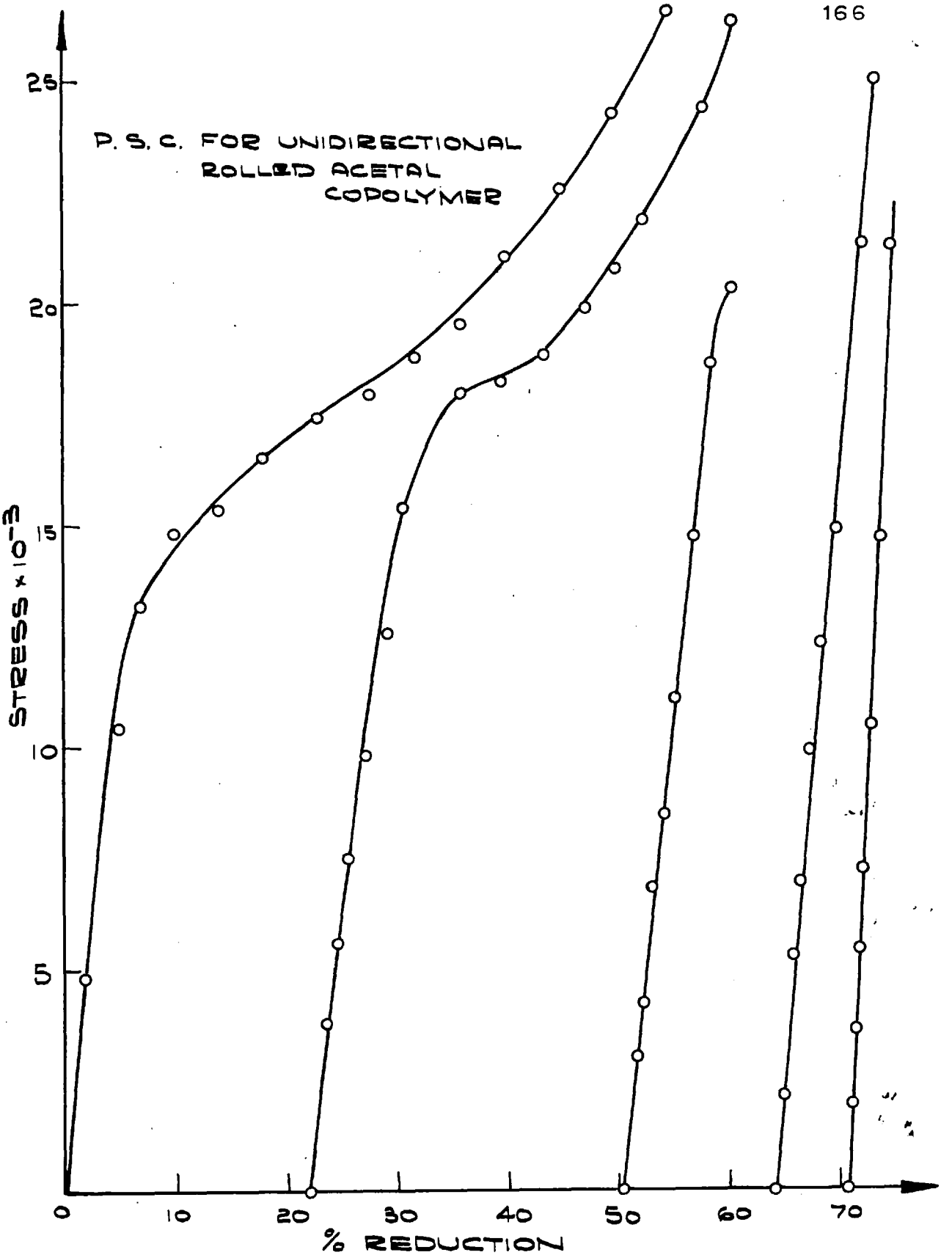

G.2.41. Plane strain compression tests for unidirectional rolled Acetal copolymer

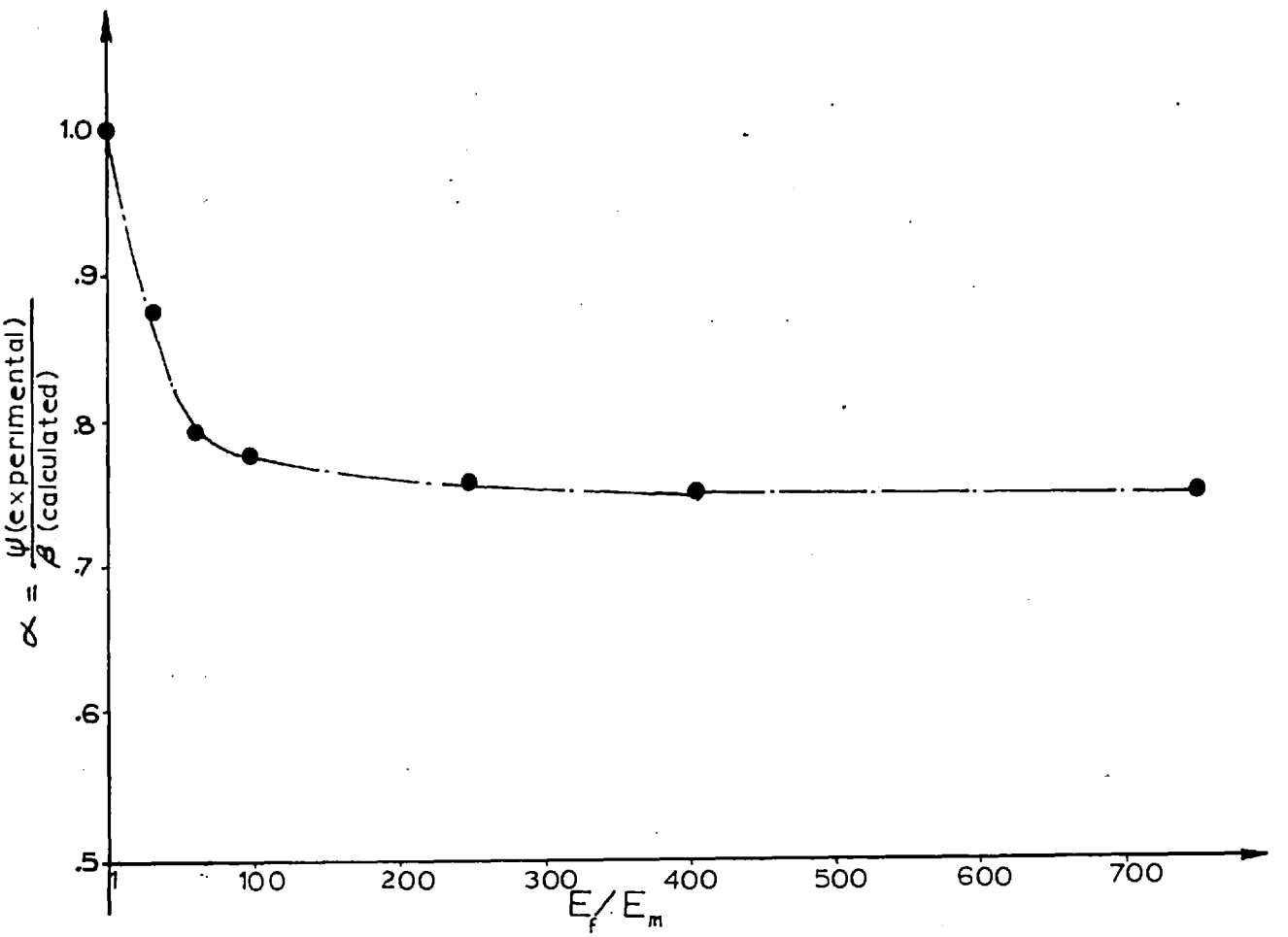

G.2.42 The variation of the calculated α with respect to moduli ratio (for randomly distributed fibres).

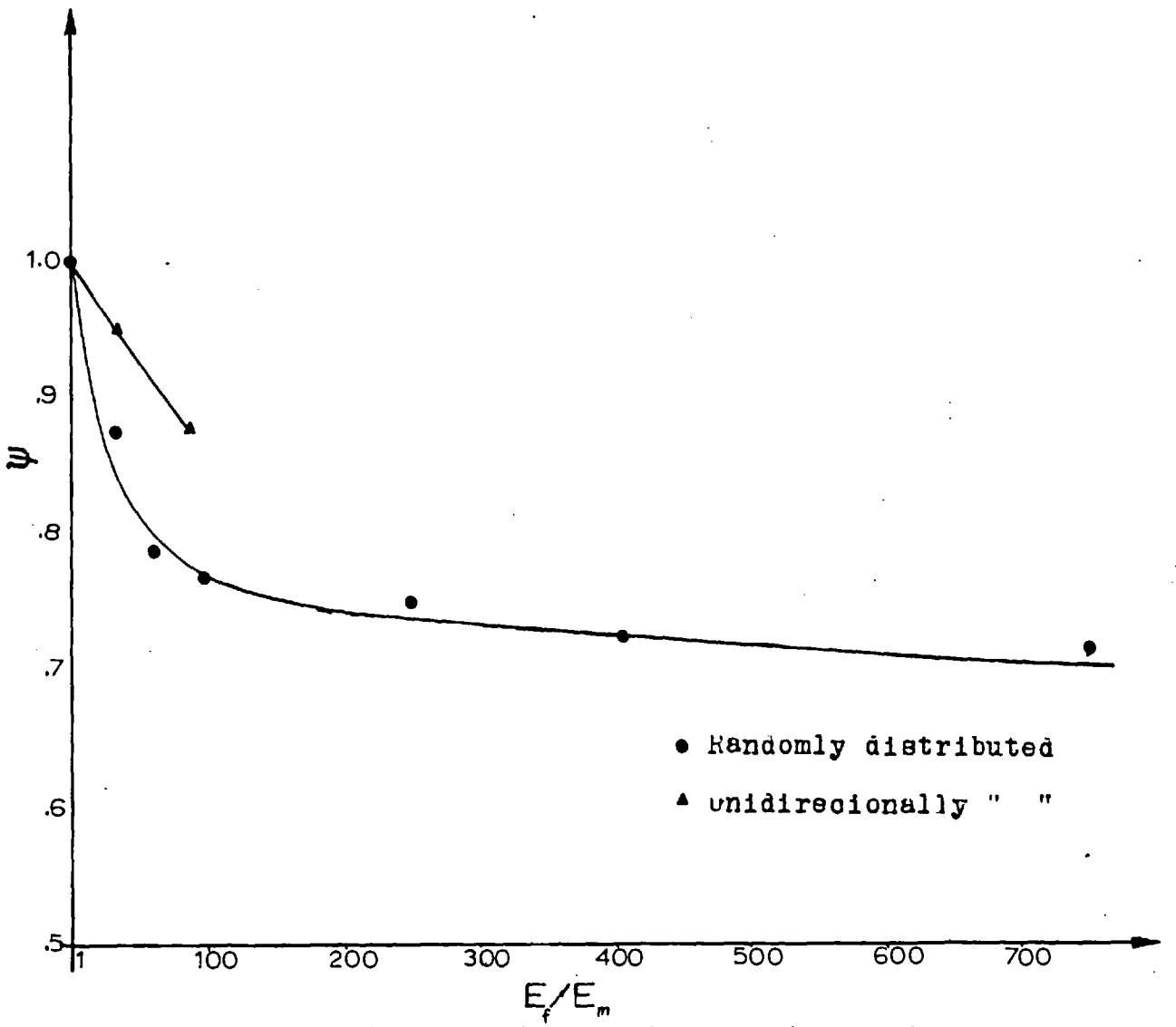

G.2.43 The variation of the strain transfer efficiency coefficient ψ with respect to E_f/E_m

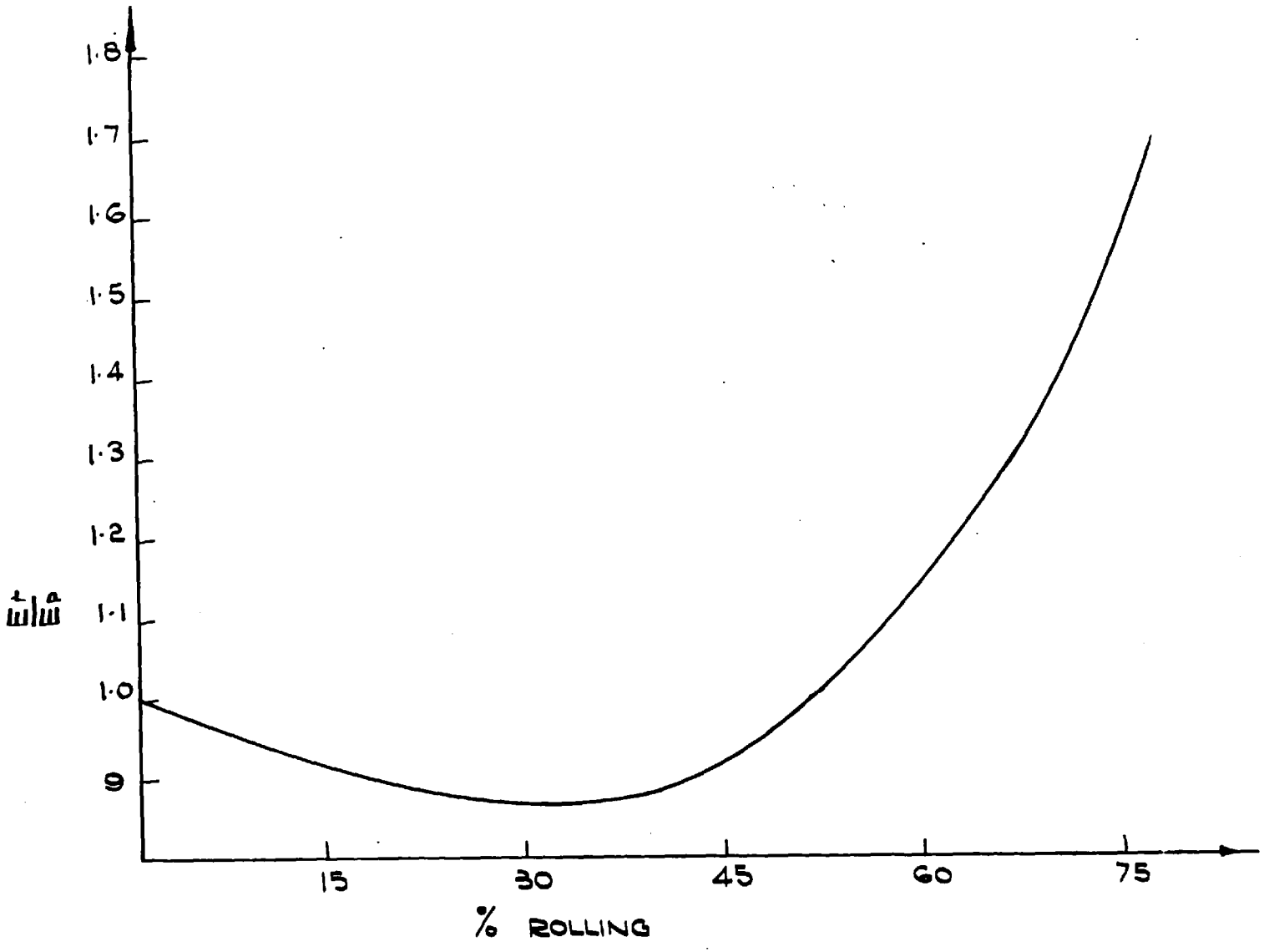

G.2.44.Variation of the L.D.Polyethylene Young's modulus with respect to degree of rolling.

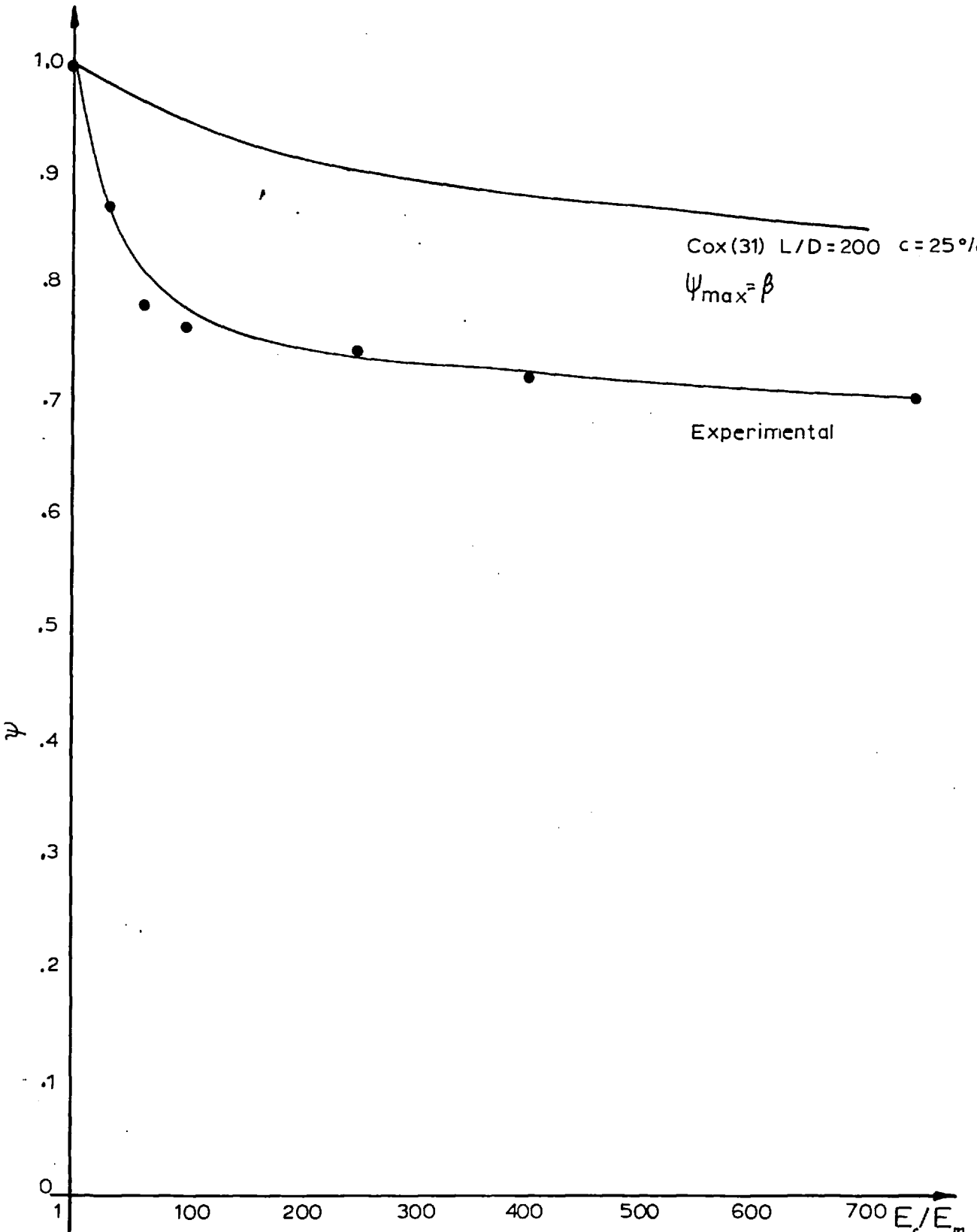

G.2.45 Comparison of theoretical and experimental variation of ψ for elastic matrix elastic fibre case.

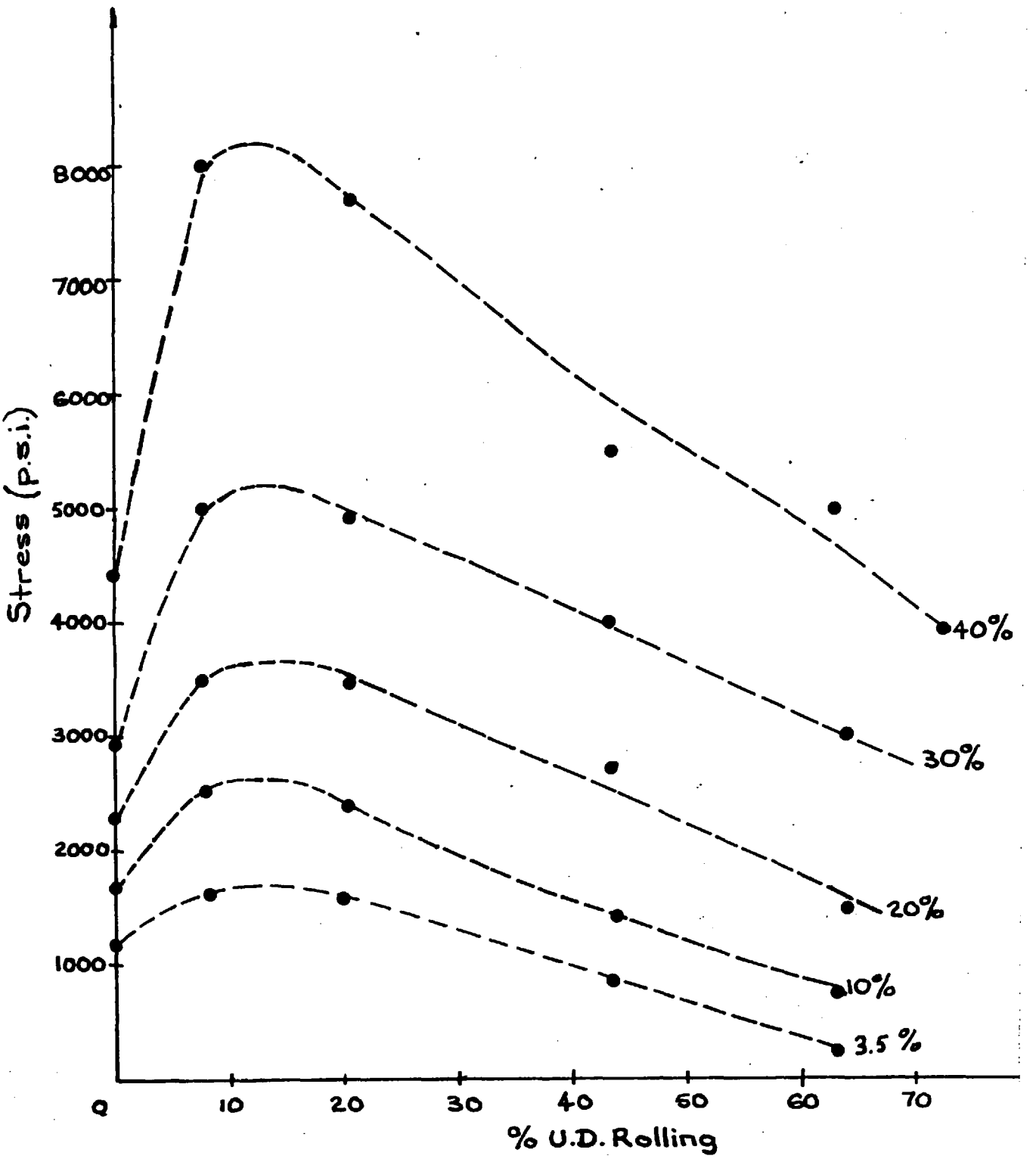

G.2.46. Variation of stress with respect to degree of rolling (1.8% randomly distributed bronze reinforced L.D. Polyethylene)

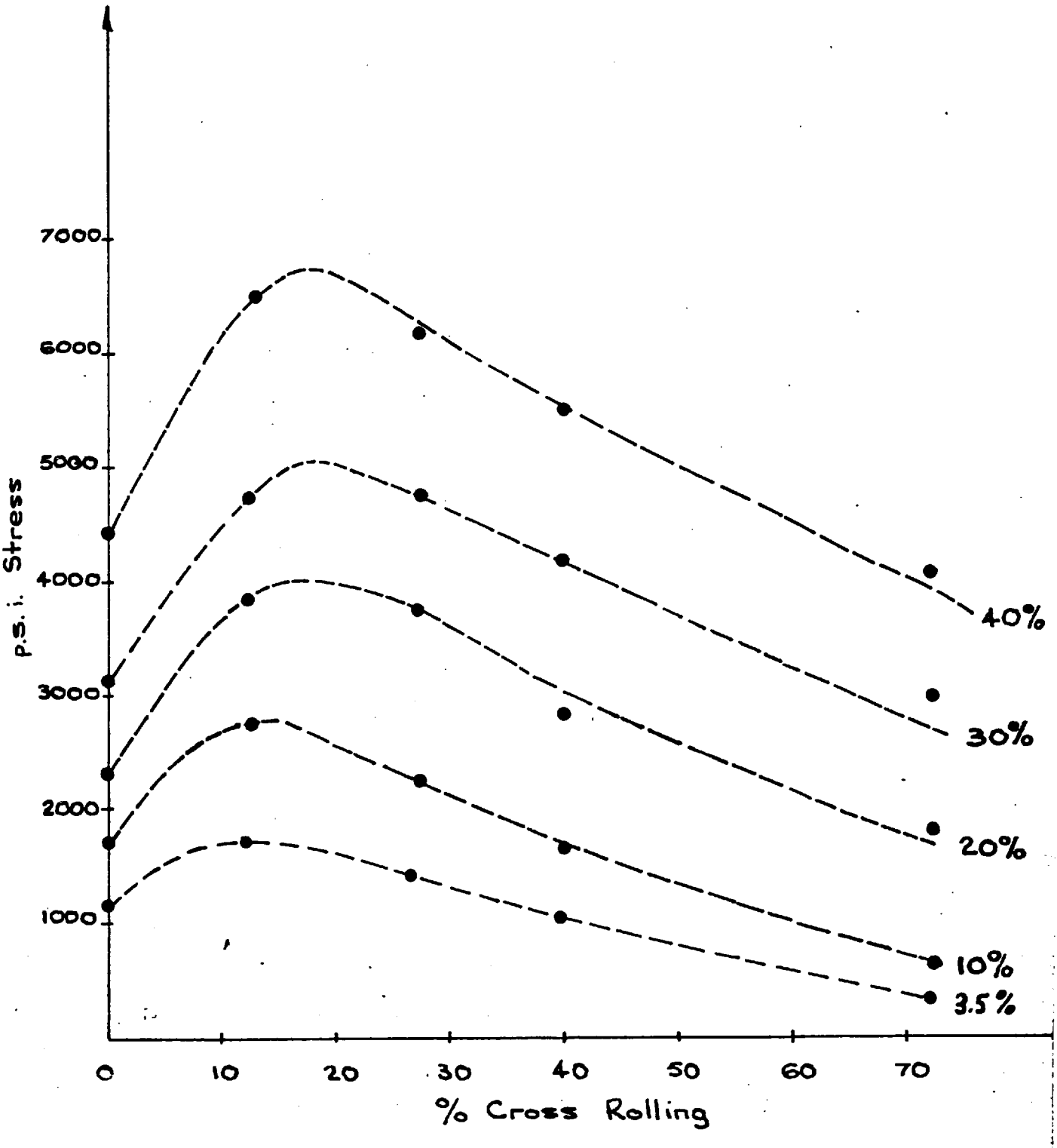

G.2.47. Variation of stress with respect to degree of rolling (1.8% randomly distributed bronze reinforced L.D. Polyethylene)